INOVAGRI
International Meeting

INOVAGRI BOOK 2014
Irrigation and Salinity: Researches and Technological Innovations

José Antônio Frizzone
Francisco de Souza
Sílvio Carlos Ribeiro Vieira Lima
Hans Raj Gheyi
Claudivan Feitosa de Lacerda

INOVAGRI
INSTITUTO DE PESQUISA E INOVAÇÃO NA AGRICULTURA IRRIGADA

INI Instituto Nacional de Ciência e Tecnologia Engenharia da Irrigação

INOVAGRI BOOK 2014 - IRRIGATION AND SALINITY: RESEARCHES AND TECHNOLOGICAL INNOVATIONS

INOVAGRI BOOK 2014 - IRRIGATION AND SALINITY: RESEARCHES AND TECHNOLOGICAL INNOVATIONS

Organizadores
José Antonio Frizzone
Francisco de Souza
Sílvio Carlos Ribeiro Vieira Lima
Hans Raj Gheyi
Claudivan Feitosa de Lacerda

INOVAGRI
INSTITUTO DE PESQUISA E INOVAÇÃO NA AGRICULTURA IRRIGADA

Fortaleza - CE
2014

INOVAGRI Book 2014 - Irrigation and Salinity:
Researches and Technological Innovations

Editoração Eletrônica
Byte Systems - Soluções Digitais

Cover
Rogis Rosemberg R. Gomes

Publication Data for Cataloging
Instituto de Pesquisa e Inovação na Agricultura Irrigada – INOVAGRI

F921i INOVAGRI Book 2014 - Irrigation and Salinity: Researches and Technological Innovations / José Antonio Frizzone, Francisco de Souza, Sílvio Carlos Ribeiro Vieira Lima, Hans Raj Gheyi, Claudivan Feitosa de Lacerda - Fortaleza, CE: INOVAGRI, 2015.
182 p. : il, 15,5 x 21,0 cm

ISBN 978-85-67668-09-3

1. Irrigation. 2. Salinity. 3. Water Resources. I. Frizzone, José Antonio. II. Souza, Francisco de. III. Lima, Sílvio Carlos Ribeiro Vieira. IV. Gheyi, Hans Raj. V. Lacerda, Claudivan Feitosa de. VI. INOVAGRI.

CDD 333.91

Preface

In April 2014, the global scientific community dedicated to the pursuit of knowledge about the issues surrounding the use of water in agriculture met in Fortaleza in the II INOVAGRI INTERNATIONAL MEETING to discuss irrigation, salinity and water resources.

The event was a realization of the Institute for Research and Innovation in Irrigated Agriculture (INOVAGRI), National Institute of Science and Technology in Irrigation Engineering (INCT- EI) and the National Institute of Science and Technology in Salinity (INCTSAL).

It was very important, especially for our country, because it is a fact, that the current situation in Brazil, related to agriculture is experiencing a period of transformation. Brazil is now, one of the largest potential for expansion of irrigated area. Regarding to the Irrigation we are sure it is necessary to find ways to increase the water use efficiency in irrigated areas.

We introduce now comprehensive texts about several subjects divided in 11 chapters, discussed in the round tables in the 2014 meeting on technological innovation, planning, management and new technologies applied in irrigation and salinity.

This book aims to promote an upgrade of the technological innovations applied to the irrigated agriculture by presenting the last event as a tool for discussion of R&D in irrigation and drainage. We hope this publication may be a guide for new researchers.

Sincerely,

Sílvio Carlos Ribeiro Vieira Lima
President of II INOVAGRI INTERNATIONAL MEETING

Acknowledgment

We would like to thank to the following institutions and people:

- The Institutions which gave us support and sponsored the organization of the II INOVAGRI INTERNATIONAL MEETING;
- The National Institute of Science and Technology in Irrigation Engineering (INCT-EI) and the National Institute of Science and Technology (INCTSAL);
- The author of each published text in special to Dr. Hans Raj Gheyi for being in charge of the organization of this textbook and all those who attended the meeting.
- All the Note Speakers of this event in special to Dr. Richard Allen by the wonderful contribution for the Irrigation in the world and for the participations at all meetings in Brazil since 2007.

Contents

1

Advances in *in situ* Measurement of Crop Evapotranspiration and Estimation of Crop Coefficients

Richard L. Snyder[1] & Cayle Little[2]

[1] University of California, California, USA
[2] California Department of Water Resources, California, USA

INOVAGRI Book 2014 - Irrigation and Salinity:
Researches and Technological Innovations
ISBN 978-85-67668-09-3

INOVAGRI
INSTITUTO DE PESQUISA E INOVAÇÃO NA AGRICULTURA IRRIGADA

Fortaleza - CE
2015

1 Irrigation Science and Technology to the Service of Farmers, Food Security, and Environment

ABSTRACT

While the instrumentation to estimate latent heat flux density (LE) with agro-meteorological measurements has improved in recent decades, there are few major advances in the ability to accurately determine actual evapotranspiration (ETa) other than with the surface renewal (SR) method. The Bowen ratio energy balance (BREB) method uses the Bowen ratio (β) estimates and the energy balance equation to calculate latent heat flux density from the ratio of sensible (H) to latent heat (LE) flux density, but errors in estimating LE (and ETa) are often problematic when the absolute value of is large, i.e., when H is large relative to LE. When H is small relative to LE, then LE≈Rn-G, where Rn and G are the net radiation and ground heat flux, and there is minimal benefit from using the BREB method. Also, the fetch requirement for the BREB method can be large for tall, rough canopies, which limits its applicability. Eddy covariance (EC) measurements are widely used to directly estimate H and LE, but it is rare that the energy balance closes in field trials, especially for irrigated crops. The reason for the lack of energy balance closure is unknown, which makes the use of EC direct LE measurements questionable at this time. In California, we have found that calculating LE as the residual of the energy balance using H from a sonic anemometer or using a thermocouple and surface renewal matches lysimeter measurements quite well. As a result, we have developed an extensive program to monitor LE as the residual of the energy balance using H from sonic anemometers and surface renewal for a wide range of crops. The results of field experiments will be presented with emphasis on the success of SR as a low-cost method to determine ETa.

1 INTRODUCTION

Efficient Irrigation and Evapotranspiration

Due to insufficient developed water supplies, there is a need to use water efficiently for on-farm irrigation. Efficient on-farm irrigation management involves applying

the water uniformly and in the correct amount so that evaporation and deep percolation (D_p) of water below the root zone are minimized. Since only water applied that contributes to evapotranspiration is considered efficiently used on farm, D_p is considered a non-useable, inefficient use of applied water. Strictly speaking, D_p recharges ground water and eventually returns as subsurface flow to rivers and streams, so it is not an inefficient use on a water basin scale. In addition, leaching of salts from a crop root zone is considered a beneficial use of water. In the short term, too much deep percolation (D_p) can limit water supplies to downstream users when water is in short supply, so minimizing deep D_p is beneficial to downstream users in addition to reducing water application energy costs and the cost of water. Except for evaporation losses from the water, surface runoff (S_R) from farm fields usually returns to the water supply, so S_R is generally not considered an inefficient use of water unless it flows into a salt-water body, gets contaminated, or evaporates without contributing to crop production or returning to the water delivery system.

In general, on-farm irrigation application efficiency can be defined as the ratio of water applied that contributes to crop evapotranspiration divided by the water applied. This ratio is often estimated as:

$$A_E = 100\left(\frac{A_N}{A_G}\right) \tag{1}$$

where A_E, A_N, and A_G are the application efficiency (%), net application (mm) and gross application (mm), respectively. Before an irrigation, A_N is commonly estimated as the soil water depletion (D_{SW}) relative to field capacity, and the soil water depletion from a well-drained soil depends mainly on the actual evapotranspiration (ET_a) since the last rainfall or irrigation. One can determine the D_{SW} by measuring the soil water content or by computing a soil water balance using water additions including effective precipitation (P_E), seepage from water tables (S_{PG}), and A_G, and water losses to ETa, D_P, and S_R. For well-drained soils, ET_a is the main mechanism for water losses, so ET_a, D_P, and S_R are employed to estimate the change in soil water content between irrigation events.

From the previous discussion, the importance of ET_a in estimating the water balance to determine water demand and for irrigation scheduling is clear. For well-drained soils, the A_G is estimated as:

$$A_G = S_R + \left(\frac{F_C - S_{WC}}{D_U}\right) \tag{2}$$

where F_C is the volumetric water content of the crop root zone at field capacity, i.e., the S_{WC} after drainage of gravitational water, and S_{WC} is the soil water content on the

irrigation date within the root zone and D_U is the distribution uniformity fraction. The D_U is the ratio of the mean depth of water soaked into the low quarter (i.e., the fourth of the field infiltrating the least water) divided by the mean depth of water soaked into the entire field. Therefore, using Eq. 2 to determine the A_G will lead to an approximate refilling the soil water content to field capacity in the low quarter of the field and some deep percolation over the other ¾ of the field. Maintaining a high D_U reduces the A_G required to refill the low quarter to F_C.

Daily change in soil water content (ΔS_{WC}) on an irrigation date is estimated as:

$$\Delta S_{WC} = A_N + P_E + S_{PG} - ET_a - D_P - S_R \quad (3)$$

On days without irrigation, the ΔS_{WC} equation is given by:

$$\Delta S_{WC} = P_E + S_{PG} - ET_a \quad (4)$$

Assuming no precipitation, seepage, or irrigation for a crop grown on a well-drained soil, the equation for ΔS_{WC} simplifies to:

$$\Delta S_{WC} = -ET_a \quad (5)$$

Thus, for well drained soils, the ΔS_{WC} between rainfall and irrigation is approximately equal to the sum of the actual crop evapotranspiration (ΣET_a) between irrigation events. Therefore, for a soil without seepage or effective rainfall, one can easily estimate S_{WC} each day between irrigation events to determine F_C-S_{WD} using Eq. 5. In locations where there is seepage and/or precipitation, the estimation process is more difficult, but one can use Eq. 4 with estimated S_{PG} and/or P_E to estimate the F_C-S_{WC} on an irrigation date.

Soils with high water tables make it difficult to determine F_C-S_{WC} because the ET_a can be the same in soils with water tables or that are well drained, but seepage of water upward from the water table to the crop root zone replaces some of the water loss due to ET_a. Thus, using ET_a to estimate changes in S_{WC} can lead to overestimation of F_C-S_{WC} in soils with water tables. At this time, we have no universal method to estimate the contribution of water tables to ET_a from crops.

Effective precipitation is often difficult to estimate due to lack of information and special variability. In addition, fog interception, dew deposition, and light rainfall often lead to errors in estimating the daily water balance from ET_a information alone. Like soils with water tables, the tendency is to overestimate the F_C-S_{WC} in crops where fog, dew, and light rainfall are common. There is no easy way to measure the contribution of these sources to the water balance, but a method to estimate the contributions was reported by Moratiel et al. (2012). The method estimates the fog, dew, or light rainfall contributions using ET_a and the approximate time of day when the crop dries using

the equation. The following equation estimates the fraction (F) of the daily ET_a that comes from nighttime fog interception, dew deposition, and light rainfall:

$$F = 1 - \frac{1}{1 + e^{\left(\frac{t-12.5}{1.65}\right)}} \quad (6)$$

where $0 < t < 24$ is the approximate local standard time when water dries from the crop surface. The product of ETa and F determines how much of the daily evapotranspiration came from fog, dew, or light rainfall, and (1 - F) × ETa is how much of the evapotranspiration came from the soil.

Reference Evapotranspiration in California

In California, standardized reference evapotranspiration for short canopies (ET_o) is widely available from the CIMIS - California Irrigation Management Information System (Snyder and Pruitt, 1992), which was developed by the University of California (UC) and the California Department of Water Resources (DWR). CIMIS has nearly 150 automated weather stations located throughout most of the State over irrigated grass for estimating ET_o. The network is near real-time in that the data are only a few hours delayed from the current time. The data are free and readily available to the public at no charge.

While CIMIS has many stations, it does not completely cover all microclimates within the State. As a result, spatial CIMIS was developed by the UC and DWR to estimate ET_o on an 4×4 Km grid using remote sensing, CIMIS data, and GIS. The remote sensing is used to estimate solar radiation and GIS is used to estimate weather variables between CIMIS stations that account for topography. Like CIMIS, spatial CIMIS is near real-time and data are available up through the previous day.

For shallow rooted crop and crops that are frequently irrigate in small amounts, there is an advantage in having estimated ET_o prior to the irrigation date so that controllers can be set to provide the correct application amount. Since the US National Weather Service (NWS) provides timely, reasonably accurate weather forecasts, UC and DWR worked with the NWS to develop a 7-day forecast ET_o product. The ET_o is estimated using the daily standardized reference evapotranspiration equation. The NWS does not forecast solar radiation, but it does forecast cloud cover, so the solar radiation is estimated from cloud cover using the relationships in the UN FAO publication 24. The NWS forecast is disseminated on forecast office websites throughout California and they service is expanding to other states in the USA. Everyone has free access to the ETo forecast, which is called FRET. The procedure is to find your location on a map using a postal zip code, latitude and longitude, or a nearby city name. Once a site is selected, the website provides a forecast for up to seven days.

Crop Coefficients

California has many microclimates, and research has shown that well-watered crop coefficient (K_c) values vary with microclimate. To study the effect of microclimate on K_c values, we used the standardized ET_o equation and the standardized reference evapotranspiration equation for tall canopies (ET_r), to calculate the K_c value for the 50 cm tall alfalfa. The four study locations are shown in Figure 1 and plots of ET_r versus ET_o are shown in Figure 2. Torry Pines is located just north of San Diego in a relatively cool, humid location. Meloland is located in a hot desert below sea level. Twitchell Island is found in a relatively cool, windy location near San Francisco Bay. Tulelake is located at a fairly high elevation in a warm, dry climate during summer. The results indicate that there is a huge difference in the K_c for tall alfalfa depending on the climate. Since this work was presented more research was completed, and a method was developed to estimate the climate effect on K_c values of any crop by estimating the aerodynamic resistance of a particular crop as an inverse function of wind speed in a base climate. Then, using the same aerodynamic resistance equation for the crop in a Penman-Monteith equation, the ratio of the estimated crop ET_c to ET_o provides an estimate of the K_c in other climates.

Figure 1. Locations for comparing ET_r and ET_o

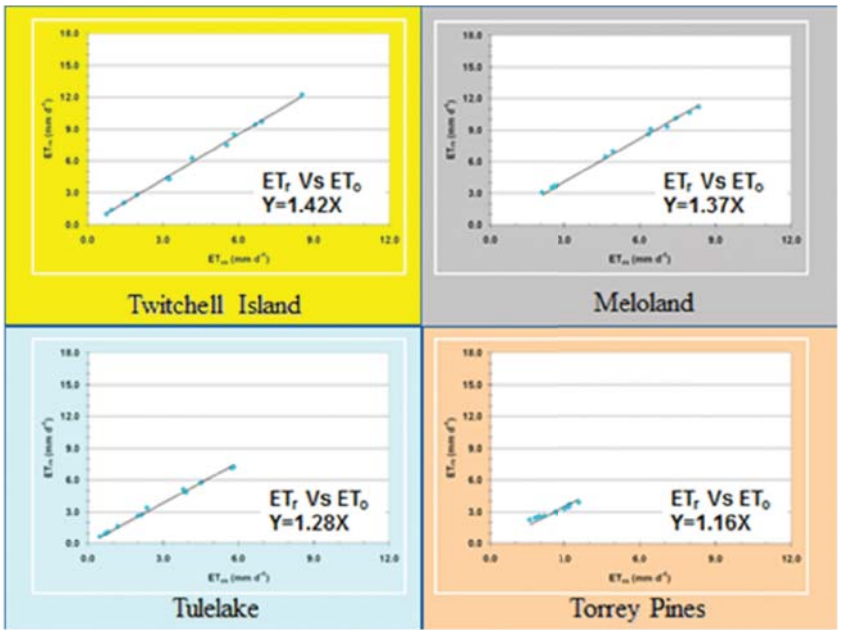

Figure 2. Plots of ET_r versus ET_o for the locations in Figure 1

Estimating Evapotranspiration

Measuring soil water content or evapotranspiration to determine F_C-S_{WC} is costly, difficult, and time consuming, so it is common to determine ΔS_{WC} by estimating ET_a using regional standardized reference evapotranspiration (ET_o) and actual crop coefficient (K_a) values as:

$$ET_a = ET_o \times K_a = ET_o \times (K_c \times K_s) = (ET_o \times K_c) \times K_s = ET_c \times K_s \quad (7)$$

Here, the variable K_s is a stress coefficient that varies between 0 and unity. When K_s = 0, then ET_a=0 and when K_s=1.00, then crop is limited by energy availability. ET_c is a special case for ET_a when there is no stress and K_s=1.00. Actual crop coefficients are determined as the measured crop evapotranspiration divided by the standardized reference evapotranspiration as:

$$K_a = \frac{ET_a}{ET_o} \quad (8)$$

Here, ET_o is the standardized reference evapotranspiration for short canopies (Allen et al., 2005). Although minimal data are currently available, the K_s in Eq. 6 is calculated as:

$$K_s = \frac{ET_a}{ET_c} \quad (9)$$

Where the $ET_c = ET_a$ of a crop that is experiencing little or no ET reducing stress.

While the instrumentation to estimate latent heat flux density (LE) with agro-meteorological measurements has improved in recent decades, there are few major advances in our ability to accurately determine actual evapotranspiration (LE and ET_a) other than with the surface renewal (SR) method. Currently, we use a residual of the energy balance method that combines the eddy covariance and surface renewal techniques to estimate sensible heat flux density (H) and estimate half-hourly ET_a as:

$$ET_a = \frac{LE}{2.45} \quad (10)$$

Where ET_a is in mm hh^{-1}, LE is in MJ m^{-2} hh^{-1} is the latent heat flux density, and L=2.45 MJ kg^{-1} is the latent heat of vaporization. The LE is calculated as the residual of the energy balance equation:

$$LE = R_n - G - H \quad (11)$$

using measured net radiation (R_n), ground heat flux density (G), and sensible heat flux density (H) in MJ m^{-2} hh^{-1}. In this paper, we discuss the measurement technique currently used in California and present some results.

2 MEASURING EVAPOTRANSPIRATION

A thorough discussion of the methods used to estimate LE using the residual of the energy balance (REB) method and H using a sonic anemometer with the eddy covariance (EC) technique or a fine-wire thermocouple and the surface renewal (SR) method is presented in Shapland et al. (2013). However, a short description of the methods is described here. Photographs of some of the sensors used to measure net radiation, ground heat flux, and sensible heat flux density are shown in Figure 3.

For the EC method, a sonic anemometer measures high frequency (10 Hz) wind speed in three directions, and the axes are rotated to force the mean vertical wind speed fluctuation equal to zero. Then, H (J $m^{-2}s^{-1}$) is estimated as the product of the product of the volumetric heat capacity (J $m^{-3}K^{-1}$) of the air and the mean covariance between fluctuations of the adjusted vertical wind speeds and fluctuations of air temperatures about their means (K m s^{-1}) over a 30 minute period (Shaw and Snyder, 2003).

The SR method collects high frequency (10 Hz) thermocouple data and statistically analyzes the data to determine an average temperature ramp over a 30 minute

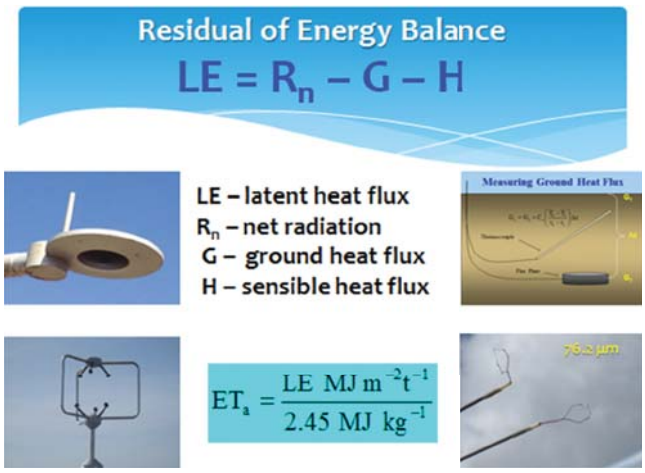

Figure 3. The residual of the energy balance equation and sensors used to measure net radiation, ground heat flux, and latent heat flux

period. The ratio of the amplitude to the duration of the average temperature ramp is an approximation for the change of temperature with time, so the product of the volumetric heat capacity of the air, the ratio of the amplitude to the duration of the ramp, and the volume divided by a unit area (i.e., the measurement height) provides an estimate of the sensible heat flux density. If the mean ramp increases during the 30 minute period, the atmospheric surface layer is unstable and the heat flux is upward. If the mean ramp temperature decreases, the near surface air is stable and the flux is downward. Because smaller diameter thermocouples have a tendency to break frequently, we decided to use 76.2 µm diameter thermocouples for SR measurements. While the larger thermocouples were more rugged, we found that calibration against a sonic anemometer was needed to correct SR estimates of H (H') to better match EC measurements of H. The SR data were calibrated for both stable (when H'<0) and unstable (when H'>0) atmospheric conditions. The calibrations were achieved by calculating the slope of the linear regression through the origin of sonic H versus uncalibrated surface renewal H'. More recently, we were able to show that aerodynamically compensating for the thermocouple size allows us to compute H' directly without the need for calibration (Shapland et al., 2014). However, in this paper, we only report results where the SR H' values were calibrated.

For net radiation measurements, we used model Q7.2 net radiometer from REBS, Inc., Seattle, Washington, USA during the early studies and model NR Lite net radiometers from Kipp & Zonen B.V., Delft, The Netherlands in recent years. The sensors were changed mainly to reduce the maintenance time and costs for repairing plastic domes. Ground heat flux was measured with model HT3 heat flux plates from REBS, Inc. and model Tcav soil temperature averaging sensors from Campbell Scientific Inc.

Logan, Utah, USA. The energy balance data were collected using model CR1000 and model CR3000 data loggers from Campbell Scientific Inc., Logan, Utah, USA.

In early studies, it was assumed that the soil volumetric heat capacity was fixed at 2.0×10^6 MJ $m^{-3}K^{-1}$. While this might have introduced small errors into the half hour measurements, it likely had little effect on the diurnal estimates of G, which are normally close to zero. Recently, we began to adjust the volumetric heat capacity for volumetric heat capacity, which we measure with model EC5 volumetric water content sensors from Decagon Devices, Pullman, Washington, USA. The surface ground heat flux density was calculated following the procedures in de Vries (1963).

3 RESULTS

Rice Evapotranspiration

Rice evapotranspiration data were collected in 19 fields during the period 2001 through 2013 in the Sacramento Valley of California. In each experiment, the ET_a and K_c data showed similar results to those shown in Figure 4 from the 2001 experiment. Figure 4 also shows that the general shape of the K_c curve is likely due to the trend in net radiation. Figure 5 shows diurnal energy balance curves during the initial growth and midseason periods of the season. The energy balance during initial growth shows net radiation over the flooded field is considerably higher than the typical clear sky R_n=650 W m^{-2} expected over a grass surface. It also shows that much of the high net radiation contributed to heating the water during the day and the energy storage in water was lost during the evening and night. It also shows that there was little or no sensible heat flux exchange over the flooded rice during initial growth when there was minimal vegetation. This was most likely due to the laminar air flow over the smooth water surface. During midseason, the crop canopy caused more turbulence and led to positive sensible heat flux in the morning when sunlight raised the surface

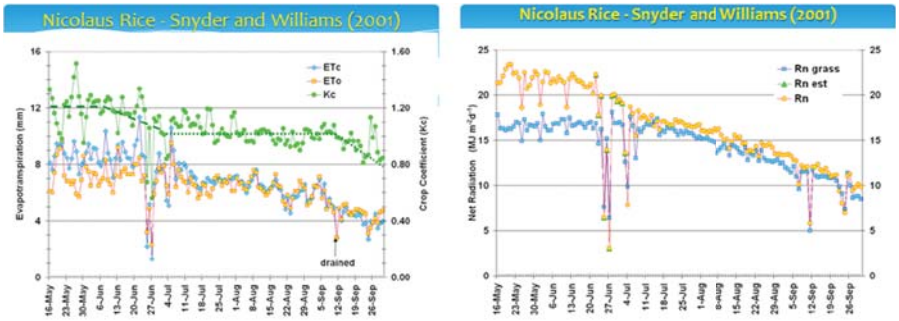

Figure 4. Rice evapotranspiration and crop coefficients measured in 2001 near Nicolaus, California (left) and the corresponding net radiation over grass and over rice (right)

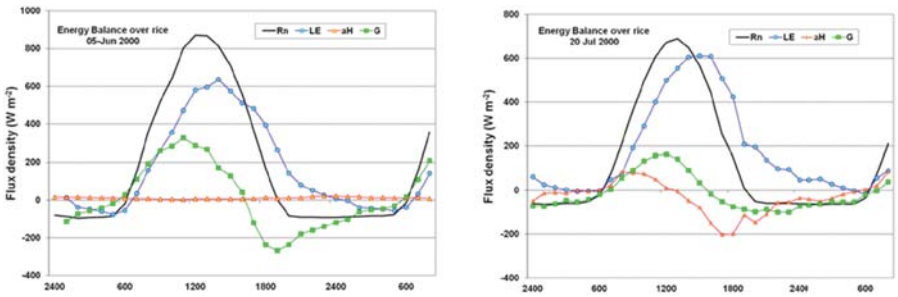

Figure 5. Diurnal energy balance plots during initial growth on 5 Jun 2000 (left) and the midseason period on 20 Jul 2000 (right). Note that net radiation (R_n) is positive to the surface, latent heat flux (LE) and calibrated surface renewal sensible heat flux (aH) are positive upward, and G is positive downward

temperature relative to air temperature and negative sensible heat flux in the afternoon when ET cooled the canopy relative to air temperature.

Validating the REB Method to Determine ET_a

To verify that the residual of the energy balance (REB) method for estimating ET_a was accurate, a micrometeorlogical station was set up over a winter wheat crop nearby the 6.1 m diameter weighing lysimeter in Davis, California, USA during the winter 2011-12. Figure 6 shows the lysimeter and the station and a plot of the ET_a measured by lysimeter and using the REB method with H from the sonic anemometer. Except for a period during March, when the data logger malfunctioned and late in the season, the ET_a from the lysimeter and from the REB estimate matched well. The discrepancy during the late period was due to water stress within the lysimeter and not

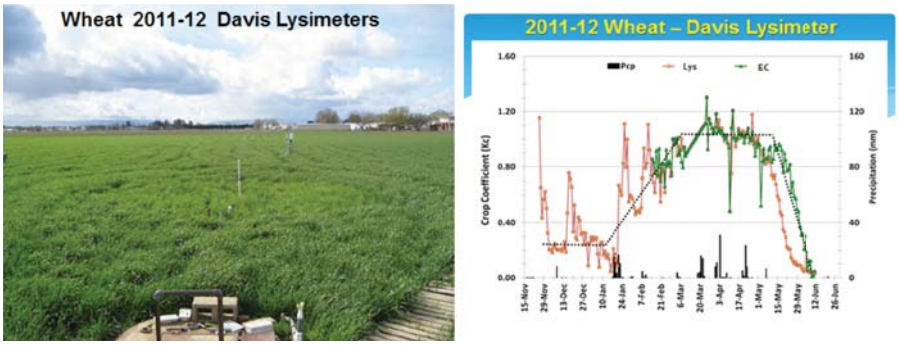

Figure 6. The Davis weighing lysimeter planted to winter wheat and a micrometeorological station for measuring ETa with the REB method using an RM Young sonic anemometer for H and the resulting daily ETa values for the lysimeter (Lys) and eddy covariance (EC)

from the surrounding field that occurred due to the lack of funding for irrigation. The data clearly show that the REB and lysimeter measurements give nearly identical ET_a results when functioning properly and there is no difference in water status of the crop.

Comparing ET_a Calculated with the EC and SR Methods

It was shown that the REB method using H from the EC method gives good estimates of ET_a when compared to a lysimeter. However, it is also important to show that the SR and EC methods both provide good estimates of H and LE. Figure 7 (left) shows a comparison between ET_a estimated with the REB method using both EC and SR estimates of H measured over wine grapes on a hillside near Diamond Springs, California. Figure 7 (right) shows the ET_o and ET_a calculations over turfgrass in an urban setting that was about 40 m east of a tall building in Davis, California. In both examples, the EC and SR methods gave daily ET_a values that were within 0.5 mm of each other, which indicates a good match.

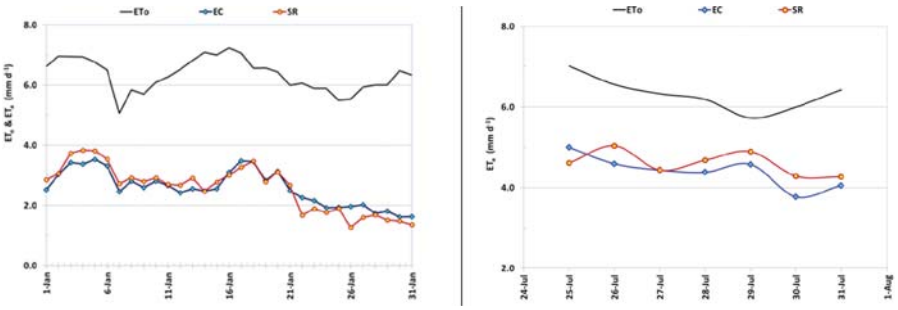

Figure 7. Plots of ET_o and ET_a measured over grapevines grown near Diamond Springs, California (left) and plots of ET_o and ET_a measured over turfgrass about 40 m east of a tall building in Davis, California (right). In both experiments, LE was measured using the REB method with H from SR and EC

4 CONCLUSIONS

We have shown that the REB method to estimate LE provides good estimates of ET_a using H from the EC method and that the SR method gives similar results. Since thermocouples are considerably less expensive than sonic anemometers and they can be mounted much closer to the canopy surface, the surface renewal method can provide accurate ET_a measurements at a lower cost and over surfaces that are too small in extent for sonic anemometers. In these studies, the SR estimates of H were calibrated to approximate H from the EC method. Recent research has shown that the SR method does not require calibration if one compensates for the thermocouple size (Shapland et al. 2014), so it is likely that we can estimate ET_a using the low-cost SR method without the need for a sonic anemometer. This is a big advance for the

science of measuring ET since it should greatly increase the ability of scientists and engineers easily collect energy balance data at a lower cost.

REFERENCES

de Vries, D.A. 1963. Thermal properties of soils. pp. 210–235, *in:* W.R. van Wijk (ed). *Physics of Plant Environment.* Amsterdam, The Netherlands: North-Holland Publishing Co.

Shapland, T.M., McElrone, A.J., Paw U, K.T. and Snyder, R.L. 2013. A turnkey data logger program for field-scale energy flux density measurements using eddy covariance and surface renewal. Italian J. of Agrometeorology, 1/2013.

Shapland, T.M., Snyder, R.L., Paw U, K.T., and McElrone, A.J. 2014. Thermocouple frequency response compensation leads to convergence of the surface renewal alpha calibration. Agricultural and Forest Meteorology, 189-190: 36-47.

Shaw, R.H. and R.L. Snyder. 2003. "Evaporation and eddy covariance." *Encyclopedia of Water Science*. Stewart, B.A. and Howell, T.A. Eds. Marcel Dekker Inc., New York, NY, 235-237.

Snyder, R.L., and Pruitt, W.O. 1992. Evapotranspiration Data Management in California, Proc., *Water Forum '92 - Irrig. & Drain. Session*, ASCE, New York, N.Y.

2

Measuring Water Use and Crop Coefficients for Full and Deficit Irrigated Crops

Thomas J. Trout[1]

[1] United States Department of Agriculture, Colorado, USA

INOVAGRI Book 2014 - Irrigation and Salinity:
Researches and Technological Innovations
ISBN 978-85-67668-09-3

INOVAGRI
INSTITUTO DE PESQUISA E INOVAÇÃO NA AGRICULTURA IRRIGADA

Fortaleza - CE
2015

2 Measuring Water Use and Crop Coefficients for Full and Deficit Irrigated Crops

ABSTRACT

As water scarcity increases in irrigated areas, precise scheduling of irrigation timing and amount becomes more critical. Farmers also must consider deficit irrigation as a way to maintain their productivity and income with limited water supplies. The USDA-Agricultural Research Service in Colorado is measuring yields and crop water use with full and managed deficit irrigation, and developing strategies to maximize "crop per drop". We have set up field plots with several deficit irrigation timings and amounts and closely monitor water applications, soil water content, and crop responses. We develop water production functions (yield per unit water use), plant stress indicators such as elevated canopy temperature and reduced growth, and estimate crop water use by the volume balance method. Deficit irrigation generally does not result in higher water productivity of field crops, but can be used to manage limited water supplies. The volume balance method is an accurate way to estimate crop water use if water applications are uniform and deep percolation is small. Canopy temperature is a good way to estimate crop stress and is closely related to soil water deficit.

1 INTRODUCTION

Irrigation water supplies in the U.S. Central Plains and much of the western U.S. are declining. Supplies originally developed for irrigated agriculture are being diverted to growing urban areas and for ecosystem restoration. Groundwater use in many areas exceeds recharge and must decrease if we are to sustain this valuable resource. Temperature increases due to climate change will likely reduce the mountain snowpack accumulation that is critical to surface water supplies. Irrigated agriculture will very likely have less water available in the future than it had in the past. Sustaining irrigated agriculture will require increasing the economic productivity per unit of water.

Careful irrigation management can lead to increased water productivity – more yield per unit water. Applying the correct amount of water at the correct time is

necessary for efficient irrigation water management. A common method to estimate crop water requirement and schedule irrigation is to use the FAO-56 procedure (Allan et al, 1998) of estimating the evapotranspiration of a reference crop from weather data, ETr, and multiplying this reference ET by a crop coefficient for the crop being grown, Kc. Crop coefficients are determined by measuring the crop ET (ETc) and dividing by the reference ET (ETr).

Crop ET can be measured by energy balance methods (Eddy Covariance, Bowen Ratio Energy Balance), or water balance (lysimetry, soil water measurement). Energy balance methods can work well for large fields (adequate fetch), but require careful use of expensive instrumentation. A weighing lysimeter is potentially the most accurate method to measure ETc, but is very expensive and difficult to manage properly. Soil water measurement can be a good alternative if rainfall is low and irrigation is carefully managed such that water loss to deep percolation and runoff are small.

Although crop coefficients are normally measured for well-watered crops, when water is limited, regulated deficit irrigation may be a desired practice. Thus, crop coefficients for deficit irrigation are also useful.

In 2008, USDA-Agricultural Research Service in Fort Collins, Colorado began a field study of the water productivity of four crops under a range of irrigation levels from fully irrigated to about 40% of full irrigation. We measure ET of the crops under each of these conditions and seek ways to maximize productivity per unit water consumed. We also strive to better understand and predict the responses of the crops to deficit irrigation so that limited irrigation water can be scheduled and managed to maximize yields. In this study, I describe the water balance method we use to measure ETc for this study and the resulting crop coefficients for corn under these conditions.

2 METHODS

A 20 hectare research farm northeast of Greeley, CO – the Limited Irrigation Research Farm, or LIRF - was developed to enable the precision water control and field measurements required to accurately measure ET of field crops. The low rainfall in the area, predominately sandy-loam soils and good groundwater well are ideal for irrigation research.

Four crops – field corn, sunflower (oil), dry beans (pinto), and winter wheat were rotated through research fields on the farm. Crops are planted, fertilized, and managed for maximum production under fully-irrigated conditions, but are irrigated at 6 levels that range from fully irrigated to about 40% of the fully irrigated amount. Deficit irrigations are timed to maximize production – usually by allowing relatively higher stress during early vegetative and late maturity stages and applying extra water to reduce stress during reproductive stages.

Each crop field was divided into 4 replications within which the 6 irrigation treatments were randomized (randomized block design). Water was regulated,

measured, and delivered to 10 m (12 row) x 40 m plots. We applied irrigation water with drip irrigation tubes placed on the soil surface along each crop row to insure that the water was applied uniformly and precisely. This was essential to be able to complete the water balance. Figure 1 shows an aerial view of the research fields in 2008.

Figure 1. Aerial view of the water productivity plots at LIRF. Crops from left to right are beans, wheat, sunflower, and corn. Lower fields contain Bowen Ratio instrumentation

A CoAgMet (Colorado Agricultural Meteorological Network) automated weather station was installed on the farm near the center of a 1 acre grass plot. Hourly weather data from the station were used to calculate ASCE Standardized Penman-Monteith alfalfa reference evapotranspiration (ETr). Soil water content between 15 cm and 200 cm depth was measured by a neutron probe from an access tube in the center of each plot. Soil water content in the surface 15 cm was measured with a portable TDR system (MiniTrase, SoilMoisture, Inc., Santa Barbara, CA). Soil evaporation was estimated based on techniques described in Allen et al. (1998). Basal crop coefficients were adapted from Table 8.8 in Allen et al. (2007) based on full cover date. Irrigations were scheduled using both predicted soil water depletions based on ETr measurements, and measured soil water depletion.

Crop ET was measured by water balance. Figure 2 shows a diagram of the water balance for an irrigated field with a deep water table (no upward water movement). In the diagram:

$$ETc = I + P - \Delta SW - DP - R$$

where: I = the irrigation amount, P = precipitation, ΔSW = change in soil water content, DP = deep percolation of water below the root zone, and R = surface runoff.

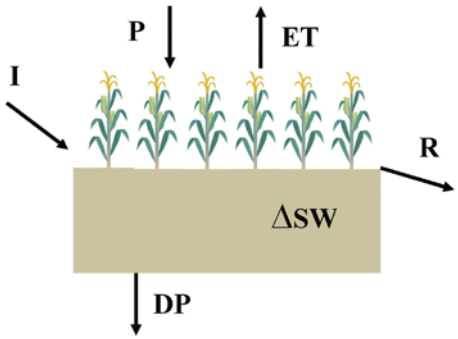

Figure 2. Water balance for irrigated crops

Because DP and R are difficult to measure accurately, the goal is to irrigate efficiently to minimize DP and R. To accomplish this we use a very uniform irrigation method (drip) and careful irrigation scheduling on the plots. The low seasonal rainfall in the area (200 mm) also reduces DP and R losses. For our trials on relatively flat fields with moderate infiltration, we assume R is zero. Deep percolation was assumed to occur only when irrigation or precipitation amount exceeded the ability of the soil to store water in the root zone (soil water depletion), and soil water content increased in layers below the root zone.

Plant measurements were taken periodically to determine crop responses to the water levels and relate the crop coefficients to plant growth stage and canopy ground cover, Fc. Canopy cover was measured with a digital camera attached to the boom of a "high boy" mobile platform and driven through the plots weekly (Figure 3).

Figure 3. High Boy reflectance tractor measuring canopy ground cover, reflectance and temperature

Indicators of crop water stress such as stomatal conductance, leaf water potential, and photosynthesis were measured periodically. Canopy temperature was measured continuously with stationary infrared thermometers and periodically with the mobile platform (Bausch et al., 2010).

At the end of the season, seed yield and quality as well as total biomass were measured from each plot.

3 RESULTS

Table 1 summarizes the overall results for the four crops in terms of water requirements and productivity. Productivity is listed in terms of kilograms of grain produced per cubic meter of water consumed, or evapotranspiration, often referred to as water use efficiency. Water consumption (ETc) was measured by water balance. Corn, although a fairly high water user, is the most efficient crop at converting water to biomass and grain. Sunflower uses a little less water than corn and tends to utilize any available soil water efficiently because of its vigorous rooting system. Winter wheat uses about the same amount of water as sunflower. Because wheat matures early, it can be a good rotation crop if well capacity or late season water supply is limited. Pinto beans use less water than the other crops studied because of the shorter season. Our beans were grown on 30 inch rows which result in a little lower water use and yields than if planted in narrower rows.

Table 1. Water productivity and total water requirements of 4 crops grown at LIRF

Crop	Water productivity	Total water requirements
Corn	2.3 kg/m^3	580 mm
Sunflower	0.8	470
Winter Wheat	1.2	550
Pinto Beans	0.8	350

I will use the 2011 corn crop (Dekalb DKC52-59 (VT3)) to demonstrate use of water balance to measure crop ETc. Figure 4 shows the seasonal water balance for the 2011 corn crop for the 6 irrigation treatments. The 200 mm of seasonal precipitation was all stored in the root zone except for the 100% irrigation treatment which lost about 10 mm to deep percolation. The high irrigation treatments (100% and 85%) ended the season with a little more water in soil storage than at the beginning while the remaining deficit treatment extracted water from soil water storage and used it for ETc. The irrigation applications varied between 450 – 170 mm. With deep percolation and storage changes, the ET varied between 630 – 370 mm. In other years, ET of the fully-irrigated crop averaged 580 mm and of the most stressed crop, 330 mm. Irrigations were timed such that plant water stress for the deficit irrigation levels was least between tasseling and soft dough (growth stages VT to R4).

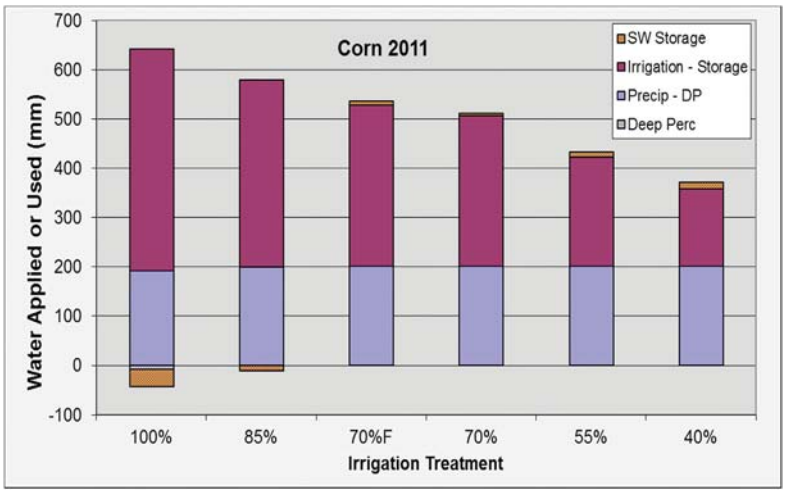

Figure 4. Water balance for the 2011 corn crop showing precipitation, irrigation, and seasonal soil water storage changes. Bars below zero represent additions to storage or deep percolation losses. Dotted areas represent irrigation or precipitation stored or percolated. Treatments represent the target percentage of full ETc

The wide range of irrigation applications resulted in substantial differences in crop growth. Figures 5 and 6 show a comparison of plant height and ground cover in early August as the corn was beginning to tassel.

Figure 5. Comparison of corn growth condition just before tasseling. Rows at the left and background are fully irrigated; rows at right are the lowest irrigation level

Figure 6. Left photo: Full irrigation with 91% ground cover. Right photo: Low irrigation with 63% ground cover

Although water balance ETc based on soil water measurement is fairly accurate over long term, such as the seasonal values shown in Figure 4, it is much more difficult to estimate ETc over the short term due to errors in soil water measurement. When a calculation is based on small differences between measurements which have can have small errors, the relative error in the difference can be large. To reduce the errors, water balance calculations should be made over several days and preferably when soil water conditions are similar such as just before irrigation.

Figure 7 shows crop coefficient curves for the 2011 fully-irrigated (100%) corn crop. The points represent individual measurements based on irrigation and precipitation amounts and changes in soil water content measured just before each irrigation. The brown line represents a smoothing of these points as an 11 day running average. Although there is some variation in the trends, the general shape of the curve is evident. The figure also shows the crop coefficient curve predicted by Allen, et al (2007) based on planting date and date of full (80%) cover (yellow line), and the crop coefficient based on the Allen et al (2007) initial and mid-season values but adjusted for the growth of the crop as represented by canopy ground cover (blue line). It is evident that the measured crop coefficients agree fairly well with the referenced values.

Figure 8 shows the measured crop coefficients for each of the irrigation treatments for the 2011 corn crop. Irrigation treatments (1 – 6) represent decreasing irrigation amounts, as listed in Figure 4. As expected, the measured crop coefficient decreases as the water deficit increases. These decreases result in the reduced crop ET shown

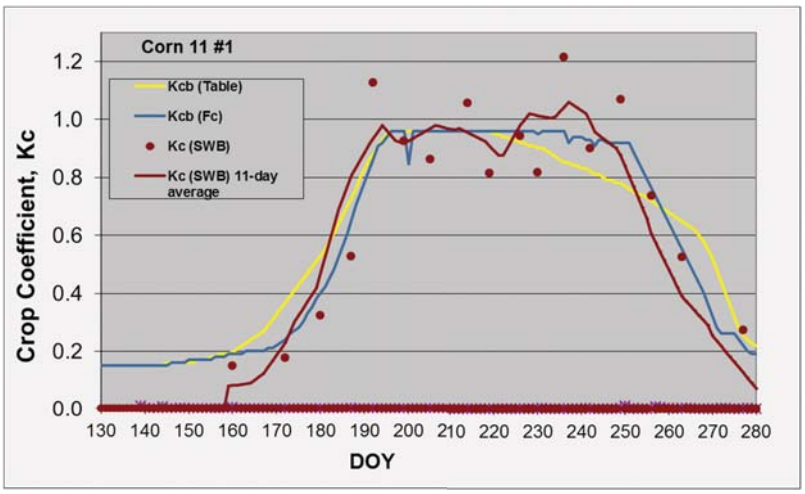

Figure 7. Crop coefficient curves (alfalfa reference) for the 2011 fully irrigated corn crop measured by water balance (brown points and line) predicted by Allen et al (2007) (yellow line) and adjusted for crop growth (blue line)

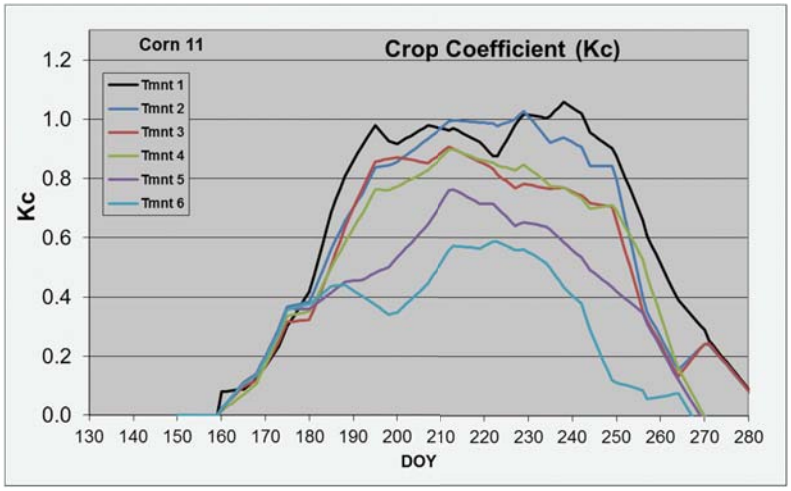

Figure 8. Measured crop coefficients (alfalfa reference) for the 6 irrigation treatments for the 2011 corn crop

in Figure 4. They are related to plant water stress that cause decreased canopy ground cover (Fig 6) and reduced stomatal conductance resulting from soil water deficits. Figure 9 shows how relative ETc (from Fig 4) and relative mid-season Kc (Fig. 8), compared to relative stress coefficient (Ks, based on soil water deficits calculated by the FAO-56 method (Allen etal 1998)) and relative measured canopy ground cover,

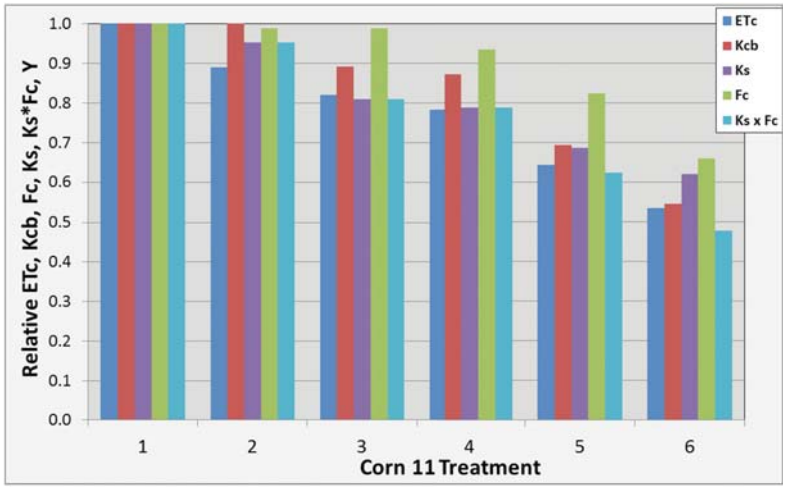

Figure 9. Relative seasonal ETc, mid-season crop coefficient, Kc, stress coefficient, Ks, canopy ground cover, Fc, and the product of Ks x Fc

Fc, and the product of these two factors. It is evident that these indicators of stress relate well to reductions in ETc and Kc.

4 CONCLUSIONS

Water balance can be used to accurately measure seasonal crop water use and to estimate crop coefficients when irrigation, precipitation, and soil water content are measured accurately, irrigation is applied uniformly, and water loss to deep percolation and runoff are small.

REFERENCES

Allen, R.G., L.S. Pereira, D.Raes, and M. Smith. 1998. Crop evapotranspiration: guidelines for computing crop water requirements. FAO Irrigation and Drainage paper # 56. FAO, Rome.

Allen, R.G., J.L Wright, W.O. Pruitt, L.S. Pereira, M.E. Jensen. 2007. Water Requirements. Ch 8 in G.J. Hoffman, R.G. Evans, M.E. Jensen, D.L. Martin, and R.L. Elliott (eds) Design and Operation of Farm Irrigation Systems (2nd Ed). ASABE, St. Joseph, MI.

Bausch, W., T.J. Trout and G. Buchleiter. 2010. Evapotranspiration estimates for deficit irrigated crops. In Proceedings of the 5th Decennial National Irrigation Symposium. Phoenix, AZ. Dec 5 – 8, 2010. ASABE, St. Joseph, MI.

3

Adoption of Irrigation Technology: Three Contrasting Cases

Luciano Mateos[1]

[1] Instituto de Agricultura Sostenible, CSIC, Córdoba, Spain

INOVAGRI Book 2014 - Irrigation and Salinity:
Researches and Technological Innovations
ISBN 978-85-67668-09-3

INOVAGRI
INSTITUTO DE PESQUISA E INOVAÇÃO NA AGRICULTURA IRRIGADA

Fortaleza - CE
2015

3 Adoption of Irrigation Technology: Three Contrasting Cases

ABSTRACT

This paper presents the processes of irrigation technology adoption using three contrasting cases. The first case will focus on center pivot site-specific variable rate irrigation, and on the adoption of this forefront technology in USA. The second case will analyze the irrigation types that have been promoted in Sub-Saharan Africa. Individual irrigation types will be presented vis-à-vis collective schemes. The success and failure of small-holder irrigation systems in Sub-Saharan Africa will be discussed. And the third case refers to the Baixo Acaraú Irrigation District, in Ceará, Brazil. Smallholder irrigation using modern technology is expected to help alleviating rural poverty in that region. An Irrigation Advisory Service operates in this district since 2010. Final remarks about irrigation technology diffusion, research, and capitalization of agricultural extension resources will close the paper.

1 INTRODUCTION

The scope of Irrigation Advisory Services is expanding from irrigation water requirement recommendations and uniformity evaluations to a more ample and integrative approach that considers the whole farming system, including collective irrigation networks, and the introduction of new technologies. Also, some modern Irrigation Advisory Services are recognizing that technology adoption in the irrigation sector occurs in an open innovation environment where multiple actors contribute to the development, adoption and adaptation of technology through interwoven processes. As irrigation technology becomes more sophisticated, the role of the irrigation industry in open innovation environments becomes more relevant.

In this transitional context, it is pertinent to reflect about current and past irrigation technology adoption processes, in order to understand failures and find avenues for sustainable irrigation that contribute to food security and rural development.

In this paper we discuss three contrasting cases of irrigation technology adoption. The first case is about the adoption of center pivot site-specific variable rate irrigation. Next, we discuss the limited expansion of irrigation in Sub Saharan Africa and the success/failure of the different irrigation types that have been introduced in that region. The third case deals with the performance of the Baixo Acarau irrigation district, where an Irrigation Advisory service operates since 2011.

2 ADOPTION OF CENTER PIVOT SITE-SPECIFIC IRRIGATION

Center pivot site-specific irrigation is one precision agriculture technology that, as other precision agriculture technologies, uses GPS, on-the-go yield monitoring, GIS, proximal or remote soil or plant sensing, wireless communication, decision support systems, etc. to vary water application to meet the specific needs of a crop in each unique zone within a field (Evans et al., 2013). The technique most widely used by site-specific irrigation practitioners to define field zones is electromagnetic induction survey of soil apparent electrical conductivity (Hedley et al., 2009; Hedley et al., 2013), although much attention is also paid to reflectance and thermal imagery based on remote sensing (O'Shaughnessy and Evett, 2010). These techniques allow obtaining maps that are used to delimitate management zones.

Site specific center pivot irrigation can be applied by varying the travel speed of the lateral, so the irrigator can control the applied water in each radial sector of the field, or by varying the application rate of each individual sprinkler (site-specific variable rate irrigation, SS-VRI), so the irrigator can apply different amounts of water to irregularly shaped management zones (Kranz et al., 2012). This is achieved by using solenoid valves, installed at the inlet of each sprinkler or set of sprinklers along the lateral, that are automatically controlled using hardware and software designed for the purpose.

Adoption of SS-VRI by producers has been slow and remains at very low levels (Evans et al., 2013). The few farmers who have adopted SS-VRI use it to site-specific non-application of water to non-cropped areas such as ponds, waterways, roads, etc. Some farmers also use their SS-VRI to treat symptoms such as over-irrigation, under-irrigation or runoff. These farmers are innovators and risk-takers.

The classic technology adoption process is well described by the diffusion theory proposed by Roger (2003) (Fig. 1). The innovators are followed by the early adopters of new technologies, progressive farmers who are often more highly educated. The subsequent early majority are more prudent in their consideration of risk and benefits while the late majority are skeptical about new technologies. Few technologies progress beyond the early adopter level, and this is the case of SS-VRI. This is attribute to the so called chasm between early adopters and early majority caused by the gap between the actual capacities of the new technology and user expectations.

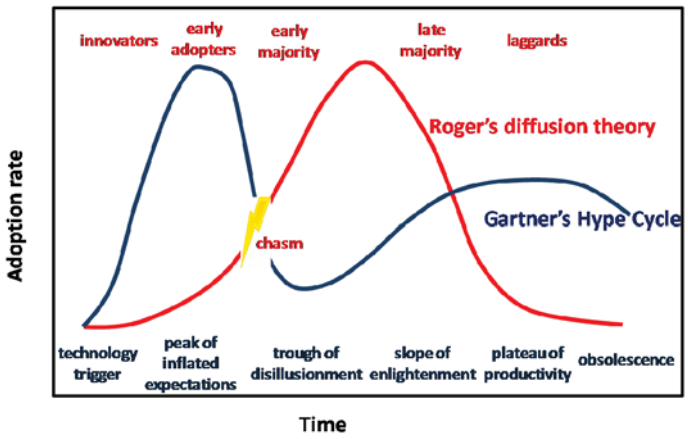

Figure 1. Representation of technology adoption processes according to Roger's (2003) diffusion theory in red line and font, and Gartner Hype-Cycle (Fenn and Raskino, 2008) in blue line and fonts

However, the adoption of much of the new technology is not fully described by Roger's diffusion theory. That may be the case for SS-VRI, which has been driven forward primarily by researchers and the industry. With the appearance of a new technology, often industry and media create unrealistic levels of expectation. More than once we have heard claims of water savings derived from the application of this or that fanciful new technology. Specifically, SS-VRI commercial services are offered showing attractive brochures with colorful maps that claim undemonstrated water savings. These hypes prompt rapid expansion of the technology followed by a decrease of its adoption and the so called trough of disillusionment (Fig. 1). Researchers and center pivot manufacturers who were involved in the earliest research on SS-VRI sometimes think that rather than a solution to a problem SS-VRI is a solution looking for a problem (Evans and King, 2012; Evans et al., 2013). According to the researchers who have analyzed the so called "Gartner Hype-Cycle" (Fenn and Raskino, 2008), the trough of disillusionment can be followed by a slope of enlightenment up to its actual plateau of productivity.

Although some hyping may be desirable, extensionists and researchers should introduce rationality in the process to narrow the chasm between early adopters and early majority or, in other words, to control hyping and avoid the trough of disillusionment. "Inappropriate application of a technology or practice can do as much harm to adoption as product failure" (Lamb et al., 2008). We are working with a group of researchers from the University of Nebraska trying to move up the slope of enlightenment by understanding the conditions under which SS-VRI is really an advantage (Lo et al., 2014). We hope to eventually bring SS-VRI up to its actual plateau of productivity. Basic concepts in this thinking follow.

Figure 2 shows the spatial variability of the water holding capacity of the soil down to the depth that the roots can reach potentially. In arid environments, the soil is naturally dry. The irrigation schedule can be based on refilling periodically the soil when the management allowable depletion is reached at the field zone with less water holding capacity. This may mean relatively high irrigation frequency, something center pivots are designed for. Therefore, little or none benefits should be expected from SS-VRI in arid environment. However, if rainfall accounts for a significant contribution to crop water consumption, SS-VRI can be used to exploit the soil water storage by applying less water where storage is greater. In the example in Fig. 2 it is assumed that the rainfall contribution is in the soil at the beginning of the irrigation season. SS-VRI in a relatively homogeneous soil (Fig. 2a) would mean greater irrigation savings compared to uniform irrigation than in a more heterogeneous soil (Fig. 2b).

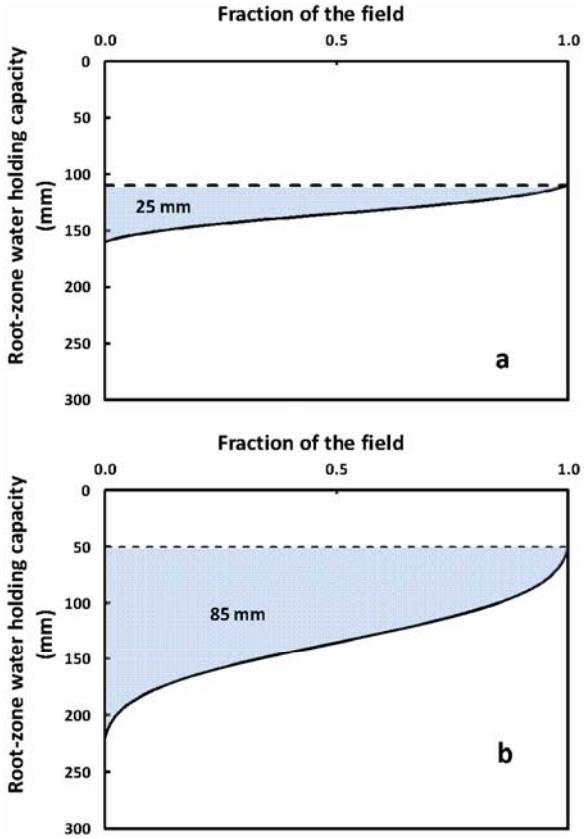

Figure 2. Variation of the root zone soil water holding capacity of two hypothetical soils: (a) uniform soil, (b) heterogeneous soil. The area between the dashed and the solid lines represents the potential for rain water use under SS-VRI irrigation

In summary, contrary to common expectations, SS-VRI should be in Mediterranean and sub-humid climates more advantageous than in arid and semiarid climates. The potential SS-VRI advantages should be exacerbated by soil variability.

3 TYPES OF IRRIGATION SYSTEMS IN SUB-SAHARAN AFRICA (SSA)

Recent studies have reported that water is abundant in many parts of SSA (MacDonald et al., 2012; Wada et al., 2012), where more than 25% of the population suffers from chronic hunger, the great majority small farmers. The challenge is therefore to extend irrigation (only 4% of the SSA cropland is currently irrigated) but doing it in such a way that does not repeat past mistakes elsewhere in the world.

Two main groups of smallholder irrigation schemes have been tested in SSA: large-scale schemes have several hundred or thousand hectares and their water supply is centrally-managed by public agencies; small-scale schemes comprise a variety of distributed irrigation types, including village community-managed schemes, women gardens, private farms owned by individuals, and others.

The development of large-scale irrigation in SSA has been relatively limited. Despite significant investment in the 1960s and 1970s, followed by attempts at improving management since the late 1980s, large-scale irrigation schemes have largely missed forecasted performance and, in the 1990s, their low performance discouraged donors and governments from further investment. Since then, development policies have advocated for small-scale distributed irrigation as most appropriate for achieving economic growth and rural development, although often with subsidized technologies (Turner, 1994; Vincent, 1994).

More recent studies either advocate for even smaller scale (private and individual) irrigation (Burney et al., 2013; de Fraiture and Giordano, 2014), usually using groundwater, or, at the other extreme, see possibilities of a rice Green Revolution in SSA driven by large-scale irrigation (Nakano et al., 2011).

Studies of large-scale rice irrigation schemes (namely Office du Niger in Mali) have showed promises of sustainability result of partnerships between the government and pro-reform stakeholders (Aw and Diemer, 2005). However, more recent studies conducted also at the Office du Niger have showed that subsequent intervention of large corporations that compete for land and water with the smallholders (the so called land and water grabbing) may threaten sustainability seriously (Hertzog et al., 2012).

On the other hand, despite general support to community-managed irrigation schemes, there are numerous examples of poor performance or failure (e.g. Comas et al., 2012; Borgia et al., 2013) as well as examples of successful unplanned individual irrigation around reservoirs that were constructed for communal use (de Fraiture et al., 2014).

The appropriateness of modern irrigation technology such as drip irrigation for smallholder farming is also controversial. While some expected drip irrigation to have significant impact on alleviating hunger and poverty (Postel et al., 2001; Woltering et al., 2011), others warn that expectations of increased performance associated with

drip will only be realized in very specific circumstances (van der Kooij et al., 2013). Failure of drip irrigation technology adoption is often the result of overlooking the local context, usually very different from that in which the technology originated, evolved, and operates successfully (Garb and Friedlander, 2014).

This quick review of the types of irrigation systems in SSA and the evolution of how they have been judged by international academia and investors points out to perception processes that, as for SS-VRI, may be described by the Hype-Cycle theory. This is showed in Fig. 3, where the trajectories are not more than personal first appreciations; they do not mean to represent actual evolutions but just to illustrate that the introduction of irrigation in SSA has been driven by top-down decisions. Apparently, the slope of enlightenment has followed tortuous paths distorted by internal and external factors that make difficult discerning whether irrigation has reached its productivity level for each type so far tested. Uncertainty remains about what are the appropriate irrigation types for each situation and what are their actual productivity levels. Recent irrigation technology adoption experiences in Northern Africa show processes driven by bottom-up forces (Benouniche et al., 2014), which one may expect that will follow more sagacious adoption trajectories; however, the irrigation industry is participating actively, therefore these processes may involve some hyping risk. Participatory action research, training and education are highly needed to effectively move up on the enlightenment slope in the adoption of non-exclusive irrigation types in SSA.

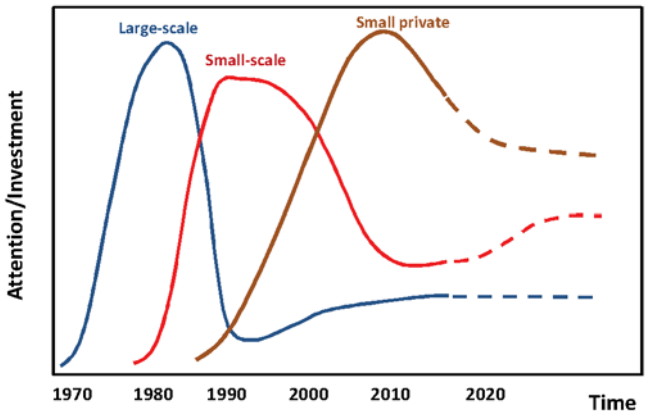

Figure 3. Representation of the adoption of irrigation types in SSA based on Gartner Hype-Cycle (Fenn and Raskino, 2008)

4 BAIXO ACARAU IRRIGATION DISTRICT

The Baixo Acarau Irrigation District is located in Ceará, Brazil. Water is supplied to the district by a pumping station at the Acaraú River; then it is distributed to farmers

through an open channel distribution system. Water is pumped again and filtered at the entrance of the farm lots to be applied with drip/trickle and micro-sprinkler systems. The district covers more than 8 thousand hectares, divided into lots of large, medium and small sizes. The typical small, family lot has 8 ha, divided into 8 irrigation subunits. The main crops are coconut and banana.

Inovagri operates an Irrigation Advisory Service at the Baixo Acarau Irrigation District since 2010 (Lima et al., 2012). The Irrigation Advisory Service provides weekly recommendations of irrigation requirements and performs evaluations of irrigation uniformity. It uses an Internet-based software and mobile-phone technology to process information and transmit it to the farmers. It also keeps a dynamic inventory.

Evaluation of field irrigation systems showed that a considerable part of the irrigation systems present good or excellent uniformity, although some systems show poor uniformity (Santos Neto et al., 2012). Recent yet unpublished research that has examined the whole farm irrigation system (based on measurements of motor-pump efficiency, pressure losses at the filtering system, main pipeline head losses, pressures at the tail end of the system, and water use) have shown that pumping efficiency is often poor (which means waste of energy), filtering is inadequate (which means energy losses, emitter clogging and low distribution uniformity), operation does not conform to design criteria or current system state (thus under-irrigation is common). Although the irrigation system was developed by the government subsidizing modern irrigation technology, most farmers have adopted the technology, which is demonstrated by the proliferation of local irrigation equipment dealers.

There are two issues in the performance of the Baixo Acaraú Irrigation District that are worth noting. One is the failure in water planning at basin scale (government responsibility) that has conducted to recurrent water shortage and is threatening the sustainability of the district. The other issue has to do with the inappropriate filtering systems that were install along the collective network and at the entrance of the farm lots, which causes great energy losses and emitters clogging. In response to this, a local artisan developed one PVC-made filter that has spread accross the district and neighbor districts, a good example of "bricolage" (Benouniche et al., 2014) that takes place in an open innovation environment.

5 CONCLUDING REMARKS

We have presented three very different cases of irrigation innovation. The three of them present immature adoption states of irrigation technologies, from the very specific SS-VRI to adoption of irrigation as agricultural practice, passing by the adaptation of modern micro-irrigation to the conditions of a smallholder irrigation district. The Hype-Cycle theory help to understand the early stages of irrigation technology adoption. The introduction of irrigation in SSA seems to be better described by multiple hype-cycles that have happened during the last 50 years as

consequence of changing public policies. The incipient adoption of SS-VRI in US seems to be a clearer adoption process. Smallholder irrigation in the Baixo Acaraú Irrigation District shows a process first entirely driven by public interventions and later evolving as an open innovation system where "bricolage" plays a relevant role. Even recognizing that adoption of irrigation technology is much more effective in open innovation environments, we advocate that research, extension, training and education should play a relevant role in that environment, contributing to rise the productivity level, controlling hyping, and closing the adoption chasm between early adopters and early majority adopters.

6 ACKNOWLEDGEMENTS

The ideas presented in this paper are result of discussions with three groups of researchers. They are: 1) for the case of SS-VRI: T. H. Lo, D. M. Heeren, J. D. Luck, D. L. Martin, and D. E. Eisenhauer, from the University of Nebraska-Lincoln; 2) for the case of SSA: C. Borgia, H. Gómez-Macpherson, J. Comas, and D. Connor; 3) for the case of the Baixo Acaraú Irrigation District: A.C.S. Almeida, J.A. Frizzone, S.C.R.V. Lima, J.A. Beltrão, and the irrigation systems evaluation team. This paper was prompted by the invitation to the II INOVAGRI International Meeting held in Fortaleza, Brazil, in 13-16 April 2014.

REFERENCES

Aw, D., Diemer, G., 2005. Making a Large Irrigation Scheme Work: A Case Study from Mali. Washington, DC. The World Bank. http://siteresources.worldbank.org/INTARD/Resources/making_a_large_scale_irrigation_system_work_DID.pdf

Benouniche, M., Zwarteveen, M., Kuper, M. 2014. Bricolage as innovation: Opening the black box of drip irrigation systems. Irrigation and Drainage, 63, 651-658.

Borgia, C., García-Bolaños, M., Li, L., Gómez-Macpherson, H., Comas, J., Connor, D., Mateos, L., 2013. Benchmarking for performance assessment of small and large irrigation schemes along the Senegal Valley in Mauritania. Agricultural Water Management 121, 19-26.

Burney, J.A., Naylor, R.L., Postel, S.L., 2013. The case for distributed irrigation as a development priority in sub-Saharan Africa. PNAS 110 (31), 12513–12517.

de Fraiture, C., G.N. Kouali, H. Sally, P. Kabre. 2014. Pirates or pioneers? Unplanned irrigation around small reservoirs in Burkina Faso. Agricultural Water Management, 131, 212-220.

de Fraiture, C., Giordano, M., 2014. Small private irrigation: A thriving but overlooked sector. Agricultural Water Management 131, 167-174.

Evans, R.G., B.A. King. 2012. Site-specific sprinkler irrigation in a water limited future. Transactions of the ASABE 55:493–504

Evans, R.G., J. LaRue, K.C. Stone, B.A. King. 2013. Adoption of site-specific variable rate sprinkler irrigation systems. Irrigation Science 31:871–887

Fenn, J., M. Raskino. 2008. Mastering the Hype Cycle: How to Choose the Right Innovation at the Right Time. Harvard Business Press.

Garb, Y., Friedlander, L., 2014. From transfer to translation: Using systemic understandings of technology to understand drip irrigation uptake. Agricultural Systems 128, 13-24.

Hedley, C.B., I. J. Yule, M. P. Tuohy, I. Vogeler. 2009. Key performance indicators for simulated variable-rate irrigation of variable soils in humid regions. Transactions of the ASABE 52: 1575-1584

Hedley, C.B., P. Roudier, I.J. Yule, J. Ekanayake, S. Bradbury. 2013. Soil water status and water table depth modelling using electromagnetic surveys for precision irrigation scheduling. Geoderma 199:22–29

Hertzog, T., J-C Poussin, B. Tangara, I. Kouriba, J-Y Jamin. 2014. A role playing game to address future water management issues in a large irrigated system: Experience from Mali. Agricultural Water Management, 137, 1-14.

Kranz, W.L., R.G. Evans, F.R. Lamm, S.A. O'Shaughnessy, R.T. Peters. 2012. A review of mechanical move sprinkler irrigation control and automation technologies. Applied Engineering in Agriculture 28:389–397

Lamb, D.W., P. Frazier, P. Adams. 2008. Improving pathways to adoption: putting the P's in precision agriculture. Computers and Electronics in Agriculture 61:4–9

Lima, S.C.R.V, Frizzone, J. A., Sousa, A. E., Beltrão J. A., Ferreira, R. P., Garcia, D. R. 2012. Aplicação da tecnologia da informação e a adoção pelo agricultor: a avaliação inicial do envio de mensagens pelo serviço de assessoramento ao irrigante. Revista Brasileira de Agricultura Irrigada, v.6, p. 314-328.

Lo, T.H., L. Mateos, D.M. Heeren, J.D. Luck. 2014. The applicability of VRI for managing variability in infiltration capacity and plant-available aater: A preliminary discussion and GIS study. CSBE/ASABE Annual International Meeting, July 13-16 2014, Montreal, Canada

MacDonald, A.M.,Bonsor,H.C.,Dochartaigh,B.E.O.,Taylor,R.G.,2012.Quantitative maps of groundwater resources in Africa. Environmental Research Letters 7.

Nakano, Y., Bamba, I., Diagne, A., Otsuka, K., Kajisa, K., 2011. The Possibility of a Rice Green Revolution in Large-scale irrigation schemes in Sub-Saharan Africa (Policy Research Working Paper No 5560). The World Bank, Washington, DC. http://www-wds.worldbank.org/external/default/WDSContentServer/WDSP/IB/2011/02/07/000158349_20110207101601/Rendered/PDF/WPS5560.pdf

O'Shaughnessy, S.A., S.R. Evett. 2010. Developing wireless sensor networks for monitoring crop canopy temperature using a moving sprinkler system as a platform. Applied Engineering in Agriculture 26:331–341

Postel, S., Polak, P., Gonzales, F., Keller, J. 2001. Drip irrigation for small farmers: a new initiative to alleviate hunger and poverty. Water International 26, 3-13.

Santos Neto, A., Braga, A., Silva, M., Lima, S.C.R.V., Frizzone, J., Gomes Filho, R. 2011. Auditoria de Desempenho de Sistemas de Irrigação II: Avaliação e Correção da Uniformidade de Emissão de Água no Distrito de Irrigação do Baixo Acaraú, CE. Revista Brasileira de Agricultura Irrigada: 5 (4):272 – 279.

Turner, B., 1994. Small-scale irrigation in developing countries. Land Use Policy 11, 251−261.

van der Kooij, S., Zwarteveen, M., Boesveld, H., & Kuper, M., 2013. The efficiency of drip irrigation unpacked. Agricultural Water Management, 123, 103-110.

Vincent, L., 1994. Lost chances and new futures. Land Use Policy 11, 309−322.

Wada, Y., van Beek, L. P. H., Bierkens, M. F. P., 2012. Non sustainable groundwater sustaining irrigation: A global assessment. Water Resources Research 48, W00L06

Woltering, L., Ibrahim, A., Pasternak, D., & Ndjeunga, J. 2011. The economics of low pressure drip irrigation and hand watering for vegetable production in the Sahel. Agricultural Water Management 99, 67-73.

4

Designing Farm Reservoirs under Climate Change Uncertainty

Keith Weatherhead[1] & Michael Green[2]

[1] Cranfield University, UK
[2] Anglia Ruskin University, Cambridge, UK

INOVAGRI Book 2014 - Irrigation and Salinity:
Researches and Technological Innovations
ISBN 978-85-67668-09-3

INOVAGRI
INSTITUTO DE PESQUISA E INOVAÇÃO NA AGRICULTURA IRRIGADA

Fortaleza - CE
2015

4 Designing Farm Reservoirs under Climate Change Uncertainty

ABSTRACT

Climate change in England is expected to simultaneously increase water demand and reduce summer water availability. Our farmers are being encouraged to build on-farm irrigation reservoirs as an adaptation to water resource shortages. However, building farm reservoirs is much more expensive than using direct abstraction from rivers or boreholes. Optimising the reservoir capacity raises issues of balancing the high costs against the uncertainty in climate change predictions.

Climate change projections are increasingly being presented in terms of probability distributions rather than median or "most-likely" values. The current UK national climate change projections, UKCP09, provide 10,000 probabilistic projections for each of three future emission scenarios (high, medium, low). This highlights some (though still not all) of the uncertainty in climate change forecasts, but complicates the adaptation planning.

This chapter describes the application of probabilistic climate change projections to the design of irrigation reservoirs at three sites in England. We compare the optimum reservoir sizes calculated using the median or "most likely" projection against the sizes calculated using all 10,000 probabilistic projections, using alternative decision making criteria.

The results show that the differences in optimum reservoir capacity between the three emission scenarios were actually very small. However, there is a substantial range in the optimum capacity across the 10,000 probabilistic projections within each emission scenario. Some extreme scenarios suggested doubling the median capacity, whilst other suggested not building a reservoir at all.

Whether and how that additional information should affect the choice of reservoir capacity depends on the risk appetite of the farmer.

Keywords: Farm reservoirs, probabilistic scenarios, uncertainty, UKCP09, adaptation planning.

1 INTRODUCTION

Although most crops in the UK can be grown with rainfall alone, irrigation is essential for the production of some high value crops, such as potatoes, soft fruit and vegetables, where continuous and reliable supplies of premium quality are demanded by the major food processors and supermarkets. Irrigation is particularly important in the drier south and east. However, this is also the region where water resources are in highest demand for public water supply, and environmental pressures are most intense. In most catchments, no more water is available, and in many the government needs to reduce the volumes already licensed for abstraction (Figure 1).

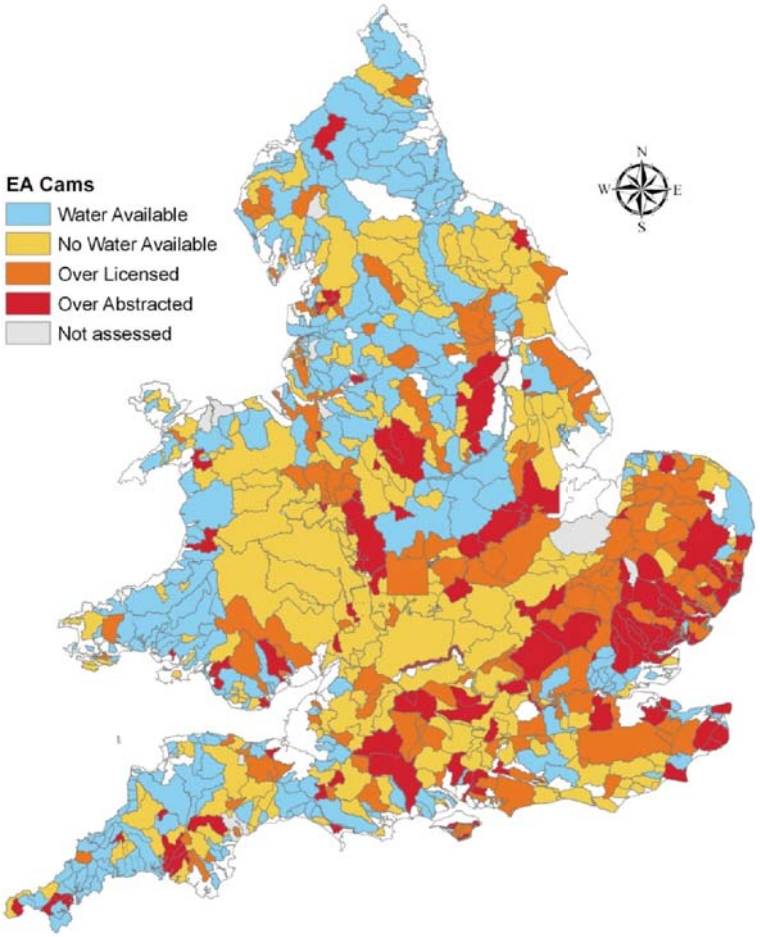

Figure 1. Summer water available for abstraction licensing in England and Wales. Source: Environment Agency

Faced with these water shortages and the declining reliability of direct abstraction from rivers and boreholes, our farmers are being encouraged to build on-farm reservoirs. Most of these reservoirs are constructed off-stream, with 360 degree embankments, avoiding the environmental, safety, regulatory and cost issues that building a dam across a river would create. They are typically designed with balanced cut and fill, whereby the soil excavated in the centre provides the material for the embankments – hence the bottom is below ground level and the top is well above ground level. The water is pumped in when available in the winter months, and then pumped out again when needed in the summer months. Capacities range from 5,000 to 250,000 m^3. Survey data suggests there could already be around 2000 reservoirs, with a total capacity around $100x10^6$ m^3; this is about 30% of the total volume licensed for irrigation.

Reservoirs are expensive to construct, with the major costs in earth moving and bank compaction. Unless constructed in suitable clay soils, the reservoirs also have to be lined to ensure they are watertight, using either some form of plastic material or imported clay. A survey of 73 recently constructed on-farm reservoirs (Patel, 2012) was used to estimate costs (Figure 2). Unexpectedly, the results did not show declining marginal costs as the scale increased. After an initial fixed cost, perhaps related to site surveys, legal fees and planning studies, further costs were linearly related to additional storage capacity. These marginal capital costs were about £0.72

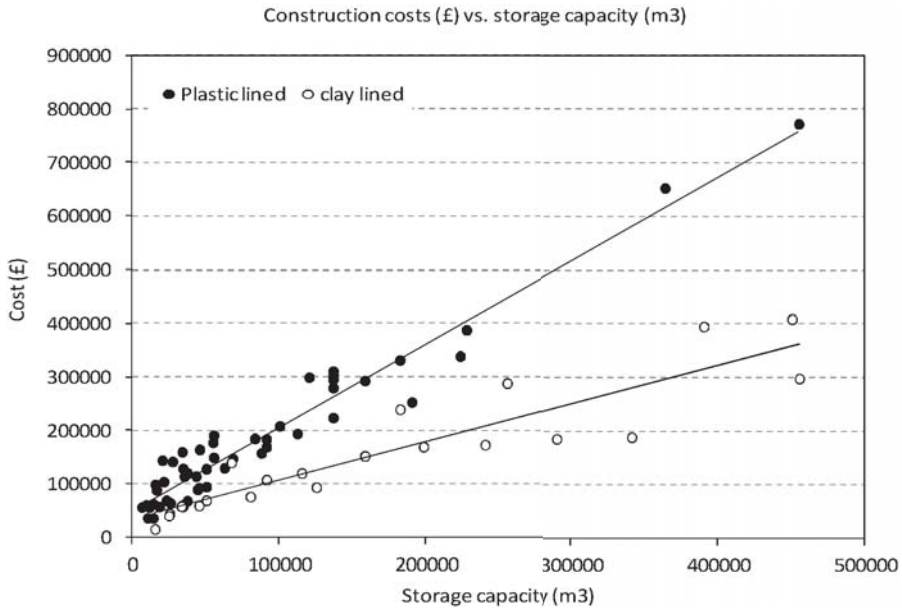

Figure 2. Reported construction costs for farm reservoirs in the UK (Patel, 2012)

(US$1.2) /m^3 capacity for unlined (clay) reservoirs, and £1.4 (US$2.4) /m^3 for plastic lined reservoirs.

Optimising the capacity of the reservoir to the area and crop to be irrigated is important. Too small a reservoir would run out of water in a dry year; too large a reservoir would be too expensive to provide a positive financial return. Modelling is therefore used to calculate the required irrigation need. Traditionally the irrigation needs of each crop have been modelled using the last 20 years of weather data. The needs are then ranked from low to high (i.e. wet summers to dry summers) and the design capacity selected, typically using the 16th driest year in the 20 (e.g. Figure 3).

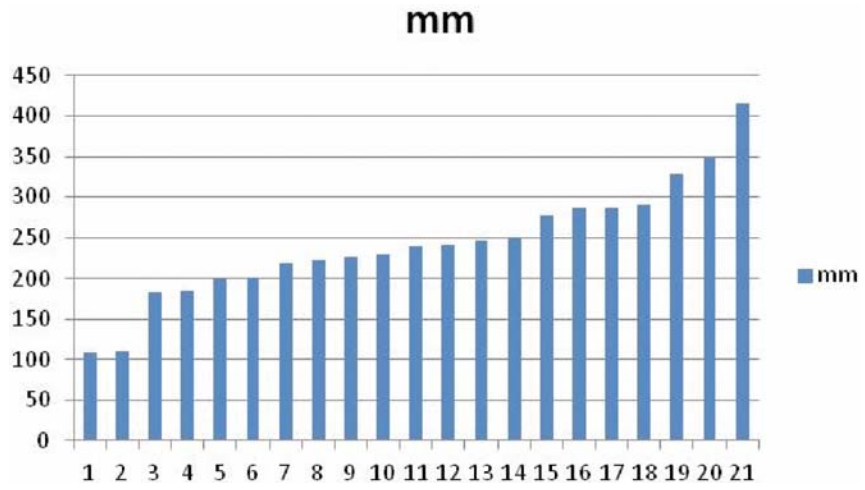

Figure 3. Ranked modelled irrigation needs (mm per year) for potatoes grown near Cambridge, England

2 RESEARCH QUESTION

Climate change is now complicating this process. For England, the climate change forecasts are mostly for warmer wetter winters and warmer drier summers. This would both increase the water required for irrigation (e.g. Daccache et al., 2011) and reduce the summer flow in many rivers, clearly worsening the water shortages But there remains a lot of uncertainty in these forecasts.

Most climate change forecasts still provide only a central scenario, perhaps for a few different emissions scenarios. However, the latest climate change projections for the UK are presented in a probabilistic format. For any given site, year and emission scenario, the previous UKCP02 dataset gave one single mean projection. Now UKCP09 provides 10,000 probabilistic projections (PP) and also 11 spatially coherent projections (11SCP), plus a calibrated weather generator. The SCPs are recommended for use in studies covering an area rather than a point, for example catchment studies.

This extra data should theoretically be highly valuable in calculating the optimum reservoir size, but it certainly complicates the process and is often not used.

The research question we addressed (Green and Weatherhead, 2015) therefore was: how should knowledge of this uncertainty affect the design of irrigation reservoirs?

3 METHODOLOGY

We modelled the present and future irrigation need at three sites, two sites in the East and one site in the North West of England. Brooms Barn is located in the county of Suffolk, near Bury St Edmunds, approximately 30 km east of Cambridge. Woburn is situated in the county of Bedfordshire, 50 km north-west of London. It is marginally wetter than Brooms Barn and has slightly lower annual evapotranspiration. Slaidburn is further north in an area of lower irrigation need. Observed daily weather data was extracted for the 30 year baseline period from the weather station record for each site.

For future scenarios, this baseline data was perturbed with the UKCP09 monthly change factors for that site, to give 30 year daily weather data for each site; this produced 10,000 scenarios from the probabilistic projections for each site for each emission scenario, as well as for the 11 SCPs.

The computer model WaSim used to calculate irrigation need for the baseline and each scenario. WaSim is a one-dimensional daily, soil water balance capable of simulating soil water storage, infiltration and evapotranspiration and drainage of water in response to climate, irrigation and seepage where relevant (Hess and Counsell, 2000). WaSim has proven invaluable across a range of previous studies including determining irrigation requirements, optimising water management, assessing the performance of sub-surface drainage systems and studying the effects of climate change on water resources.

Typical costs and benefits for clay agricultural reservoirs were obtained from a concurrent study (Patel, 2012). The economic benefit of the water contained within each reservoir was calculated on the basis of average water use, assuming an average net benefit (for potatoes) of £1.56.m^{-3} of water used (Morris et al., 1997).

The observed baseline and each of the 10,000 sequences was then used to calculate the net present value (NPV) of a range of reservoir sizes, with usable storage capacities equivalent to 0 to 1,000mm over the area irrigated (i.e. 0 to 10,000 $m^3.ha^{-1}$). The reservoir capacities that would be designed were selected by applying different non-probabilistic decision making criteria (Laplace; Maximin; Maximax; Minimax regret; Hurwicz's criterion) to each of the 10,000 projections and the 11SCP, plus various sub-samples of the complete probabilistic dataset obtained using different sampling techniques, for each site and emission scenario. The differences in irrigation reservoir capacities were then assessed.

4 RESULTS

Irrigation Water Requirements

The calculated irrigation requirements showed an increase in the average depth needed, as expected, but with a significant scatter across the 10,000 projections (e.g. Figure 4) for both emission scenarios.

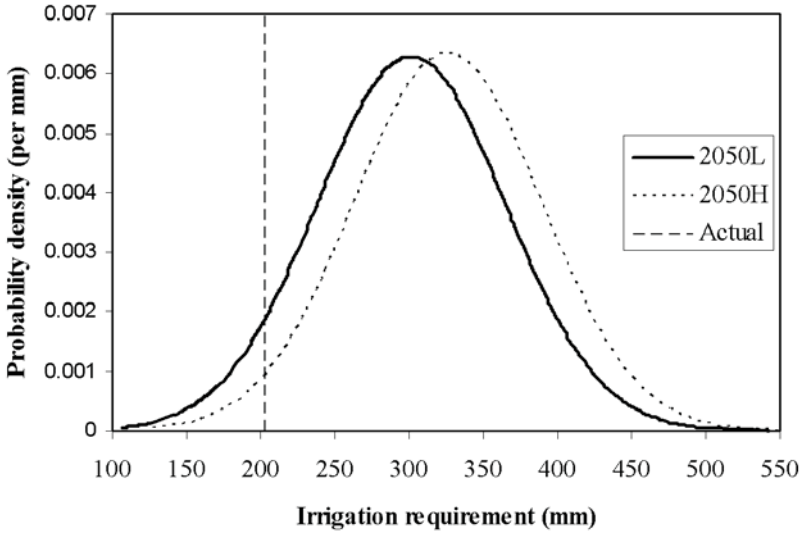

Figure 4. Example of effect of climate change and emission scenario on optimum reservoir capacity for potatoes grown near Cambridge, England

Irrigation requirements for the high emission scenario were typically around 10% higher than for the low emission scenario. Once converted into optimum reservoir capacities however, using the Laplace decision criteria (which averages the Net Present Value across all the projections), the differences between the emission scenarios are not so evident. The optimum capacity for the high scenario was only a few % larger than for the low scenario at both sites in the East, and all three emission scenarios suggesting not building a reservoir at Slaidburn (Table 1).

Table 1. Optimum reservoir capacities (as mm on the irrigated area) calculated using Laplace across all of the 10,000 probabilistic projections (PP) and the 11 spatially coherent projections (11SCP), for Brooms Barn, Slaidburn and Woburn, for the 2050s low, medium and high emission scenario

Case study	Site emission	Brooms barn			Slaidburn			Woburn		
		L	M	H	L	M	H	L	M	H
Optimum capacity	PP	390	410	400	0	0	0	360	380	390
	11SCP	350	350	360	0	0	0	280	280	290

Range of PP and 11 SCP Projections

The ranges in the optimum reservoir capacities obtained from the full datasets were compared with those using just the 11 spatially coherent projections. The comparison showed that while the 11 SCPs did show some variation between the 11 projections, there were much bigger ranges within the 10,000 probabilistic datasets, and slightly larger median capacities (e.g. Figure 5). Using the 11 SCPs would therefore give a misleading impression.

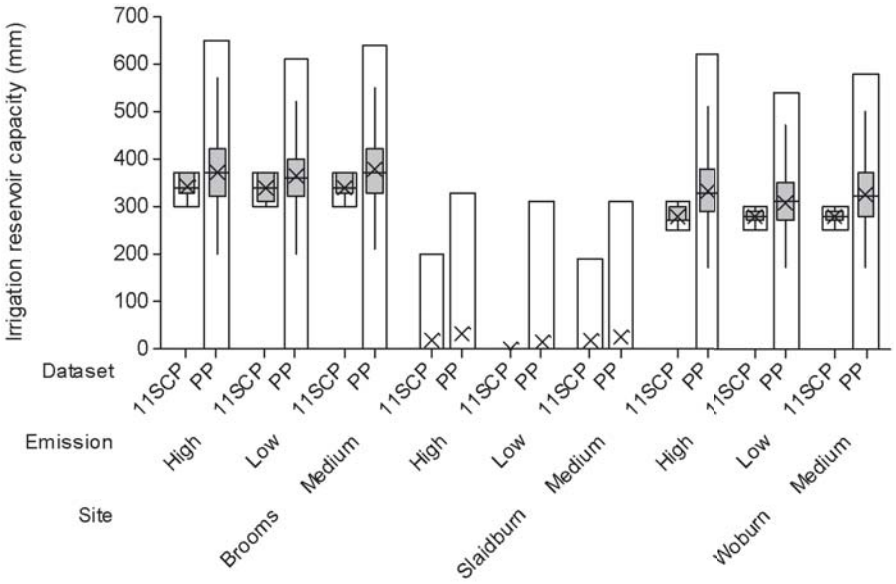

Figure 5. Comparison of range in optimum irrigation reservoir (mm) capacities for Brooms Barns, using each of the 10,000 probabilistic projections and each of the 11SCP projections individually. {Plots show minimum, Q1 (25th percentile), median, mean (X), Q3 (75th percentile) and maximum optimum irrigation reservoir capacity for each dataset. Upper error bar calculated using Q3 + 1.5 (Q3-Q1), lower error bar calculated ysing Q1 – 1.5 (Q3-Q1)}

Effect of Decision Criteria

The choice of decision making criterion has a major impact on the decision outcome, as might be expected. What was noticeable was how this interacted with the size of the dataset. The decision outcomes resulting from an individual who considers themselves risk neutral (i.e. someone who would typically use Laplace, based on mean net present value) would not be substantially different regardless of whether the "most likely" projection was used instead of the complete dataset. In contrast, the differences when using the other decision criteria were much larger and far more variable. When used with the complete probabilistic dataset certain decision criteria

such as Maximax and Maximin resulted in very extreme and sometimes contrasting decision outcomes such as taking no action or building very large reservoirs. With increasingly large datasets, methods based on extreme values will choose increasingly extreme and unlikely outcomes.

Effect of Sub-Sampling

A sub-sample size of 30 was used here to reflect practical applications. The results of multiple sub- samples were compared to each other and the results using the full datasets.

The Laplace results were reproduced well from the sub-sampling. However, sub-sampling again highlighted the shortcomings of some of the other decision methods: the reservoir capacities using Maximin, Maximax and Hurwicz's criterion were poorly reproduced.

Simple random sampling, optimum LHS and Maximin LHS performed comparably. It has been suggested previously that LHS is an appropriate sampling approach for use with the probabilistic dataset; however, it did not noticeably improve the "reproducibility" of the design reservoir capacities from the sub-samples. All three sampling approaches yielded similar decision outcomes to each other, regardless of the decision criteria and site used.

5 CONCLUSIONS

Four of the main conclusions are highlighted here:

Using probabilistic projections highlights (some of) the potential range (uncertainty) in future climates, and alerts users to potentially unexpected outcomes. However, many uncertainties are still not included. In situations where uncertainty can even reverse the recommendation, it may be better to aim for flexibility rather than to optimise.

The difference between emission scenarios in the decision outcome is small relative to the uncertainty from the modelling. Using different emission scenarios to illustrate the possible future range could give a very misleading indication of the uncertainty present.

The choice of decision making criteria is an important consideration - Laplace and the median projection gave similar reservoir capacities, but some decision criteria gave extreme results when used with the probabilistic projections.

Finally, all sampling methods risk missing extreme vales; random sampling was unexpectedly a good as the more complicated Latin Hypercube Sampling

6 ACKNOWLEDGEMENTS

The authors would like to thank the UK's Engineering and Physical Sciences Research Council (EPSRC) and HR Wallingford for funding this research.

REFERENCES

Daccache, A., Knox, J.W., Weatherhead, E.K., and Stalham, M.A. (2011). Impacts of climate change on irrigated potato production in a humid climate. Agricultural and Forest Meteorology 151(12) 1641-1653. doi:10.1016/j.agrformet.2011.06.018

Green, M. and Weatherhead, E.K. (2015). The application of probabilistic climate change projections: A comparison of methods of handling uncertainty applied to UK irrigation reservoir design. Journal of Water and Climate Change, doi:10.2166/wcc.2014.125

Morris, J, Weatherhead, E K, Mills, J, Dunderdale, J A L, Hess, T, Gowing, D J G, Sanders, C, Knox, J W (1997) Spray irrigation cost benefit study. Final report to Environment Agency. Cranfield University, Bedford.

Patel, A. (2012). The costs of on-farm reservoirs and infrastructure. Unpublished MSc Thesis. School of Applied Sciences, Cranfield University, Bedford.

5

Performance and Efficiency: Interaction between Large Scale Distribution System and On-Farm Sprinkler Irrigation

Nicola Lamaddalena[1], Andrè Daccache[1] & Roula Khadra[1]

[1] Land and Water Resources Management Department, CIHEAM, Bari Institute, Italy

INOVAGRI Book 2014 - Irrigation and Salinity:
Researches and Technological Innovations
ISBN 978-85-67668-09-3

INOVAGRI
INSTITUTO DE PESQUISA E INOVAÇÃO NA AGRICULTURA IRRIGADA

Fortaleza - CE
2015

5 Performance and Efficiency: Interaction between Large Scale Distribution System and On-Farm Sprinkler Irrigation

ABSTRACT

In on-demand water distribution systems, hydrant pressure is subjected to large fluctuations depending on the number of hydrants simultaneously opened. The impact of hydrant pressure variation on the performance of on-farm sprinkler network was assessed in this study. The pressure values at the hydrants were calculated by a stochastic simulation model using a random procedure to generate a large number of different operating scenarios.

An iterative model was developed for generating the characteristic curve of the on-farm sprinkler irrigation network. The pressure and discharge variation downstream the hydrant were computed by intersecting the characteristic curves of the hydrant and that of the on-farm sprinkler network.

An application of such a methodology was carried out on an existing irrigation system operating in Southern Italy.

This study highlighted that the performance of the on-farm sprinkler network is greatly affected by the variation of the pressure head at the hydrant and by its technical characteristics.

1 INTRODUCTION

During the last decades pressurized distribution systems have been developed with considerable advantages over open canals as they guarantee better services to the user and higher distribution efficiency. On-demand delivery offers great flexibility to farmers to manage their irrigation in the best way according to their needs. Water flowing in these systems vary considerably depending on the number of hydrants simultaneously opened hence on the cropping pattern, meteorological conditions and farmers' behaviour. The number of hydrants opened will inevitably affect the hydrants pressure serving the on-farm sprinkler networks (Lamaddalena & Sagardoy, 2000).

During peak demand periods, hydrant pressure head may drop to unacceptable values, causing a decline in the uniformity and in the amount of water applied to the field by the sprinkler network (Tizaoui *et al.*, 1997; Lamaddalena et al., 2007).

Due to the lack of application uniformity, parts of the field will be over-irrigated and others under-irrigated. Over irrigation may result in poor soil aeration, nutrient leaching and water losses. Under-irrigated areas instead will be subjected to water stress with negative consequences on yield and quality (Francisco, 1998). Under low irrigation uniformity conditions, if the farmer decides to apply enough water to adequately dampen the dry spots, he will be placing too much water on the wet spots. On the other side, if he decided to manage the wet spots appropriately he will be exacerbating the water stress on the dry spots. Both of these two scenarios make healthy plants and efficient water use a difficult proposition (Wilson and Zoldoske, 1997). Therefore, any yield analysis at field level should take into consideration the combined effects of irrigation efficiency and distribution uniformity (Sepaskhah & Ghahraman, 2004).

The purpose of this study is to analyse the effect of pressure head variation at a given hydrant on the performance of an on-farm sprinkler network. The characteristic curve of the hydrant and the water distribution pattern of a typical sprinkler were studied in a hydraulic laboratory, while the characteristic curve of the on-farm network was generated using an iterative model developed by Daccache et al. (2010).

Hydrant pressure variation under different operating conditions was assessed using a stochastic simulation model (Lamaddalena & Sagardoy, 2000). The performance of the on-farm network performance is then evaluated using the classical uniformity indicators: Uniformity Coefficient (CU), Distribution Uniformity (DU) and Distribution Efficiency (DE).

2 THE PROPOSED APPROACH

Performance Analysis of On-Demand Distribution Systems

Distribution system analysis is used to determine the adequacy of the existing irrigation systems, to identify the causes of their deficiencies and to develop the most cost-effective improvements (Lee & al., 1989). AKLA model (Lamaddalena & Sagardoy, 2000) allows the performance analysis of an on-demand pressurized irrigation system by computing the pressure head at each hydrant of the system under different operating conditions. This pressure head is compared with the minimum pressure required for appropriate on-farm network operation, so a measure of hydraulic performance for each hydrant is obtained through the computation of a performance indicator called relative pressure deficit (Eqn (2)). The model is applicable under the hypothesis that the hydrants may deliver a constant discharge for a wide range of operating pressure heads. This hypothesis is acceptable when the system's hydrants are fitted with a proper flow regulator (Lamaddalena, 1997; Lamaddalena & Sagardoy, 2000).

The model is based on multiple generations of a pre-fixed number of hydrants simultaneously operating (referred to as configuration) using a random number generator having a uniform distribution function. Within each generated configuration *r*, a hydrant j is considered to be satisfied when the following relationship is verified:

$$H_{j,r} \geq H_{min} \quad (1)$$

where:

$H_{j,r}$ is the head in m of the hydrant j, within the configuration *r*;

H_{min} is the minimum required head in m for the appropriate operation of the on-farm network.

The relative pressure deficit, $\Delta H_{j,r,}$ at each hydrant *j* within each configuration *r*, is defined as:

$$\Delta H_{j,r} = \frac{H_{j,r} - H_{min}}{H_{min}} \quad (2)$$

Head losses are computed using the Darcy-Weisbach equation.

$\Delta H_{j,r}$ may be represented on a Cartesian plane (Fig. 4); in this way, the hydrants more subject to insufficient pressure head are clearly identified and classified according to table 1 (Lamaddalena & Khadra; 2001).

Table 1. Hydrant performance classified based on Relative Pressure Deficit indicator

	Good	Fair	Poor
Relative pressure deficit	≥ 0	-0.1 – 0	< -0.1

Flow Regulator

The presence of a flow regulator in a hydrant solves the problem of flow variations caused by pressure head fluctuations. At high pressures, such device reduces the outlet cross-section, thus increasing the head loss; consequently the discharge is maintained almost equal to the hydrant nominal discharge. Such head losses are less significant for discharges lower than the hydrant nominal discharge, Qn, as shown in Fig. 1.a obtained through laboratory test.

Head losses into the flow regulator cause a reduction in pressure head downstream the hydrant. In Figure 1.b, an example of such reduction is shown for a given hydrant, j, having an upstream pressure head H_j.

Performance Analysis of the On-Farm Sprinkler Network

Irrigation uniformity and distribution efficiency were used to identify the performance of the on-farm sprinkler irrigation network at each operating condition.

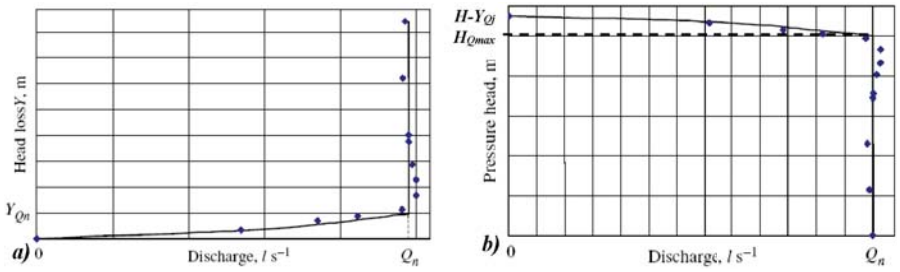

Figure 1. a) Head losses induced by the hydrant flow regulator b) Hydrant characteristic curve

The two main indicators used to assess the water application uniformity are (Heermann et al., 1990):

(i) The Distribution Uniformity (DU), which indicates the uniformity of application throughout the field:

$$DU = 100\frac{Z_{lq}}{Z_{av}} \tag{3}$$

where:

Z_{lq} average of the lowest one-quarter of the measured values, $cm^3\ cm^{-2}$

Z_{av} average applied depth in the entire field, $cm^3\ cm^{-2}$

(ii) The Coefficient of Uniformity (CU), developed by Christiansen (1942):

$$CU = 100\left(1 - \frac{\sum|Z - m|}{\sum Z}\right) \tag{4}$$

where:

Z - individual depth of catch observations from uniformity test, $cm^3\ cm^{-2}$

$|Z-m|$ - absolute deviation of the individual observations from the mean, $cm^3\ cm^{-2}$

m - mean depth of observations, $cm^3\ cm^{-2}$

The water distribution efficiency (DE) is used to strengthen the concept of CU (Keller and Bleisner, 2000). It is expressed as:

$$DEpa = \frac{\text{Minimum net depth received by wet test } \{Pa\} \text{ of area}}{\text{Average net depth received over entire area}} \times 100 \tag{5}$$

where:

DE_{pa} - distribution efficiency for the desired percentage adequacy, %
Pa - percentage of adequately irrigated area, %

3 MATERIALS AND METHODS

Site Description

In order to better clarify the interaction between the operating parameters of both the distribution system and the on-farm networks, the proposed approach was applied on an existing Italian pressurized distribution system equipped with hydrants serving an on-farm sprinkler network.

The selected distribution system is district 4 of the *'Sinistra Ofanto'* irrigation scheme *(Fig.2)*, managed by the *Consorzio of Capitanata* (Altieri, 1995) covering a topographic area of 3256 ha in the province of Foggia (Southern Italy). District 4 is supplied by a daily storage and compensation reservoir with a capacity of 28 000 m^3, where the maximum and minimum water levels are 143 m a.s.l. and 139 m a.s.l., respectively.

The district 4 network starts from the reservoir with a steel pipe of 1200 mm in diameter. It crosses the whole district and serves 32 sectors. The recorded upstream peak discharge and piezometric elevation of the system are 1200 l s^{-1} and 140 m a.s.l., respectively. Pressure head at the hydrants was identified by AKLA (lamaddalena and Sagardoy, 2000) model with respect to a minimum pressure head, H_{min} = 35 m (Fig.3).

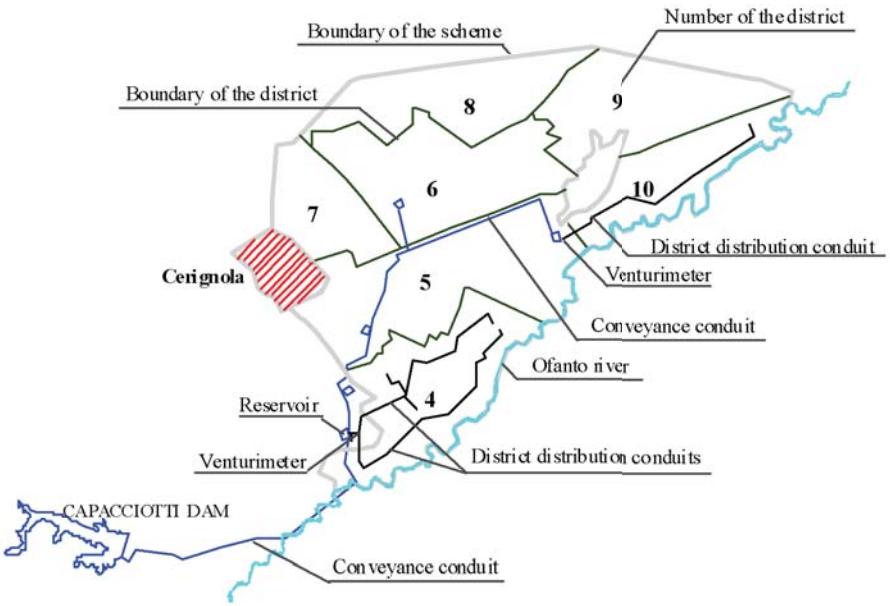

Figure 2. The Sinistra Ofanto irrigation scheme

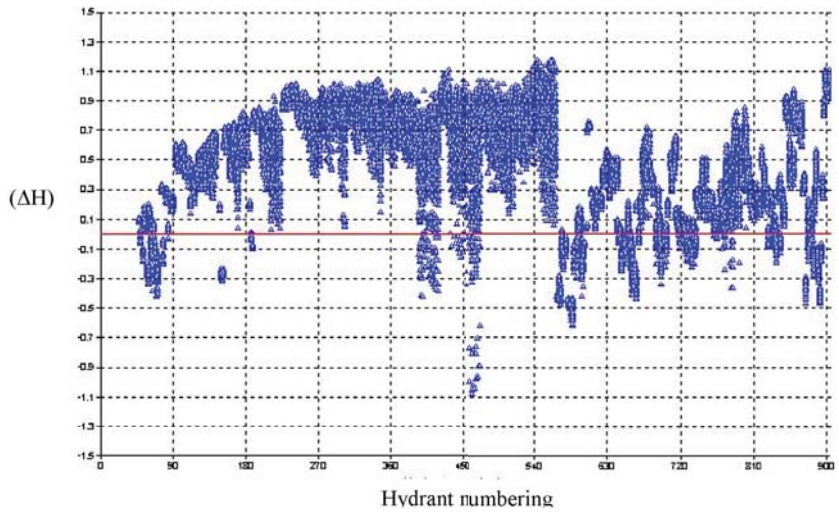

Figure 3. Analysis of the District 4 system using AKLA model

The hydrant used in this study has a nominal discharge of 15 l s^{-1} and serves a sprinkler (double nozzle Agros 40) network designed on a flat field. The on-farm sprinkler network consists of a main line with six laterals carrying seven sprinklers each, with a 18 m x 18 m sprinkler spacing (*Fig 4*). Pipes are made of PVC with diameters of 108.7 mm for the manifold and 44.6 mm for the laterals.

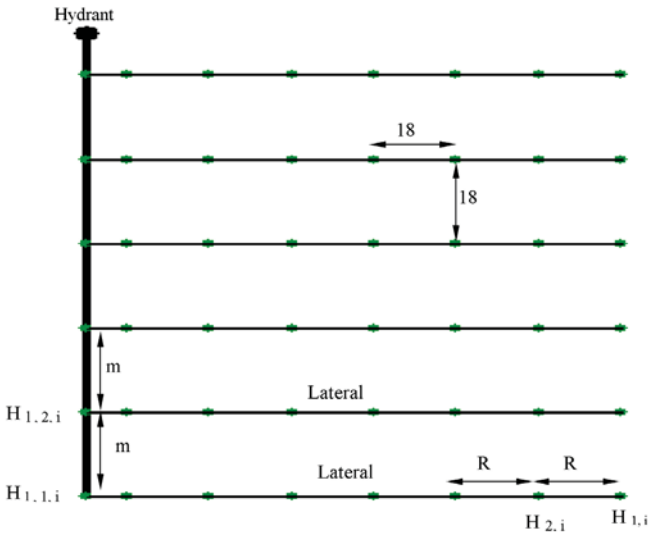

Figure 4. Layout of the on-farm sprinkler irrigation network supplied by hydrant n. 462 (i represents the number of iterations from 0 to N)

Sprinkler characteristic equations relating pressures, discharges and wetted radius are:

$$q = K_1 \times H^{0.5} \tag{6}$$

$$R = K_2 \times H^{\beta} \tag{7}$$

where:

q - discharge, $m^3 h^{-1}$

H - working pressure head, m

R - wetted radius, m

Parameters K_1, K_2 and β primarily depend on the nozzle diameter but they also vary with sprinkler design and manufacturing.

Agros 40 sprinkler used in this study was analysed indoor in the hydraulic laboratory of Castilla la Mancha (Spain) and the following values were obtained:

$$K_1 = 0.29$$

$$K_2 = 8.5$$

$$\beta = 0.136$$

On-Farm Network Characteristic Curve

Starting from a given arbitrary low pressure head at the most downstream sprinkler ($H_{1,1}$) of the lateral, the head losses in the pipes network are calculated upward till reaching the upstream end of the lateral. Consequently, the obtained pair of pressure-discharge constitutes the first point of the lateral characteristic curve.

The same procedure is repeated but with a pressure head at the downstream sprinkler of the lateral slightly increased respect to the one used in the previous iteration and consequently another point (pair of pressure-discharge) on the lateral curve will be obtained. The iterations will continue with a gradual increase of the downstream pressure head until enough points to fit the lateral characteristic curve are obtained.

The pressure head of sprinkler *K* at iteration *i* is obtained using the following equation:

$$H_{k,i} = \left[\sum_{ii=1}^{K-1} \left(H_{ii,i} + Y_{ii,i} + hL_{ii,i} \right) \right] + \left(Z_1 - Z_K \right) \quad \text{with} \quad K \neq 1 \tag{8}$$

where:

$H_{k,i}$ - Pressure head corresponding to emitter *k* and iteration *i* ,*m*

Z_K - Elevation head at the dripper *k* , *m a.s.l.*

ii - index of the pipe located upstream the emitter *K*

$Y_{ii,i}$ - Head losses (Darcy-Weisbach) within the pipe *ii* of the iteration *i* , *m*

$hL_{ii,i}$ - Local loss within the pipe *ii* of the iteration *i*, *m*

$$hL_{ii,i} = K_{Loss\ ii,i} \frac{V_{ii,i}^2}{2g} \tag{9}$$

where

$K_{Loss\ ii,i}$ - Local loss coefficient depend on the nature of local resistance within the pipe *ii*

$V_{ii,i}$ - downstream mean velocity within the pipe *ii* of the iteration *i*, $m.s^{-1}$

g - gravity acceleration, $m.s^{-2}$

$$Y_{ii,i} = f \frac{L_{ii}}{D_{ii}} \frac{\left(\sum_{jj=1}^{K} Q_{jj,i}\right)}{2gA_{ii}^2} \tag{10}$$

where:

L_{ii} - Length of pipe *ii* corresponding to the upstream reach of dripper *ii* , *m*

D_{ii} - Diameter of pipe *ii* , *m*

A_{ii} - Cross sectional area of pipe *ii* , m^2

$Q_{jj,i}$ - Flow Discharge of emitter *jj*, at iteration *i* , $m^3.h^{-1}$

f - Friction factor depends on Reynolds number *(Re)* and on the relative roughness of the pipe

The general equation of the lateral characteristic curve has the following form:

$$QL = K_L HL^{X_L} \tag{11}$$

where:

QL - Discharge at the upstream end of the lateral, m^3h^{-1}

HL - Pressure head at the upstream end of the lateral, *m*

K_L and X_L - parameters depending on the lateral hydraulic characteristics and on the plot topography.

Once the characteristic curve of all the lateral of the network are generated, the head losses calculation from the downstream end of the manifold, with a low pressure head at the most downstream lateral, upward till reaching the hydrant will reveal the first point (pair of pressure-discharge) of the network curve. A new iteration with a slight pressure increment at the downstream lateral will add another point on the network

curve. The iteration will continue until enough points to plot the characteristic curve of the network are obtained. Finally, the equation that fit the network characteristic curve is as following:

$$Qm = K_m Hm^{X_m} \quad (12)$$

where:

Qm - Discharge at the upstream end of the network, $m^3.h^{-1}$

Hm - Pressure head at the upstream end of the network, *m*

K_m and X_m - parameters depending on the network hydraulic characteristic and on the field topography

4 RESULTS AND DISCUSSION

The range of pressure variation at hydrant level varies in time but also depends on the hydrant location. With AKLA, hydrant analysis is expressed in probability of occurrence (Lamaddalena, 1997), defined as the probability that a certain value of the hydrant pressure head (or higher values) may be obtained during the operation of the system. As an example, the analysis of the district 4 distribution network, with a peak discharge of 1200 l s^{-1} and minimum required pressure head (H_{min}) for appropriate operation of the on-farm sprinkler network is 35 m is presented in Fig. 2. Hydrants with negative values of the relative pressure deficit (Eqn (2)) are considered to be unsatisfied as the hydrant pressure for this particular configuration result a pressure head lower than H_{min}.

Figure 4 shows that district 4 hydrants have a wide range of pressure variation ($-0.3 < \Delta H < +0.6$) with probability occurrence of 90% and 10%, respectively.

Hydrant number 462 supplying the sprinkler network under study shows a relative pressure deficit of -0.25, 0.11 and 0.54 for a probability of occurrence of 90%, 60% and 10% respectively. These values of relative pressure deficit, according to Eqn (2), correspond to a hydrant pressure head equal to H_{462} = 26 m, H_{462} = 39 m, H_{462} = 54 m, respectively.

These pressure head values are obtained from 1000 random generations of hydrants simultaneously opened (configuration) that simulate a wide number of possible operating conditions of the system (Lamaddalena & Sagardoy, 2000).

The intersection point between the sprinkler network and the hydrant characteristic curves (at different probabilities of occurrence) provides the actual pressure and discharge available at the upstream end of the on-farm network.

For an upstream hydrant pressure head of 26m (90% probability of occurrence), the actual pressure head at the upstream end of the on-farm sprinkler network is 21

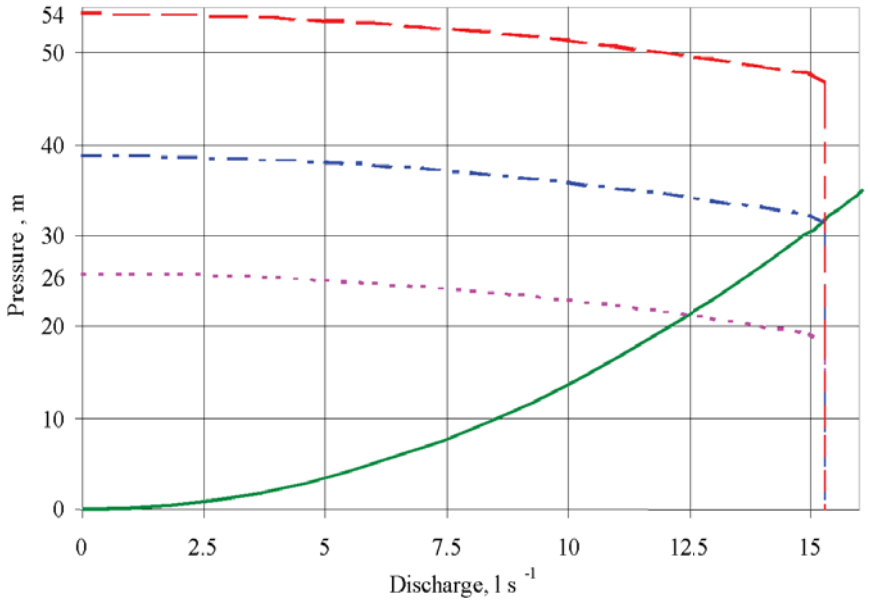

Figure 5. Interaction between on-farm network and hydrant characteristic curves at various probability of occurrence (Example of hydrant 462): red - 10% probability of occurrence; blue - 60% probability of occurrence; pink - 90% probability of occurrence; green - network characteristic curve

m, and the actual discharge is 12.5 l s^{-1} (Fig.6). For an upstream hydrant pressure head higher than 39 m (60% probability of occurrence), the actual pressure head and discharge at the upstream end of the on-farm sprinkler network are 31 and 15.3 l s^{-1}, respectively.

This example highlights that, even with high pressure head available at the hydrant, the actual pressure available at the on-farm network depends on its characteristic curve. In fact, hydrant pressure heads higher than 39 m have no effect on the actual pressure head available for the on-farm network but they only produce great localised head losses inside the flow regulator.

In case of hydrant pressure head lower than 39 m, the available pressure head at the on-farm network is reduced, together with the on-farm network discharge.

Once the pressure and the discharge at the upstream end of the on-farm network are obtained, by calculating the head losses down to the on-farm network, it is possible to obtain the pressure head and consequently the discharge at each sprinkler in the network.

The on-farm network performance is expressed through irrigation uniformity and distribution efficiency, as reported in section 2.4. Such performance indicators depend on the sprinkler characteristics and their operating pressure. The wetted patterns at

various pressure heads (15, 25, 35, 45 and 55 m) and the corresponding radius were measured for a sprinkler type Agros 40 (Lamaddalena et al. 2007).

Furthermore, a linear model was formulated to assess - on the basis of the wetted patterns measured indoor - the wetted pattern of each sprinkler in the network depending on its actual operating pressure. Then, the above said performance indicators were computed by using the Eqns (5, 6, 7).

The wetted pattern overlapping was obtained by taking into account the distance between sprinklers, and consequently the amount of water applied to the field was assessed and imported in GIS to facilitate the visual analysis.

The main advantage of this approach is that it provides a tool whereby a designer can assess the over and under-irrigated areas of the field for different operating conditions of the distribution system and thereby gain an insight as to how the design could be improved.

The graphical analysis in *Fig. 7a* and *Fig. 7b* shows the water applied to the field when the hydrant pressure head is 26 m and at a pressure equal or higher than 39 m, respectively.

The analysis shows that the on-farm Distribution Efficiency varies from 80%, for pressure head at hydrant greater than 39 m (60 % probability of occurrence and lower), to 62% for of an upstream hydrant pressure head equal to 26 m (90 % probability of occurrence).

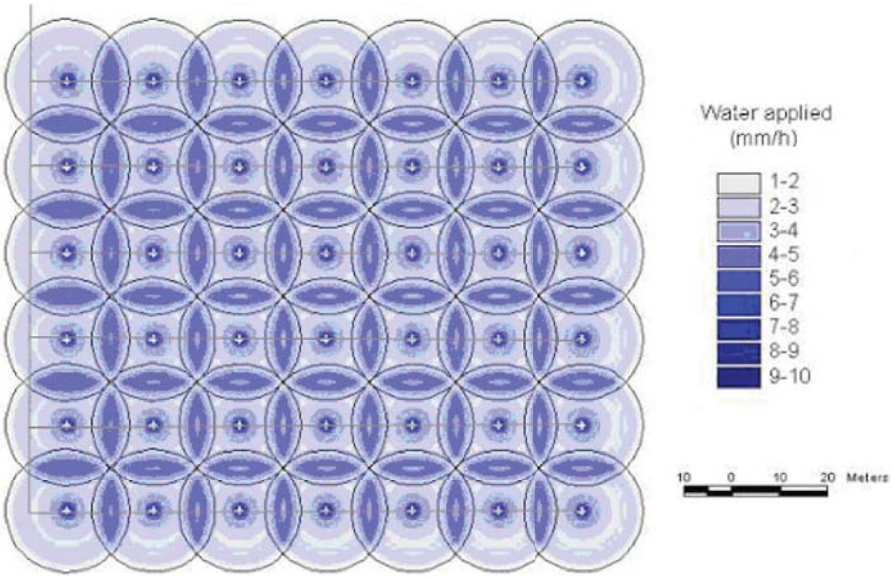

Figure 7a. Graphical analysis of the on-farm network working at a hydrant pressure head of 26 m (90% probability of occurrence)

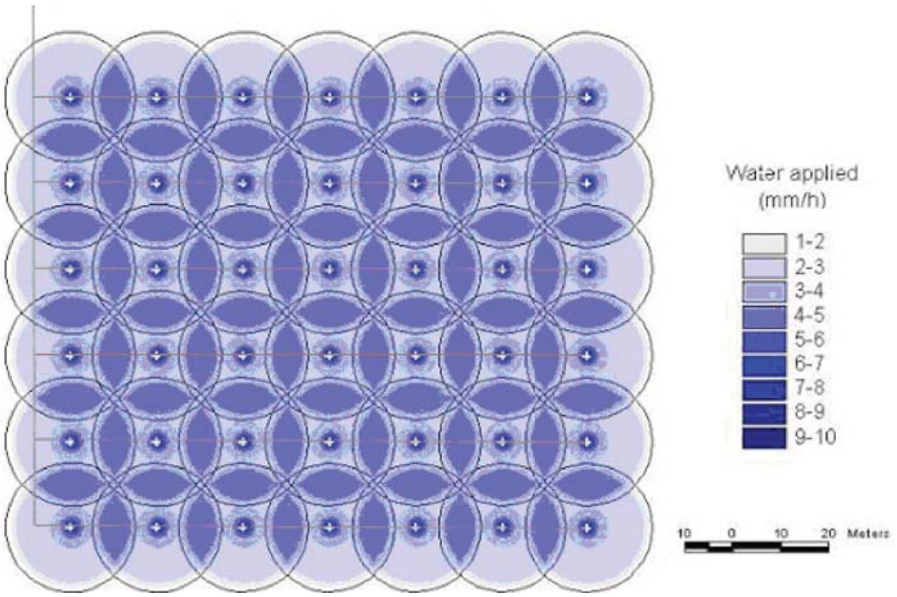

Figuew 8b. Graphical analysis of the on-farm network working at a hydrant pressure head higher than 39 m (60% probability of occurrence)

5 CONCLUSIONS

On-farm network design is usually based on a fixed upstream pressure head that usually corresponds to the best on-farm irrigation performance. This assumption is not realistic when on-farm networks are supplied by on-demand pressurized distribution systems. In fact, in this case, the hydrant pressure head is subjected to high fluctuations depending on the operating condition of the distribution system.

In order to understand the influence of the pressure head variation at the hydrant on the performance of the on-farm network, a detailed analysis was performed on an existing irrigation system.

This study highlighted that the performance of the on-farm sprinkler network is greatly affected by the variation of pressure head at the upstream hydrant. As by the analysed case study, it was demonstrated that the on-farm Distribution Efficiency can strongly vary in time.

In this case, the analysis shows that the on-farm Distribution Efficiency can vary from 80%, for pressure head at hydrant greater than 39 m, to 62% for of an upstream hydrant pressure head equal to 26 m.

Therefore, a model to simulate the interaction between the irrigation distribution system and the on-farm sprinkler network is an useful decision-support tool for the design and management phases.

REFERENCES

Altieri S. 1995. Sinistra Ofanto irrigation scheme: management and maintenance problems. Bonifica, L.S: Pereira (ed.) 1-2, 40-47

Christiansen J E (1942). Irrigation by sprinkling. California Agric.Exp.Sta.Bull.670. University of California, Berkeley.

Daccache, A.; Lamaddalena, N.; Fratino, U. (2010). On-demand pressurized water distribution system impacts on sprinkler network design and performance. Irrigation Science, Vol. 28, Issue 4, pp 331-339

Francisco L. Santos (1998). Evaluation of alternative irrigation technologies based upon applied water and simulated yields. J. Agric. Eng. Res. 69, 73D83.

Heermann D F; Wallender W W; Bos G M (1990). Irrigation efficiency and uniformity. In : Hoffman G.J., Howell T.A., Solomon K :H :, Management of farm irrigation systems. ASAE, St Joseph, MI, 125-149.

Jiusheng Li (1997). Effect of pressure and nozzle shape on the characteristics of sprinkler droplet spectra. J. Agric.Eng. Res. 66, 15-21

Keller J; Bleisner R D (2000). Sprinkler and trickle irrigation. The Blackburn press, 68-69.

Lamaddalena N (1997). Integrated simulation modelling for design performance analysis of on-demand pressurized irrigation systems. PhD. Thesis, Instituto Superior de Agronomia, Technical University of Lisbon.

Lamaddalena N; Khadra R (2001). "An integrated tool for the management of large scale irrigation systems". Rivista di Irrigazione e drenaggio (in Italian), 48, 31-36.

Lamaddalena N; Sagardoy JA (2000). Performance analysis of on-demand pressurised irrigation systems. Irrigation and Drainage Paper, FAO 59. Ch 5

Lamaddalena, N.; Fratino, U.; Daccache, A. (2007). On-farm sprinkler irrigation performance as affected by the distribution system. Biosystems Engineering, vol. 96, Issue 1, pp 99-109

Lee C; Brestler P.T.; Buttle J.L; Howard C.D.D. (1989). Distribution network analysis for water utility. American Water Works Association, Manual of Water Supply Practices, Denver, Colorado, USA.

Sepaskhah A R; Ghahraman B (2004). The effects of irrigation efficiency and uniformity coefficient on relative yield and profit for deficit irrigation. Biosystems Engineering 87 (4), 495-507.

Tizaoui C; Pereira L S ; Lamaddalena N (1997). Irrigation par aspersion et localisée : conditions hydrauliques, performances et production. In: Proceedings of the International conference on "Collective Irrigation Systems", Bari, Italy, 55-75.

Wilson T ; Zoldoske D (1997). Evaluating sprinkler irrigation uniformity. CATI Publication # 970703. July 1997.

6

Avanços no Conhecimento sobre a Tolerância e a Aclimatação de Plantas à Salinidade

Enéas Gomes-Filho[1], Elton Camelo Marques[1] & José Tarquinio Prisco[1]

[1] Instituto Nacional de Ciência e Tecnologia em Salinidade, Universidade Federal do Ceará, Fortaleza, CE, Brasil

INOVAGRI Book 2014 - Irrigation and Salinity:
Researches and Technological Innovations
ISBN 978-85-67668-09-3

INOVAGRI
INSTITUTO DE PESQUISA E INOVAÇÃO NA AGRICULTURA IRRIGADA

Fortaleza - CE
2015

6 Avanços no Conhecimento sobre a Tolerância e a Aclimatação de Plantas à Salinidade

RESUMO

A salinidade é um dos estresses abióticos que mais afetam o crescimento e a produção vegetal. Acredita-se que o esclarecimento dos mecanismos de tolerância e susceptibilidade à salinidade seja de fundamental importância para o desenvolvimento de novas técnicas de manejo das culturas, possibilitando a produção nessa condição estressante. Essa tarefa, no entanto, não tem sido fácil, dada a complexidade desse tipo de estresse, o qual envolve dois componentes distintos: o osmótico e o iônico. Muitos pesquisadores têm tentado aumentar a tolerância das plantas à salinidade através da manipulação gênica, e a definição de quais os genes em potencial para esse tipo de estudo requer o conhecimento prévio das alterações induzidas pela salinidade no padrão proteico (proteoma) dos diversos órgãos da planta. Em geral, esses estudos têm apresentado resultados promissores quando desenvolvidos em casa de vegetação, porém a eficácia dessa prática no campo ainda é limitada. Como alternativa à manipulação gênica, têm-se pré-tratado as plantas com compostos orgânicos, inorgânicos ou reguladores do crescimento, a fim de induzir a aclimatação à salinidade. As evidências de que essa abordagem condiciona as plantas a responderem mais rápida e eficientemente a estresses múltiplos são cada vez mais concretas. Avanços significativos no conhecimento também têm sido obtidos ao se estudar genótipos com tolerância diferencial à salinidade, através da análise da expressão gênica e do proteoma, permitindo, assim, a identificação de genes e proteínas relacionados a essas características. Pretende-se mostrar e discutir alguns resultados recentes relacionados à tolerância e à aclimatação de plantas à salinidade, contribuindo assim para o avanço do conhecimento sobre esses processos.

Palavras-chave: estresse oxidativo; estresse salino; proteoma; expressão gênica

1 INTRODUÇÃO

No contexto biológico, define-se o termo estresse como sendo qualquer alteração nas condições ótimas de um ser vivo, a qual modifica todos os seus níveis funcionais, limita o seu desenvolvimento e pode reduzir as suas possibilidades de sobrevivência (LARCHER, 2000; TAIZ; ZEIGER, 2009). As plantas estão sempre sujeitas a condições de estresses múltiplos, os quais podem ter origem biótica ou abiótica (LARCHER, 2000). Entre os inúmeros estresses abióticos aos quais as plantas estão expostas, encontra-se o estresse salino, um dos que mais comprometem a produtividade agrícola mundial (FLOWERS, 2004; MAHAJAN; TUTEJA, 2005), chegando a afetar mais de 800 milhões de hectares no mundo (MUNNS; TESTER, 2008; TÜRKAN; DEMIRAL, 2009; HASEGAWA, 2013).

Os solos salinos podem ser encontrados em todos os continentes (exceto a Antártida) e em qualquer zona climática, mas se concentram em regiões de clima árido e semiárido, onde a evaporação intensa e a lixiviação incompleta concorrem para a concentração dos sais no solo e nas águas superficiais (RENGASAMY, 2006; BUI, 2013). Nessas regiões, a salinização do solo é praticamente irreversível, pois a lixiviação dos sais acumulados é limitada, em razão da escassez de água doce, seja pluvial, seja subterrânea (ROZEMA; FLOWERS, 2008).

A salinização dos solos também resulta da ação antrópica, a qual está relacionada fortemente a certas práticas agrícolas, tais como o uso de água de irrigação de baixa qualidade, associado a uma drenagem e a um manejo do solo inadequados (RENGASAMY, 2006; YADAV *et al.* 2011; PLAUT; EDELSTEIN; BEN-HUR, 2013). Em 2000, estimou-se que 19,5% das áreas irrigadas em todo o mundo — correspondentes a 45 milhões de hectares — enfrentavam problemas de salinidade, e no Brasil esse percentual encontrava-se entre 20 e 25%, concentrado principalmente na região Nordeste (FAO, 2000).

As consequências da salinidade às plantas devem-se principalmente aos efeitos desse estresse no crescimento e no desenvolvimento vegetal, os quais podem ser de natureza iônica, osmótica ou de ambas (HASEGAWA *et al.*, 2000; MUNNS; TESTER, 2008; HASEGAWA, 2013). Os efeitos iônicos resultam da elevada absorção de íons, especialmente Na^+ e Cl^-, que alteram a homeostase iônica da célula quando em altas concentrações, a qual é de importância fundamental para a atividade de muitas enzimas citosólicas e para a manutenção do potencial de membrana celular (HASEGAWA *et al.*, 2000; MUNNS; TESTER, 2008). Os efeitos osmóticos, por sua vez, são decorrentes da redução do potencial hídrico do ambiente radicular, que acarreta a diminuição da disponibilidade de água para a planta (MUNNS, 2002; MUNNS; TESTER, 2008). Secundariamente, a salinidade também induz o estresse oxidativo, ao provocar o acúmulo de espécies reativas de oxigênio (EROs), que são prejudiciais à célula quando em altas concentrações, causando danos oxidativos às biomoléculas (MITTLER, 2002; AZEVEDO NETO; GOMES-FILHO; PRISCO, 2008). Sob estresse salino, os

principais processos fisiológicos da planta, tais como a fotossíntese, a respiração, a síntese proteica, as relações hídricas e as reações enzimáticas são afetados (MUNNS, 2002; PARIDA; DAS, 2005), podendo o excesso de sais conduzir a planta à morte (MANSOUR; SALAMA, 2004).

O grau com que a salinidade afeta as plantas depende de fatores intrínsecos ao indivíduo (espécie, cultivar e estádio de desenvolvimento), fatores relacionados ao estresse (tipo de sal, concentração salina, tempo de exposição aos sais e seu modo de aplicação) e fatores ambientais (luz, temperatura e umidade relativa do ar, composição iônica e granulometria do solo), bem como da interação entre eles (SHANNON; GRIEVE, 1999; BRAY; BAILEY-SERRES; WERETILNYK, 2000). Enquanto algumas espécies apresentam elevada tolerância à salinidade (halófitas), requerendo inclusive um ambiente salino para que seu ciclo de vida seja completado, outras são altamente susceptíveis aos sais (glicófitas). Acredita-se que o esclarecimento dos mecanismos de tolerância e susceptibilidade à salinidade seja fundamental para o desenvolvimento de novas técnicas de manejo das culturas, possibilitando a produção nessa condição estressante. Além disso, tais conhecimentos também podem ser utilizados no melhoramento genético, visando aumentar a tolerância ao estresse.

A resposta de uma planta à salinidade irá depender de uma sequência de reações que ocorrem desde o início da exposição ao estresse até quando seus efeitos na planta passam a ser visualizados (PRISCO; GOMES-FILHO, 2010). A primeira dessas etapas compreende a percepção dos componentes osmótico e iônico do estresse salino, que é mediada por sensores (receptores) presentes na membrana plasmática. Após a percepção do estresse, há um aumento na concentração citoplasmática de cálcio, que, por sua vez, funciona como um mensageiro secundário e induz uma cascata de sinalização, que culmina em mudanças no funcionamento das células (TÜRKAN; DEMIRAL, 2009; MAATHUIS, 2014). Essa série de reações, que constitui a transdução do sinal, pode ser bastante complexa, envolvendo proteínas, lipídios, alguns hormônios vegetais e EROs (PRISCO; GOMES-FILHO, 2010). Enquanto essas alterações no metabolismo acontecem, as plantas realizam ajustes metabólicos, estruturais e fisiológicos a fim de alcançar seu equilíbrio homeostático, bem como desintoxicam suas células; a esse conjunto de ajustes, dá-se o nome de aclimatação, e ao final dele, pode haver tolerância ou susceptibilidade ao estresse salino (PRISCO; GOMES-FILHO, 2010). O esquema apresentado na Figura 1 resume as mudanças fisiológicas e bioquímicas que ocorrem quando as plantas são submetidas à salinidade e tem servido de modelo para nossos estudos sobre fisiologia e bioquímica do estresse salino.

2 TOLERÂNCIA E ACLIMATAÇÃO À SALINIDADE

As plantas respondem primariamente ao estresse salino através da ativação de um ou mais mecanismos, adquiridos durante o seu processo evolutivo. Entre eles, podem-

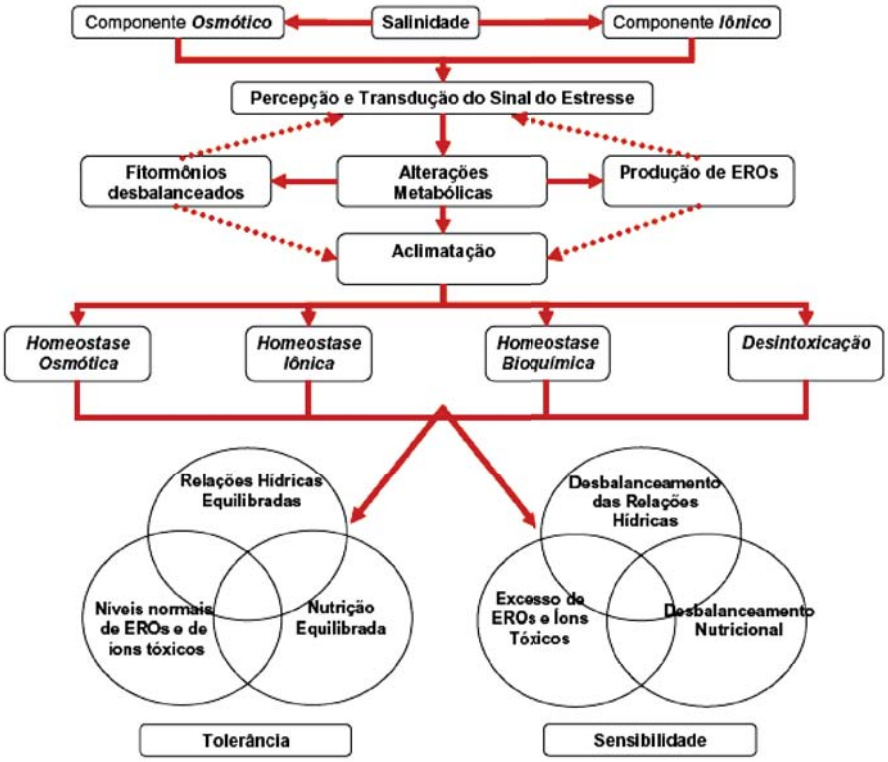

Figura 1. Sequência de mudanças fisiológicas e bioquímicas que ocorrem quando plantas são submetidas a estresse salino. Fonte: Prisco e Gomes-Filho (2010)

se citar: a) controle da absorção de íons pela raiz e do seu transporte para as folhas; b) compartimentação de íons, no nível celular ou na planta inteira; c) acúmulo de solutos orgânicos compatíveis no citoplasma; d) alterações na estrutura da membrana plasmática; e) indução da expressão e da atividade de enzimas antioxidantes; e f) alteração no balanço hormonal. Isoladamente ou em conjunto, esses mecanismos têm por finalidade minimizar os danos causados pelo estresse salino às plantas, culminando no restabelecimento da homeostase celular e, finalmente, na retomada de seu crescimento, mesmo que a uma velocidade reduzida (HASEGAWA *et al.*, 2000; MANSOUR; SALAMA, 2004; PARIDA; DAS, 2005; MUNNS; TESTER, 2008). Espécies incapazes de restaurarem sua homeostase e de crescerem nessas condições estressantes, devido à ausência ou à ineficiência dos mecanismos citados, sofrerão invariavelmente mais danos.

Muitos pesquisadores têm se esforçado para identificar os genes envolvidos na tolerância à salinidade. Como resultado desses esforços, sabe-se atualmente que tal característica está associada a genes que codificam: a) proteínas transportadoras de íons, envolvidas no controle da taxa de absorção de sais a partir do solo e do seu

transporte através da planta; b) enzimas envolvidas com a biossíntese de solutos compatíveis; c) proteínas do metabolismo energético; d) enzimas de regulação do metabolismo oxidativo; e) proteínas com participação em vias de transdução do sinal de estresse; f) proteínas com funções protetoras; e g) proteínas reguladoras do crescimento de células e tecidos. Baseando-se nesse conhecimento, têm-se tentado aumentar a tolerância à salinidade por meio da manipulação gênica, especialmente através da superexpressão de um ou mais "genes do estresse". Outra prática tem sido a transferência de um ou mais "genes do estresse" de uma espécie ou cultivar tolerante para outra sensível.

Em uma dessas primeiras tentativas, o gene *NHX1* (do inglês, *Na*$^+$*/H*$^+$ *exchanger*) responsável por codificar o transportador antiporte Na^+/H^+ da membrana vacuolar, envolvido na compartimentação de Na^+ no vacúolo, foi superexpresso em plantas de *Arabidopsis*, e tal intervenção garantiu o crescimento e o desenvolvimento das plantas em concentrações de NaCl de até 200 mM (APSE *et al.*, 1999). Apesar de esses autores terem destacado à época a viabilidade do aumento da tolerância à salinidade via engenharia genética, a ausência de produtos comerciais resultantes dessa abordagem na atualidade indica que tal prática não é totalmente eficaz. Muitos desses estudos são desenvolvidos em laboratório e casa de vegetação, e frequentemente tais resultados não são extrapoláveis a condições de campo, tornando-se premente que eles sejam repetidos nessas condições. Além disso, a tolerância ao estresse salino depende da expressão coordenada de vários genes (resposta multigênica), e não pode ser conseguida com a simples transferência ou superexpressão de um ou dois genes. Sendo assim, não se deve estudar a base genética e molecular da tolerância à salinidade de maneira isolada e particular, e, sim, de maneira integrada, visando entender como tais genes (e proteínas) contribuem e se relacionam para conferir tolerância à salinidade.

A sobrevivência de uma planta sob estresse depende da sua capacidade de se aclimatar a essa condição adversa. Como dito anteriormente, a aclimatação é um processo que envolve mudanças fisiológicas, bioquímicas e morfológicas, inclusive na expressão gênica, que não são transmitidas para as gerações futuras, permitindo que um indivíduo adquira maior tolerância ao estresse, em comparação àqueles que não se encontram aclimatados (PRISCO; GOMES-FILHO, 2010). Isso se dá devido a uma capacidade diferencial em perceber e induzir as respostas ao estresse necessárias para o alcance da homeostase.

Homeostase Osmótica

Uma das primeiras respostas que ocorrem em plantas sob estresse salino é o ajustamento osmótico, que tem a função principal de restabelecer a homeostase osmótica; nessa condição adversa, os potenciais osmótico e hídrico das plantas diminuem, a fim de retomar o gradiente de potencial hídrico no sistema solo-planta e consequentemente a absorção de água pelas raízes, que é prejudicada em condições de salinidade (MUNNS, 2002; MUNNS; TESTER, 2008). Isso se faz à custa do acúmulo de íons tóxicos

no vacúolo e de íons não tóxicos e solutos orgânicos no citosol, compatíveis com a manutenção da atividade metabólica das células (PRISCO; GOMES-FILHO, 2010). Esse processo, embora bastante conhecido, ainda hoje chama a atenção de diversos pesquisadores, especialmente em razão das funções exercidas pelos solutos compatíveis na proteção de proteínas e de outras macromoléculas contra os danos causados por sais e EROs. Os solutos compatíveis mais estudados são o aminoácido prolina, o composto quaternário de amônio glicinabetaína, o açúcar-álcool manitol e o açúcar trealose (SILVEIRA *et al*., 2010). Apesar de historicamente se atribuir à prolina um papel de destaque no ajustamento osmótico, atualmente há evidências de que a concentração desse soluto nas células não é suficientemente elevada para contribuir com o potencial osmótico celular, em condições de salinidade. Em favor dessa ideia está o fato de os teores desse soluto aumentarem tanto em genótipos/cultivares sensíveis, quanto tolerantes à salinidade. Acredita-se assim que o papel da prolina nesses casos esteja mais relacionado à proteção contra os danos causados pelo estresse, que propriamente ao ajustamento osmótico (SZABADOS; SAVOURÉ, 2010; HAYAT *et al.*, 2012).

Homeostase Iônica

As mudanças que ocorrem durante o restabelecimento da homeostase osmótica têm forte associação com a homeostase iônica. Junto à compartimentação dos íons tóxicos no vacúolo, outros processos, tais como o acúmulo deles nas células do córtex da raiz, a retirada do Na^+ do xilema e seu efluxo para o solo, contribuem enormemente para o alcance da homeostase iônica em plantas sob estresse salino (ROY *et al.*, 2014). Na maioria das espécies, o Na^+ é o principal íon responsável pelos efeitos tóxicos da salinidade, com exceção de algumas arbóreas, tais como as dos gêneros *Citrus* e *Vitis*, em que o Cl^- parece ser o íon mais nocivo (WHITE; BROADLEY, 2001). Por essa razão, muitos esforços foram envidados ao longo dos anos para desvendar as respostas e os mecanismos de tolerância das plantas ao Na^+, e como resultado disso hoje se conhece bem como ele é absorvido e distribuído no interior das células e tecidos.

As principais vias envolvidas no influxo de Na^+ na célula vegetal são os canais de cátions não seletivos (NSCC, do inglês, *non-selective cation channel*), os transportadores de K^+ de alta afinidade (HKT, do inglês, *high-affinity K^+ transporter*), os transportadores de cátions de baixa voltagem (LCT, do inglês, *low-affinity cation transporter*) e os canais de cátions insensíveis à voltagem (VI-NSCC, do inglês, *voltage-insensitive nonselective cation channel*) (KRONZUCKER; BRITO, 2011). Embora o papel específico de cada sistema de transporte varie entre espécies e conforme as condições de crescimento, fortes evidências sugerem que essas vias podem operar em conjunto durante a absorção de Na^+ (SILVEIRA *et al.*, 2010). Já o efluxo de Na^+ do citosol é mediado principalmente pela proteína SOS1, um transportador antiporte Na^+/H^+ situado na membrana plasmática, que é expresso, sobretudo, na epiderme da raiz, onde contribui com a exclusão do Na^+ para o meio externo, e no parênquima do xilema, contribuindo para o carregamento de Na^+ (HASEGAWA, 2013;

MAATHUIS, 2014). Outro importante processo relacionado à tolerância ao Na^+ é a retirada desse íon do xilema, mediada pela proteína HKT1, um transportador simporte Na^+/K^+ da membrana plasmática que regula a quantidade de Na^+ que é translocada para a parte aérea através do fluxo transpiratório.

A manipulação dos genes *SOS1* e *HKT1* tem representado uma das principais intervenções realizadas pelos fisiologistas moleculares, com vistas à homeostase iônica e ao aumento da tolerância à salinidade. Plantas de fumo nas quais o gene *SOS1* oriundo de *Arabidopsis thaliana* foi inserido e superexpresso foram mais tolerantes à salinidade que as plantas do tipo selvagem (Figura 2); após 24 dias de irrigação com solução de NaCl, seguido por um período de irrigação com solução nutritiva, as plantas transgênicas recuperaram-se do estresse, e seu crescimento foi quase normal, além de terem apresentado maior taxa fotossintética e menores teores de Na^+ que as plantas do tipo selvagem (YUE *et al.*, 2012). Visando o mesmo objetivo, Munns *et al.* (2012) transferiram o gene *HKT1* de uma espécie não cultivada de trigo (*Triticum monoccocum*) para *T. durum*, que, diferentemente da primeira espécie, é sensível aos sais e não possui o gene *HKT1* em seu genoma; em condições de campo, as plantas transgênicas (apresentando o gene *HKT1*) tiveram a concentração de Na^+ na folha bandeira drasticamente reduzida. Além disso, essa intervenção aumentou em 24% a produtividade de grãos, em condições de salinidade, em comparação às plantas do tipo selvagem (MUNNS *et al.*, 2012). Apesar das implicações

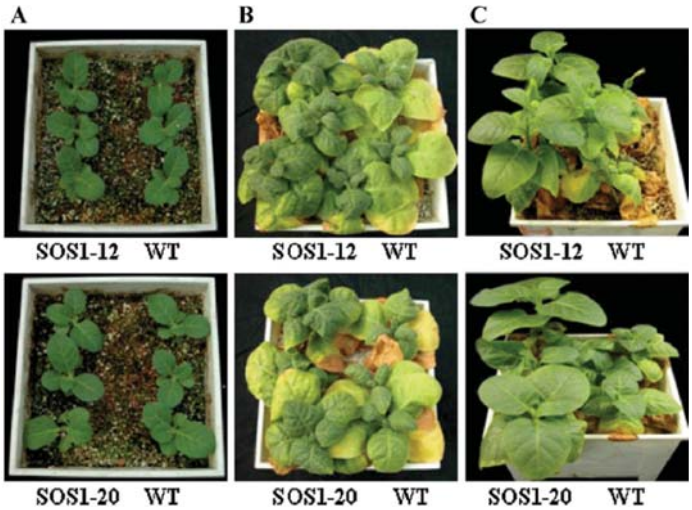

Figura 2. Tolerância à salinidade de plantas de fumo do tipo selvagem (WT, do inglês *wild-type*) ou superexpressando o gene *SOS1* (SOS1-12 e SOS1-20). (A) Plantas cultivadas por quatro semanas na ausência de NaCl; (B) plantas irrigadas com solução de NaCl (até 300 mM) por 24 dias, seguido por cultivo durante seis semanas na ausência de NaCl; (C) plantas da condição anterior, irrigadas com solução nutritiva, após três semanas de crescimento. Fonte: Yue *et al.* (2012)

que experimentos de manipulação gênica trazem, é preciso cautela e uma análise mais abrangente para considerá-los promissores.

Homeostase Bioquímica

A homeostase bioquímica é bastante complexa, pois envolve todas as reações do metabolismo; representa, portanto, os ajustes necessários para que o indivíduo mantenha-se funcional, a despeito do aumento da concentração de íons que ocorre no ambiente externo (PRISCO; GOMES-FILHO, 2010). Tais ajustes envolvem mudanças intensas na expressão gênica, que alteram o transcriptoma, o proteoma e o metaboloma das plantas (KOSOVÁ *et al.*, 2011). Apesar da importância, mudanças na transcrição gênica nem sempre correspondem a mudanças no proteoma; sendo assim, estudar as alterações no perfil proteico durante a aclimatação é significante, uma vez que as proteínas são os efetores diretos das respostas das plantas a estresses. Tais alterações podem envolver enzimas, componentes da maquinaria de transcrição e tradução, bem como proteínas da membrana plasmática e do citoesqueleto (KOSOVÁ *et al.*, 2011), sendo possível visualizá-las, de forma qualitativa e quantitativa, quando se compara as proteínas presentes em um determinado órgão de uma planta que foi submetida a estresse salino, com outra cultivada sob condições normais.

O uso de genótipos/cultivares com tolerância diferencial à salinidade associado à análise proteômica é uma estratégia adequada para se identificar quais proteínas encontram-se relacionadas à tolerância ou à susceptibilidade das plantas ao estresse salino. Com esse propósito, Abreu *et al.* (2014) estudaram o perfil proteico de folhas de dois cultivares de feijão-de-corda, Pitiúba (tolerante) e TVu 2331 (sensível), após submetê-los aos tratamentos controle (ausência de NaCl, por 17 dias), salino (NaCl a 75 mM, por 17 dias) e de recuperação (cultivo em condições de salinidade por 12 dias, seguido por 5 dias sem estresse) (Figura 3). Eles observaram que, em condições de estresse, os cultivares de feijão-de-corda apresentaram respostas distintas para superar os danos causados pelos sais, que se relacionaram com sua tolerância diferencial ao estresse. No cultivar Pitiúba (tolerante), houve um aumento, em relação ao controle, na expressão de proteínas envolvidas no metabolismo fotossintético e energético, tais como as enzimas ativase da rubisco, quinase da ribulose-5-fosfato e descarboxilase da glicina, bem como uma proteína componente do complexo de liberação de O_2, presente no fotossistema II (Figura 4). Por outro lado, no cultivar TVu 2331 (sensível), tais processos foram profundamente afetados, como indicado pela diminuição na expressão da rubisco, da anidrase carbônica e de proteínas componentes do complexo de liberação de O_2, e em conjunto tais mudanças, possivelmente, prejudicaram o metabolismo energético e consequentemente o crescimento das plantas. Além disso, após o tratamento de recuperação, muitas proteínas voltaram a ser expressas em níveis comparáveis ao do controle; nessas condições, em que o estresse havia cessado, o nível de expressão dessas proteínas contribuiu para a retomada do crescimento das plantas de feijão-de-corda (Figura 4) (ABREU *et al.*, 2014).

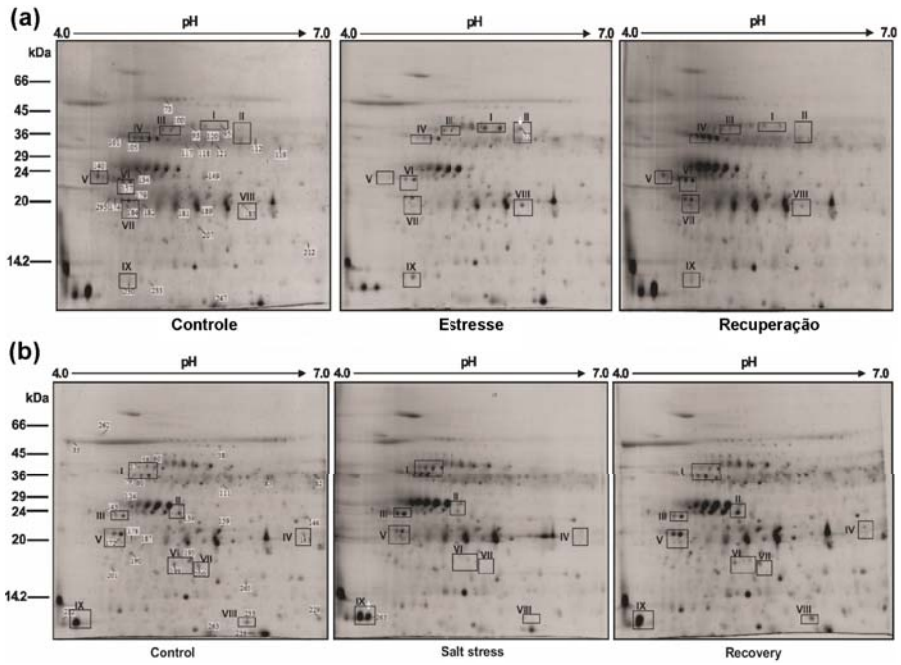

Figura 3. Eletroforese bidimensional de proteínas foliares de plantas de feijão-de-corda, cultivares Pitiúba (a) e TVu 2331 (b), submetidas aos tratamentos controle, salino e de recuperação. A comparação entre os três perfis proteicos, em cada cultivar, permitiu identificar quais proteínas tiveram sua expressão regulada pelos tratamentos aplicados. Fonte: Abreu *et al.* (2014)

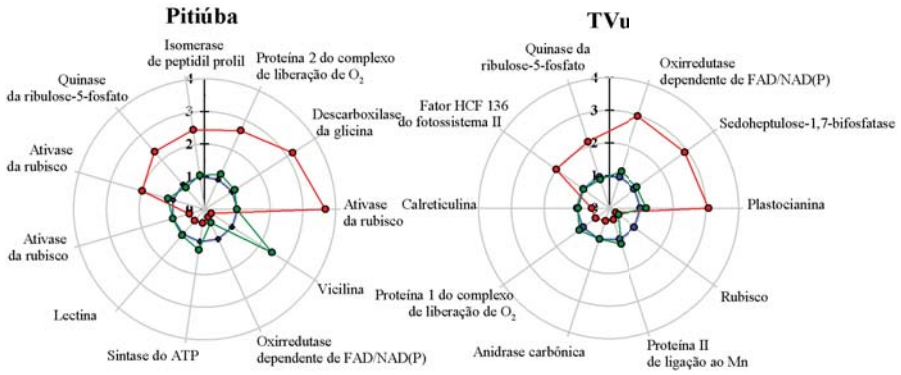

Figura 4. Expressão relativa de proteínas foliares de plantas de feijão-de-corda, cultivares Pitiúba e TVu, submetidas aos tratamentos salino (em vermelho) e de recuperação (em verde). O tratamento controle foi tomado como referência (em azul). Fonte: Adaptado de Abreu *et al.* (2014)

Desintoxicação

Associados aos processos de homeostase osmótica, iônica e bioquímica, estão aqueles que contribuem para a desintoxicação das plantas, por exemplo, a compartimentação dos íons tóxicos no vacúolo (comentado anteriormente) e a remoção de EROs. Genes (e proteínas) relacionados a esses dois mecanismos de defesa têm sido objeto de estudo de pesquisadores em todo o mundoA compartimentação de Na^+ no vacúolo é mediada por um transportador antiporte Na^+/H^+, presente no tonoplasto; a manipulação do gene que o expressa (*NHX1*) tem mostrado a importância desse processo para o alcance da tolerância à salinidade. Por exemplo, quando o gene *NHX1* da halófita *Salsola soda* foi inserido e superexpresso em alfafa, as plantas conseguiram crescer em condições severas de salinidade (NaCl a 400 mM) (Figura 5); apesar do acúmulo inevitável de Na^+ nas plantas, ele não foi suficiente para causar danos sérios às células, e segundo os autores isto pode ser devido à atividade aumentada do transportador NHX1, que manteve baixa a concentração de Na^+ no citosol (Li

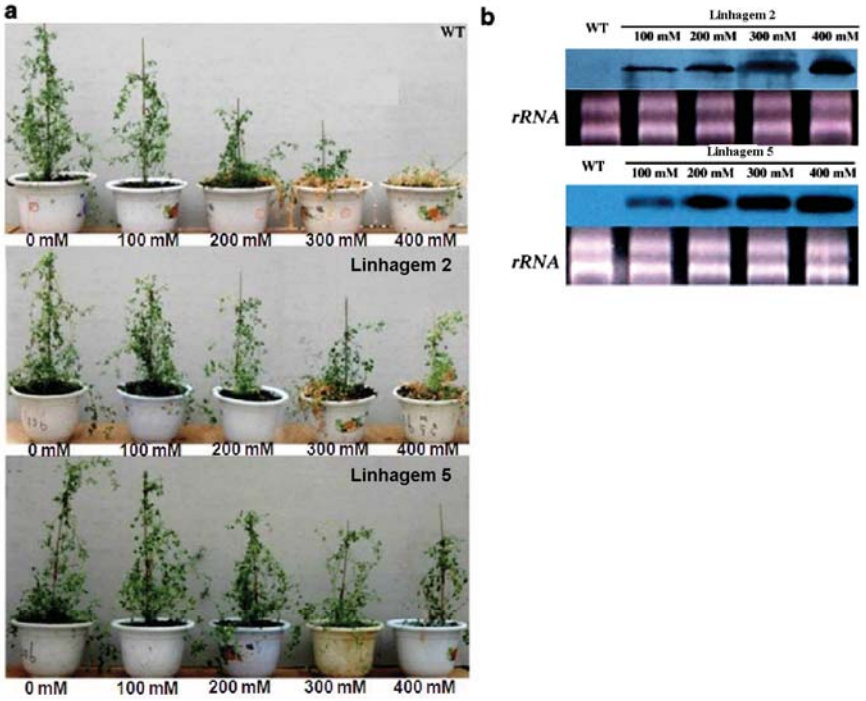

Figura 5. (a) Tolerância à salinidade (NaCl de 0 a 400 mM) de plantas de alfafa do tipo selvagem (WT) e de duas linhagens transgênicas superexpressando o gene *NHX1* oriundo de *Salsola soda*. (b) Northern blot indicando a expressão do gene *NHX1* em plantas transgênicas de alfafa. rRNA: RNA ribossomal. Fonte: adaptado de Li *et al.* (2011)

et al., 2011). A compartimentação do Na^+ no vacúolo, bem como sua exclusão da célula (discutida anteriormente) são totalmente dependentes da atividade das bombas de prótons de membrana plasmática (H^+-ATPases) e tonoplasto (H^+-ATPases e H^+-PPases). Além de manter as membranas celulares polarizadas, tais bombas são cruciais para a geração da força motriz de prótons que dirige o transporte de Na^+ (e demais íons) através das membranas, e um aumento de sua expressão contribuiu para o alcance da tolerância à salinidade em várias espécies (OTOCH *et al.*, 2001; XU *et al.*, 2011).

Um dos eventos bioquímicos que ocorrem nas plantas e em outros seres aeróbicos é a produção de EROs, que são subprodutos inevitáveis do metabolismo celular aeróbico e dos processos fotoxidativos (HALLIWELL; GUTTERIDGE, 1985; NOCTOR; FOYER, 1998). As EROs mais comumente encontradas são o peróxido de hidrogênio (H_2O_2) e os radicais superóxido ($^{\bullet}O_2^-$) e hidroxil ($HO^{\bullet}$) (APEL; HIRT, 2004; AZEVEDO-NETO; GOMES-FILHO; PRISCO, 2008). Sob condições ótimas, a produção de EROs nas plantas é mantida em níveis compatíveis com o metabolismo normal, entretanto, em condições adversas, ela pode ser drasticamente aumentada, gerando um estresse secundário, o estresse oxidativo (VAIDYANATHAN *et al.*, 2003), que é definido pelo desequilíbrio na relação entre compostos oxidantes e antioxidantes, em favor dos primeiros (GILL; TUTEJA, 2010). Nessa condição, as EROs podem causar danos aos diversos componentes da célula, como ácidos nucleicos, lipídios e proteínas (MITTOVA *et al.*, 2002; APEL; HIRT, 2004; MØLLER; JENSEN; HANSSON, 2007).

Embora sejam consideradas subprodutos do metabolismo celular, as EROs passaram a ser empregadas pelas plantas, ao longo da evolução, como moléculas sinalizadoras em diferentes processos celulares, tais como no crescimento e desenvolvimento, no ciclo celular, na apoptose, na senescência e nas respostas aos estresses bióticos e abióticos (FINKEL, 2003; MILLER; SHULAEV; MITTLER, 2008). Uma vez que as EROs possuem esse duplo papel, é necessário haver pelo menos dois processos de regulação das concentrações dessas espécies nas células: um que as tornem capazes de modular as EROs em níveis baixos, para propósitos de sinalização, e outro que permita a eliminação de EROs em excesso, especialmente em condições de estresse (MITTLER, 2002). Em função disso, as plantas desenvolveram mecanismos para manter a relação produção/eliminação de EROs constante no interior das células (APEL; HIRT, 2004), utilizando, para esse fim, os sistemas de defesa enzimático e não enzimático (ASADA, 1999). A importância da coordenação entre esses dois sistemas no processo de remoção de EROs está cada vez mais evidente e isso está relacionado com a tolerância das plantas à salinidade (MITTOVA *et al.*, 2002; MELONI *et al.*, 2003; AZEVEDO NETO *et al.*, 2005).

Muitos estudos foram desenvolvidos nos últimos anos visando o aumento da tolerância à salinidade, por meio da manipulação dos genes que codificam as enzimas do sistema antioxidativo, bem como daquelas envolvidas na síntese de compostos antioxidantes (LEE *et al.*, 2007; LUO *et al.*, 2013). Como já destacado, os resultados

positivos obtidos até então têm contribuído principalmente para a compreensão do papel desses genes (e proteínas) na tolerância das plantas à salinidade.

Quando a aclimatação a um determinado estresse é intensificada pela exposição a um estresse anterior (de mesmo tipo ou diferente), têm-se a tolerância cruzada. Nas condições de campo, as plantas estão submetidas frequentemente a estresses múltiplos, os quais variam em intensidade e duração, afetando diferencialmente o desempenho delas, o qual dependerá ainda do estádio de desenvolvimento em que elas se encontrem (COMINELLI *et al.*, 2013). É nesse contexto que a tolerância cruzada torna-se importante, principalmente para a agricultura, pois, através desse processo, as plantas podem ser selecionadas por tolerarem mais de um tipo de estresse (AZEVEDO-NETO; GOMES-FILHO; PRISCO, 2008).

Uma das técnicas utilizadas para aumentar a aclimatação a estresses abióticos é a aplicação de compostos orgânicos, inorgânicos ou reguladores do crescimento no meio de cultivo das plantas, sendo as raízes, nesse caso, o órgão que entra em contato com a substância, ou por aspersão desses compostos nas folhas (ASHRAF *et al.*, 2008). Em todos esses casos, as plantas podem ser mantidas na presença dessas substâncias exógenas durante todo o desenvolvimento delas, ou apenas em um período que antecede a exposição ao estresse (pré-tratamento). As evidências de que essa abordagem condiciona as plantas a responderem mais rápida e eficientemente a estresses múltiplos são cada vez mais concretas.

Entre as substâncias utilizadas para induzir aclimatação, estão aquelas que, dependendo da sua concentração, ora atuam como indutores de estresse, ora como moléculas sinalizadoras; o H_2O_2 e o óxido nítrico (NO) são exemplos delas (FILIPPOU *et al.*, 2013). Partindo desse conhecimento, Azevedo Neto *et al.* (2005) avaliaram o efeito do H_2O_2 na indução da aclimatação à salinidade em plantas de milho. Para isso, eles pré-trataram plantas de um genótipo sensível à salinidade (BR 5011) com H_2O_2 a 1 mM, aplicado na solução nutritiva, por dois dias, e em seguida, submeteram-nas à salinidade (NaCl a 100 mM). Ao final do tratamento salino, as plantas que estiveram sob estresse e que foram pré-tratadas com H_2O_2 cresceram bem mais que aquelas não pré-tratadas, sob as mesmas condições (Figura 6). Além disso, houve mudanças favoráveis no sistema enzimático antioxidativo das plantas pré-tratadas, tanto nas folhas, quanto nas raízes. Assim, eles concluíram que o H_2O_2 foi capaz de induzir tolerância cruzada e que provavelmente esteve envolvido na sinalização ocorrente durante a aclimatação à salinidade em milho (AZEVEDO NETO *et al.*, 2005). Quando se testou a aplicação foliar de H_2O_2 em plantas de milho, observou-se um resultado semelhante, em que as plantas pré-tratadas com essa molécula tiveram seu crescimento menos afetado pela salinidade e seu sistema antioxidativo enzimático foi induzido, especialmente a catalase, que é a principal enzima removedora de H_2O_2 (Figura 7) (GONDIM *et al.*, 2012) .

Uma alternativa para induzir aclimatação é o uso desses compostos já mencionados no tratamento das sementes, antes da semeadura (ASHRAF *et*

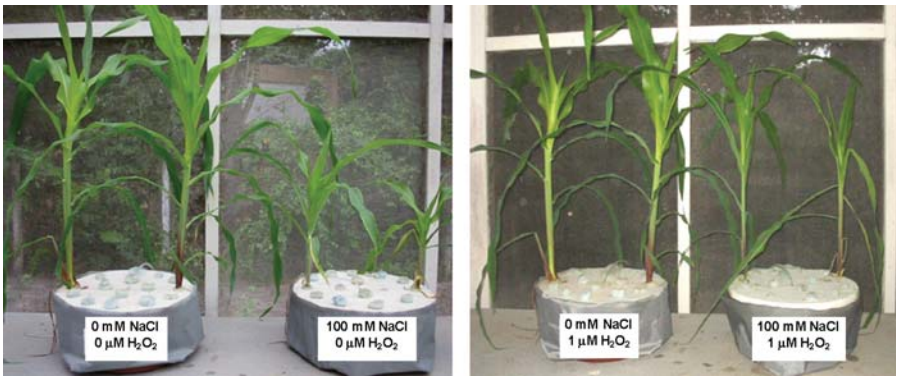

Figura 6. Efeitos do pré-tratamento com H_2O_2, aplicado via solução nutritiva, no crescimento de plantas de milho submetidas aos tratamentos controle (NaCl a 0 mM) e salino (NaCl a 100 mM). Fonte: Azevedo Neto (2005).

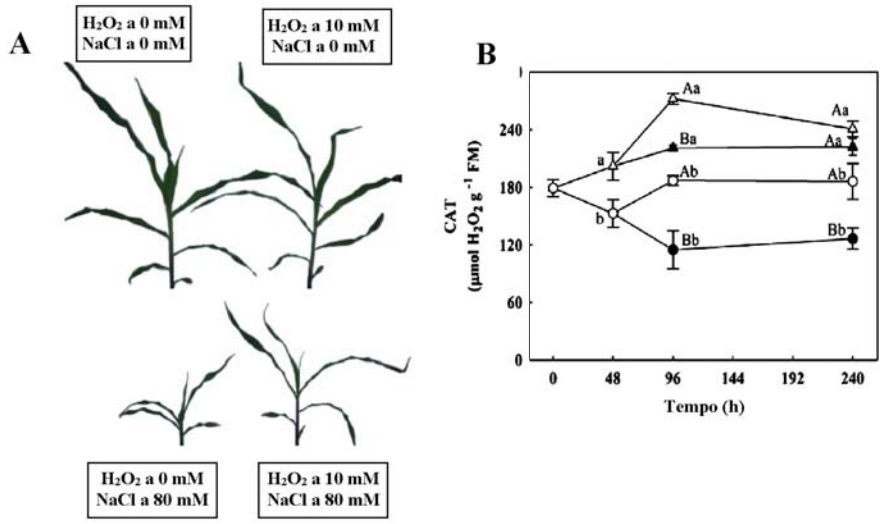

Figura 7. Crescimento (A) e atividade da catalase (CAT; B) em folhas de plantas de milho pré-tratadas com H_2O_2 (0 ou 10 mM) via pulverização foliar e submetidas à salinidade (NaCl a 0 ou 80 mM). As plantas foram coletadas antes (0 h) e após (48 a 240 h) a pulverização da solução de H_2O_2, e o tratamento salino iniciou-se decorridas 48 h do pré-tratamento. Tratamentos: ( ) H_2O_2 a 0 mM/NaCl a 0 mM; ( ) H_2O_2 a 10 mM/NaCl a 0 mM; ( ) H_2O_2 a 0 mM/NaCl a 80 mM; ( ) H_2O_2 a 10 mM/NaCl a 80 mM. Nos tempos de 96 e 240 h, letras minúsculas iguais, em um mesmo nível de salinidade, ou letras maiúsculas iguais, em um mesmo nível de pré-tratamento com H_2O_2, não diferem estatisticamente entre si ($p > 0,05$). Fonte: Gondim *et al.* (2012)

al., 2008), visando obter uma germinação rápida e um estande de plântulas uniforme; se os efeitos nocivos do estresse puderem ser atenuados nos estádios iniciais do desenvolvimento, as chances da planta estabelecer-se com sucesso são consideravelmente aumentadas (ASHRAF; FOOLAD, 2005). Ainda utilizando o H_2O_2, Gondim *et al.* (2010) observaram que o pré-tratamento das sementes com essa substância, na concentração de 100 mM, acelerou a germinação de milho, e essa resposta esteve associada, pelo menos em parte, a um aumento significativo na atividade das enzimas catalase e peroxidase do ascorbato. Ademais, plantas oriundas de sementes pré-tratadas com H_2O_2 a 100 mM também foram mais tolerantes à salinidade que aquelas oriundas de sementes não pré-tratadas, indicando que os efeitos desse pré-tratamento na semente perduraram até as plantas terem se desenvolvido.

3 CONSIDERAÇÕES FINAIS

Os estudos de fisiologia e bioquímica das plantas são a base para o entendimento dos mecanismos de tolerância à salinidade. Atualmente há um número cada vez maior de pesquisadores dedicados a entender tais mecanismos, e muitos têm usado da manipulação gênica e de outras ferramentas de biologia molecular para o alcance desse objetivo, porém é necessário ter em mente que a tolerância é uma resposta complexa e multigênica, além de ser uma característica do indivíduo, e não de um tecido ou órgão. Sendo assim, não se deve estudar a base genética e molecular da tolerância à salinidade de maneira isolada e particular, e, sim, de maneira integrada, visando entender como os genes (e proteínas) do estresse contribuem e se relacionam para conferir tolerância à salinidade. A abordagem proteômica tem contribuído para isso, por permitir a identificação de proteínas relacionadas com a tolerância à salinidade, especialmente ao se estudar genótipos com tolerância diferencial.

Apesar de ainda não haver produtos comerciais viáveis, resultantes da manipulação gênica voltada ao aumento da tolerância à salinidade, há alternativas que têm se mostrado promissoras para a indução de aclimatação a esse estresse, como o pré-tratamento das plantas ou sementes com substâncias indutoras de tolerância cruzada, e os resultados obtidos têm apresentando potencial para uso no campo.

4 AGRADECIMENTOS

Ao Conselho Nacional de Desenvolvimento Científico e Tecnológico (CNPq), à Coordenação de Aperfeiçoamento de Pessoal de Nível Superior (CAPES) e à Fundação Cearense de Apoio ao Desenvolvimento Científico e Tecnológico (FUNCAP), que direta ou indiretamente financiaram parte das pesquisas aqui relatadas.

REFERÊNCIAS

ABREU, C.E.B.; ARAÚJO, G.S.; MONTEIRO-MOREIRA, A.C.O.; COSTA, J.H.; LEITE. H.B.; MORENO, F.B.M.B.; PRISCO, J.T.; GOMES-FILHO, E. Proteomic analysis of salt stress and recovery in leaves of *Vigna unguiculata* cultivars differing in salt tolerance. **Plant Cell Reports**, v. 33, p. 1289-1306, 2014.

APEL, K.; HIRT, H. Reactive oxygen species: metabolism, oxidative stress, and signal transduction. **Annual Review of Plant Biology**, v. 55, p. 373-399, 2004.

APSE, M.P.; AHARON, G.S.; SNEDDEN, W.A. BLUMWALD, E. Salt tolerance conferred by overexpression of a vacuolar Na^+/H^+ antiport in *Arabidopsis*. **Science**, v. 285, p. 1256-1258, 1999.

ASADA, K. The water-water cycle in chloroplasts: scavenging of active oxygen and dissipation of excess photons. **Annual Review of Plant Physiology and Molecular Biology**, v. 50, p. 187-204, 1999.

ASHRAF, M.; ATHAR, H.R.; HARRIS, P.J.C.; KWON, T.R. Some prospective strategies for improving crop salt tolerance. **Advances in Agronomy**, v. 97, p. 45-110, 2008.

ASHRAF, M.; FOOLAD, M.R. Pre-sowing seed treatment — a shotgun approach to improve germination, plant growth, and crop yield under saline and non-saline conditions. **Advances in Agronomy**, v. 88, p. 223-271, 2005.

AZEVEDO NETO, A. D. Aspectos fisiológicos e bioquímicos do estresse salino em plantas de milho. 2005. 125 f. Tese (Doutorado em Bioquímica) – Universidade Federal do Ceará, Fortaleza, 2005.

AZEVEDO NETO, A.D.; GOMES FILHO, E.; PRISCO, J.T. Salinity and oxidative stress. In: KHAN, N. A.; SINGH, S. (Org.). **Abiotic stress and plant responses**. Aligarh: IK International Group, 2008, p. 58-82.

AZEVEDO NETO, A.D.; PRISCO, J.T.; ENÉAS-FILHO, J.; MEDEIROS, J.-V.R.; GOMES-FILHO, E. Hydrogen peroxide pre-treatment induces salt-stress acclimation in maize plants. **Journal of Plant Physiology**, v. 162, p. 1114-1122, 2005.

BRAY, E.A.; BAILEY-SERRES, J.; WERETILNYK, E. Responses to abiotic stress. In: BUCHANAN, B.; GRUISSEM, W.; JONES, E. (Ed.). **Biochemistry and molecular biology of plants.** Rockville: American Society of Plant Physiologists, 2000. p. 1158-1203.

BUI, E.N. Soil salinity: A neglected factor in plant ecology and biogeography. **Journal of Arid Environments**, v. 92, p. 14-25, 2013.

COMINELLI, E.; CONTI, L.; TONELLI, C.; GALBIATI, M. Challenges and perspectives to improve crop drought and salinity tolerance. **New Biotechnology**, v. 30, p. 355-361, 2013.

FILIPPOU, P.; TANOU, G.; MOLASSIOTIS, A.; FOTOPOULOS, V. Plant acclimation to environmental stress using priming agents. In: TUTEJA, N.; GILL, S.S. (Ed.). **Plant acclimation to environmental stress**. New York: Springer Science + Business Media, 2013, p. 1-27.

FINKEL, T. Oxidant signals and oxidative stress. **Current Opinion in Cell Biology**, v. 15, p. 247-245, 2003.

FLOWERS, T.J. Improving crop salt tolerance. **Journal of Experimental Botany**, v. 55, p. 307-319, 2004.

GILL, S.S.; TUTEJA, N. Reactive oxygen species and antioxidant machinery in abiotic stress tolerance in crop plants. **Plant Physiology and Biochemistry**, v. 48, p. 909-930, 2010.

GONDIM, F.A.; GOMES-FILHO, E.; COSTA, J.H.; ALENCAR, N.L.M.; PRISCO, J.T. Catalase plays a key role in salt stress acclimation induced by hydrogen peroxide pretreatment in maize. **Plant Physiology and Biochemistry**, v. 56, p. 62-71, 2012.

GONDIM, F.A.; GOMES FILHO, E.; LACERDA, C.F.; PRISCO, J.T.; AZEVEDO NETO, A.D.; MARQUES, E.C. Pretreatment with H_2O_2 in maize seeds: effects on germination and seedling acclimation to salt stress. **Brazilian Journal of Plant Physiology**, v. 22, p. 103-112, 2010.

HALLIWELL, B.; GUTTERIDGE, J.M.C. **Free radicals in Biology and Medicine**. Oxford: Clarendon Press. 1989. 543 p.

HASEGAWA, P.M. Sodium (Na^+) homeostasis and salt tolerance of plants. **Environmental and Experimental Botany**, v. 92, p. 19-31, 2013.

HASEGAWA, P.M.; BRESSAN, R.A.; ZHU, J.-K.; BOHNERT, H.J. Plant cellular and molecular responses to high salinity. **Annual Review of Plant Physiology and Plant Molecular Biology**, v. 51, p. 463-499, 2000.

HAYAT, S.; HAYAT, Q.; ALYEMENI, M.N.; WANI, A.S.; PITCHEL, J.; AHMAD, A. Role of proline under changing environments: a review. **Plant Signaling and Behavior**, v. 7, p. 1456-1466, 2012.

KOSOVÁ, K.; VÍTÁMVÁS, P.; PRÁŠIL, I.T.; RENAUT, J. Plant proteome changes under abiotic stress — Contribution of proteomics studies to understanding plant stress response. **Journal of Proteomics**, v. 74, p. 1301-1322, 2011.

KRONZUCKER, H.J.; BRITTO, D.T. Sodium transport in plants: a critical review. **New Phytologist**, v. 189, p. 54-81, 2011.

LARCHER, W. **Ecofisiologia Vegetal**. São Carlos: Rima Artes e Textos, 2000. 531p.

LEE, S.-H.; AHSAN, N.; LEE, K.-W.; KIM, D.-H.; LEE, D.-G.; KWAK, S.-S.; KWON, S.-Y.; KIM, T.-H.; LEE, B.-H. Simultaneous overexpression of both CuZn superoxide dismutase and ascorbate peroxidase in transgenic tall fescue plants confers increased tolerance to a wide range of abiotic stresses. Journal of Plant Physiology, v. 164, p. 1626-1638, 2007.

LI, W.; WANG, D.; JIN, T.; CHANG, Q.; YIN, D.; XU, S.; LIU, B.; LIU, L. The vacuolar Na^+/H^+ antiporter gene *SsNHX1* from the halophyte *Salsola soda* confers salt tolerance in transgenic alfalfa (*Medicago sativa* L.). **Plant Molecular Biology Reporter**, v. 29, p. 278-290, 2011.

LUO, X.; WU, J.; LI, Y.; NAN, Z.; GUO, X.; WANG, Y.; ZHANG, A.; WANG, Z.; XIA, G.; TIAN, Y. Synergistic effects of *GhSOD1* and *GhCAT1* overexpression in cotton chloroplasts on enhancing tolerance to methyl viologen and salt stresses. **Plos One**, v. 8, e54002. doi:10.1371/journal.pone.0054002

MAATHUIS, F.J. Sodium in plants: perception, signaling, and regulation of sodium fluxes. **Journal of Experimental Botany**, v. 65, p. 849-858, 2014.

MAHAJAN, S.; TUTEJA, N. Cold, salinity and drought stresses: an overview. **Archives of Biochemistry and Biophysics**, v. 444, p.139-158, 2005.

MANSOUR, M.M.F.; SALAMA, K.H.A. Cellular basis of salinity tolerance in plants. **Environmental and Experimental Botany**, v. 52, p. 113-122, 2004.

MILLER, G.; SHULAEV, V.; MITTLER, R. Reactive oxygen signaling and abiotic stress. **Physiologia Plantarum**, v. 133, p. 481-489, 2008.

MITTLER, R. Oxidative stress, antioxidants and stress tolerance. **Trends in Plant Science**, v. 7, p. 405-410, 2002.

MITTOVA, V.; TAL, M.; VOLOKITA, M.; GUY, M. Salt stress induces up-regulation of an efficient chloroplast antioxidant system in the salt-tolerant wild tomato species *Lycopersicon pennellii* but not in the cultivated species. **Physiologia Plantarum**, v. 115, p. 393-400, 2002.

MØLLER, I.M.; JENSEN, P.E.; HANSSON, A. Oxidative modifications to cellular components in plants. **Annual Review of Plant Biology**, v. 58, p. 459-491, 2007.

MUNNS, R. Comparative physiology of salt and water stress. **Plant, Cell and Environment**, v. 25, p. 239-250, 2002.

MUNNS, R.; JAMES, R.A.; XU, B.; ATHMAN, A.; CONN, S.J.; JORDANS, C.; BYRT, C.S.; HARE, R.A.; TYERMAN, S.D.; TESTER, M.; PLETT, D.; GILLIHAN, M. Wheat grain yield on saline soils is improved by an ancestral Na^+ transporter gene. **Nature Biotechnology**, v. 30, p. 360-366, 2012.

MUNNS, R.; TESTER, M. Mechanisms of salinity tolerance. **Annual Review of Plant Biology**, v. 59, p. 651–681, 2008.

NOCTOR, G.; FOYER, C.H. Ascorbate and glutathione: keeping active oxygen under control. **Annual Review of Plant Physiology and Plant Molecular Biology**, v. 49, p. 249-279, 1998.

OTOCH, M.L.O.; SOBREIRA, A. M.; ARAGÃO, E.M.F.; ORELLANO, E.G.; LIMA, M.G.S.; MELO, D.F. Salt modulation of vacuolar H^+-ATPase and H^+-Pyrophosphatase activities in *Vigna unguiculata*. **Journal of Plant Physiology**, v. 158, p. 545-551, 2001.

PARIDA, A.K.; DAS, A.B. Salt tolerance and salinity effects on plants: a review. **Ecotoxicology and Environmental Safety**, v. 60, p. 324-349, 2005.

PLAUT, Z.; EDELSTEIN, M.; BEN-HUR, M. Overcoming salinity barriers to crop production using traditional methods. **Critical Reviews in Plant Sciences**, v. 32, p. 250-291, 2013.

PRISCO, J.T.; GOMES-FILHO, E. Fisiologia e bioquímica do estresse salino em plantas. In: GHEYI, H.R.; DIAS, N.S.; LACERDA, C.F. (Org.). **Manejo da salinidade na agricultura irrigada**: estudos básicos e aplicados. Fortaleza: INCTSal, 2010. p. 143-160.

RENGASAMY, P. World salinization with emphasis on Australia. **Journal of Experimental Botany**, v. 57, p. 1017-1023, 2006.

ROY, S.J.; NEGRÃO, S.; TESTER, M. Salt resistant crop plants. **Current Opinion in Biotechnology**, v. 26, p. 115-126, 2014.

ROZEMA, J.; FLOWERS, T. Crops for a salinized world. **Science**, v. 322, p. 1478-1480, 2008.

SILVEIRA, J.A.G.; FERREIRA-SILVA, S.L.; SILVA, E.N.; VIÉGAS, R.A. Mecanismos biomoleculares envolvidos com a resistência ao estresse salino em plantas. In: GHEYI, H.R.; DIAS, N.S.; LACERDA, C.F. (Org.). **Manejo da salinidade na agricultura irrigada**: estudos básicos e aplicados. Fortaleza: INCTSal, 2010. p. 161-180.

SHANNON, M.C.; GRIEVE, C.M. Tolerance of vegetable crops to salinity. **Scientia Horticulturae**, v. 78, p. 5-38, 1999.

SZABADOS, L.; SAVOURÉ, A. Proline: a multifuncional amino acid. Trends in Plant Science, v. 15, p. 89-97, 2010.

TAIZ, L.; ZEIGER, E. **Fisiologia Vegetal.** 5. ed. Porto Alegre: Artmed, 2013. 918p.

TÜRKAN, I.; DEMIRAL, T. Recent developments in understanding salinity tolerance. **Environmental and Experimental Botany**, v. 67, p. 2-9, 2009.

VAIDYANATHAN, H.; SIVAKUMAR, P.; CHAKRABARTY, R.; THOMAS, G. Scavenging of reactive oxygen species in NaCl-stressed rice (*Oryza sativa* L.) — differential response in salt-tolerant and sensitive varieties. **Plant Science**, v. 165, p. 1411-1418, 2003.

WHITE, P.J.; BROADLEY, M.R. Cloride in soils and its uptake and movement within the plant: a review. **Annals of Botany**, v. 88, p. 967-988, 2001.

XU, C.; ZHENG, L.; GAO, W.; LIU, G.; JIANG, J.; WANG, Y. Ovexpression of a vacuolar H^+-ATPase c subunit gene mediates physiological changes leading to enhanced salt tolerance in transgenic tobacco. **Plant Molecular Biology Reporter**, v. 29, p. 424-430, 2011.

YADAV, S.; IRFAN, M.; AHMAD, A.; HAYAT, S. Causes of salinity and plant manifestations to salt stress: a review. **Journal of Environmental Biology**, v. 32, p. 667-685, 2011.

YUE, Y.; ZHANG, M.; ZHANG, J.; DUAN, L.; LI, Z. *SOS1* gene overexpression increased salt tolerance in transgenic tobacco by maintaining a higher K^+/Na^+ ratio. **Journal of Plant Physiology**, v. 169, p. 255-261, 2012.

7

An Overview in to Energization of Proton Pumps in Plant Cell Membranes and Its Significance under Salt Stress

Luciana Maia Nogueira de Oliveira[1], Deborah Moura Rebouças[2], Francisco Yuri Maia de Sousa[2], Alana Cecília de Menezes Sobreira[1], Maria de Lourdes Oliveira Otoch[2] & Dirce Fernandes de Melo[2]

[1] Universidade Federal Rural de Pernambuco, Garanhuns, PE, Brasil
[2] Universidade Federal do Ceará, Fortaleza, CE, Brasil

INOVAGRI Book 2014 - Irrigation and Salinity:
Researches and Technological Innovations
ISBN 978-85-67668-09-3

INOVAGRI
INSTITUTO DE PESQUISA E INOVAÇÃO NA AGRICULTURA IRRIGADA

Fortaleza - CE
2015

7 An Overview in to Energization of Proton Pumps in Plant Cell Membranes and Its Significance under Salt Stress

1 INTRODUCTION

Food security is a major concern of plant physiologist in a climate-changing world and a growing population. World population is rapidly expanding being estimated to reach 9.6 billion by the year 2050 (DEINLEIN *et al.*, 2014). This scenario claims for an urgent increase of crop productivity through selection of tolerant cultivars or genetic engineering of cultivars tolerant to environmental stresses. Environmental constraints (e.g. drought or soil/water salinity) imply, primarily, in a decrease of water uptake resulting in high salt concentration, which disrupt the ionic and osmotic equilibrium. Consequently, these constraints lead to a reduced production of biomass and crop yield (COMINELLI *et al.*, 2013; DEINLEIN *et al.*, 2014; ROY; NEGRÃO; TESTER, 2014).

Salinity, drought and chilling are among the most hostile environmental factors that limit plant development and decrease crop productivity. Natural environmental stresses are aggravated by anthropogenic activities and in some cases leads to a lost of arable land (MAHAJAN; TUTEJA, 2005). Low temperature, generally, affects plant development through a mechanical constraint, otherwise, salinity and drought affect plant development at the cellular level. Soil salinity severely disturbs crop performance decreasing plant development and crop yield and it is expected to increase in future years, mainly due to climate changes, as well as a consequence of irrigation practices (DEINLEIN *et al.*, 2014; ROY; NEGRÃO; TESTER, 2014; SCHROEDER *et al.*, 2013) (Figure 1).

To overcome the abiotic stresses, plants have developed a highly flexible metabolism that makes it possible for them to metabolically acclimate to environmental changes. They developed the ability to sense both: the hyper-osmotic and the ionic Na^+ components (DEINLEIN *et al.*, 2014). Very little is known about the "osmotic phase" tolerance. The signal cascade involved may have a fast long-distance signaling, maybe through ROS and Ca^{2+} waves, or perhaps through long distance electrical signaling (KNIGHT; TREWAVAS; KNIGHT, 1997; MITTLER *et al.*, 2011).

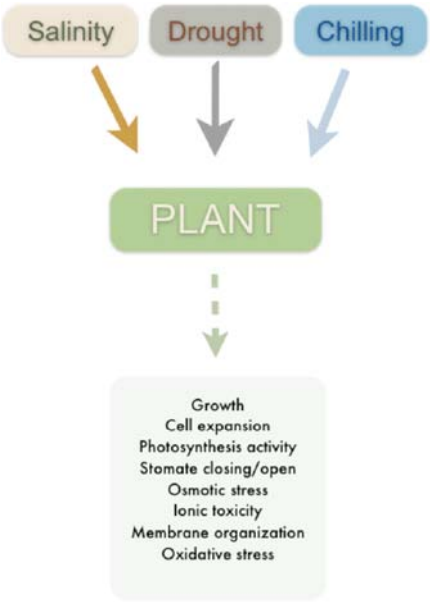

Figure 1. Overview of the different effects of stresses on plants. Salinity, drought and chilling are important environmental factors that limit plant development. Among the effects on plant metabolism are inhibition on growth, cell expansion and photosynthesis, disorder in cell membranes and osmotic stress. Salinity includes two main effects to plant: osmotic stress and ionic toxicity. One secondary effect of many stress conditions is the oxidative stress, caused by imbalance in production and scavenging of reactive oxygen species (ROS)

Aside osmotic adjustment, a key factor conferring salt tolerance is the control of intracellular ion homeostasis. Ion homeostasis could be reached by a selective ion transport and a reduction of the Na^+ and Cl^- accumulation in the leaf blade by ion exclusion and/or by ion compartmentalization into vacuoles (tissue tolerance). Exclusion of Na^+ from cytosol is therefore crucial for the maintenance of an adequate cell metabolism. The strategies that plant cells employ for ion exclusion involve a range of transporters at both plasma membrane and tonoplast (YAMAGUCHI; HAMAMOTO; UOZUMI, 2013). Exclusion of Na^+ from cytosol across the plasma membrane is driven by the SOS1 (Salt-Overly-Sensitive) transporters (QIU, Q.-S. *et al.*, 2004) or compartmentalization of Na^+ into the vacuoles by NHX-type intracellular Na^+/H^+ exchangers. The NHX-type exchangers are the best-characterized proteins involved in this process so far (BLUMWALD; AHARON; APSE, 2000). The Na^+/H^+ exchange activities are driven by the electrochemical proton gradient generated by the proton pumps such as the plasma membrane H^+ATPase or the tonoplast H^+-ATPase and H^+-pyrophosphatase (BLUMWALD; AHARON; APSE, 2000; SCHUMACHER,

2006). These mechanisms are considered to be responsible for Na^+ exclusion out of the cell or sequestration into intracellular compartments for plant tolerance under salinity stress (BASSIL; COKU; BLUMWALD, 2012; QIU, Q.-S. *et al.*, 2003, 2004). Recent advances in molecular biology and genome sequencing have recognized genes involved in salt acclimation, which, some of them, have been identified by genetic loss- and gain-of-function approaches. These genes are responsible for production of Na^+ transporters proteins that mediate its homeostasis. Another point, not less important, is the energetic demands since energy is consumed in ion transport to regulate net uptake and cellular compartmentation of Na^+ and Cl^-, as well as in the synthesis of compatible solutes (FLOWERS; COLMER, 2008).

In this chapter, we highlight the biochemical mechanisms, the transcript and protein expressions involving the proton pumps and the secondary transporters of plasma membrane and tonoplast which control plant acclimation and development under salt stress conditions. In addition, we discuss the salinity effects on plants and the mechanisms to improve salinity tolerance. Finally, we summarize the majors results obtained by our group emphasizing the latest advances in the understanding of the plants acclimation mechanisms to fight excess salt and damage generated by salt stress in cowpea cultivars with different degrees of tolerance.

2 PLANT SALINITY STRESS AND MECHANISMS OF SALT TOLERANCE

Salt tolerance is the ability of plants to grow and complete their life cycle on a substrate that contains high concentrations of soluble salt. Plants that growth in a soil with a NaCl concentration around 200mM or more are classified as halophyte, while plants that are sensible to salt in lower concentration than 200 mM are referred as glycophyte (FLOWERS; COLMER, 2008; FLOWERS; GALAL; BROMHAM, 2010; MUNNS; TESTER, 2008). The deleterious effects of salinity in plants are extensive and affect several processes, such as: photosynthesis, protein synthesis as well as energy and lipid metabolism. Considering that salt stress has many different effects on a plant, so there are also many mechanisms of tolerance as: osmotic tolerance, ion exclusion and tissue tolerance (ROY; NEGRÃO; TESTER, 2014). In this scenario, it is well known that the passive entry of Na^+ from soil into the cytoplasm of root epidermal and cortical cells is favoured by both gradient concentration and diferential voltage across the plasma membrane (CRAIG PLETT; MØLLER, 2010).

The influx of Na^+ to the root cells appears to be mediated by Ca^{2+} sensitive and insensitive processes. Indeed, calcium (Ca^{2+}) has been shown to provide salt tolerance to plant by reducing the Na^+ toxic effect, at least in part, due to the inibition of unidirectional Na^+ influx through Non Selective Cation Channels (NSCCs) (DEMIDCHIK; MAATHUIS, 2007). It must be pointed out that Na^+ influx into cells could also happen through Cyclic-Nucleotide Gated Channels (CNGCs), Non Selective Cation Channels (NSCCs), Glutamate Receptors (GLRs) which possess the properties

of NSCCs and High Affinity Potassium Transporter (HKT) (*AtHKT1;1*, *OsHKT1;4*, *OsHKT1;5* and *OsHKT2;1*).

Sodium competes with potassium for intracellular influx (AMTMANN; SANDERS, 1998; BLUMWALD; AHARON; APSE, 2000; NIU *et al.*, 1995). The influx of both can be differentiated into two categories, one with high affinity for K^+ over Na^+ and the other with lower K^+/Na^+ selectivity. The Na^+/K^+ transporter and K^+ transporters with high and low affinity may contribute substantially to Na^+ influx. It is known that K^+ is required for maintaining the osmotic balance, having a role in opening and closing of stomata and is yet an essential co-factor for many enzymes, whereas Na^+ is toxic to cell metabolism and has deleterious effect on the functioning of some enzymes (MAHAJAN; TUTEJA, 2005). The presence of Na^+ in the cytoplasm is harmful to plant cells due, not only to its toxicity but, also by the disruption of ionic equilibrium, osmotic imbalance, membrane disorganization, production of reactive oxygen species (ROS), inhibition of cell division and expansion, all of them leading to reduction in growth and reduction in photosynthesis. To improve salt stress tolerance others factors besides interplay of these ions are important and continue to be investigated. Liu and Zhu in 1998, using mutants screening, identified SOS (Salt Overly Sensitive) genes via positional cloning. SOS function is to promote the exclusion of excess Na^+ ions out of the cell through plasma membrane, via a Na^+/H^+ antiporter activity, helping to restabilish cellular ion homeostasis (MAHAJAN; TUTEJA, 2005). *AtSOS1* activity is regulated by other genes, also identified in the same screening (QIU, Q.-S. *et al.*, 2002). AtSOS3 is a Ca^{2+} binding protein (LIU; ZHU, 1998; WU, S. J.; DING; ZHU, 1996) that recruit AtSOS2, a serine/treonine protein kinase (LIU *et al.*, 2000), to the plasma membrane where AtSOS2 activates AtSOS1 by phosphorylation (QUINTERO *et al.*, 2002) and increases Na^+/H^+ exchange activity (QIU, Q.-S. *et al.*, 2003). In short, SOS1 mediates Na^+ efflux to the apoplast against the electrochemical potential through secondary active transport that is driven by the H^+ gradient across the plasma membrane (HASEGAWA, 2013).

It must be highlighted that *HKT* gene family (MUNNS; TESTER, 2008; PLATTEN *et al.*, 2006; XUE *et al.*, 2011) and SOS pathway (JI *et al.*, 2013; KUDLA; BATISTIC; HASHIMOTO, 2010; MAHAJAN; PANDEY; TUTEJA, 2008; QIU, Q.-S. *et al.*, 2002; SHI *et al.*, 2003; WEINL; KUDLA, 2009; YANG *et al.*, 2009) have been pointed out as having an important role in regulating Na^+ transport within a plant. Members of the HKT gene family have been shown to be responsible for Na^+ retrieval from the xylem and reducing transfer of Na^+ to the shoot tissue (PLATTEN *et al.*, 2006). It is possible that the individual proton-ion exchangers *(HTX)* genes might function in K^+ transport, Na^+ influx or Na^+ retrieval from the xylem according to their ion selectivity and expression pattern (CRAIG PLETT; MØLLER, 2010).

Once entering the roots Na^+ is transported to leaves, the Na^+ concentration within the cytoplasm of cells will be augmentaded and the most important strategie to the survival is the maintenance of low concentrations of Na^+. Overall, osmotic

homeostasis after salt stress is mediated by Na^+ efflux across plasma membrane and/or by its into vacuoles (MAHAJAN; TUTEJA, 2005). Central to this process is the vacuolar Na^+/H^+ antiporter (NHX) which moves Na^+ into the vacuole in exchange for H^+ (BLUMWALD; AHARON; APSE, 2000) (Figure 2).

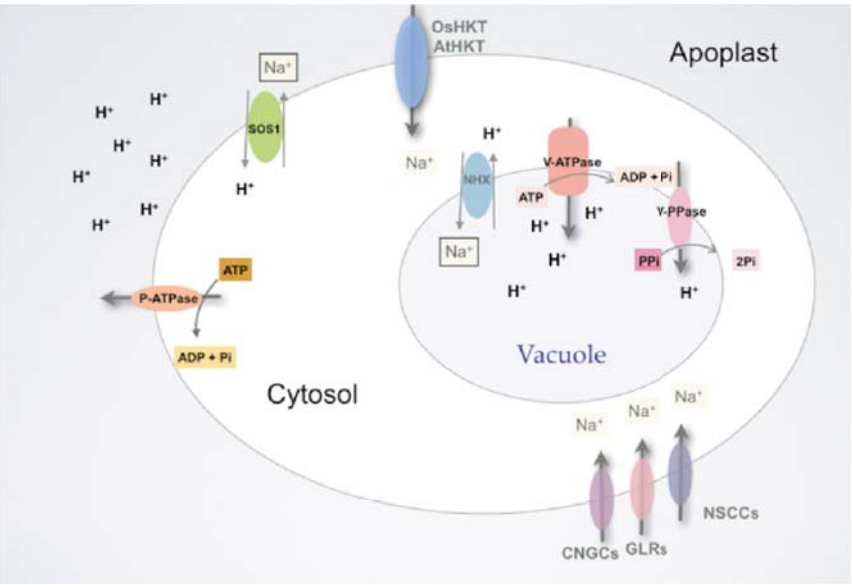

Figure 2. Primary and secondary transporters involved in the mechanism of Na^+ transport. The presence of Na^+ in the cytosol is harmful to plant cells and its concentration must be controlled. The Na^+ transport from the cytosol to apoplast or vacuole is mediated by primary and secondary transport systems. The proton pumps (P-ATPase, VATPase and V-PPase) play an important role as primary transporters and the formation of the electrochemical gradient that can be used by the secondary transport to drive Na^+ out of the cytoplasm through Na^+/H^+ antiporter (like SOS1, NHX) activities. On the other hand, HKT transporters, non-selective cation channels (NSCCs), cyclic-nucleotide gated channels (CNGCs), glutamate receptors (GLRs) have been shown to be responsible for Na^+ retrieval

3 HOW DO VACUOLAR AND PLASMA MEMBRANE PROTON PUMPS AND SECONDARY TRANSPORTERS FUNCTION IN PLANT SALT TOLERANCE?

The cellular proton pumps promote the energy available to transport Na^+ across the plasma membrane into the apoplast through SOS1, as well as, to Na^+ sequestration into the vacuole through NHX transporter. Mutational approaches involving ion transporters reveals that theirs overexpression led to increased plant salinity tolerance. The H^+ gradient requested to the work of NHX and SOS1 is maintened by both

vacuolar H^+ pumps (H^+-ATPase and H^+-PPase) and by the plasma membrane ATPase (P-ATPase). These key proton transport proteins and the SOS1 and NHX transporters are target proteins to understand salt tolerance mechanisms, which are below described:

V-ATPase

In plant cells, the vacuolar H^+-ATPase is an ATP-dependent proton pump that acidify vacuolar compartment through the transport of protons across the tonoplast (RATAJCZAK, 2000). This enzyme is composed of a peripheral V_1 domain, which is responsible for the ATP hydrolysis, and a hydrophobic membrane-embedded V_0 domain, which is responsible for proton translocation (CIPRIANO *et al.*, 2008; FORGAC, 1999). The V_1 domain contains three copies of the A and B subunits, responsible for the catalytic activity, and the subunits C, D, E, F, G and H which form a central stalk linking the V_1 to V_0 domain. The V_0 domain is composed of six subunits (a, c, c', c'', d and e), which forms a proton-conducting channel into the vacuole (FORGAC, 1999; GAXIOLA; PALMGREN; SCHUMACHER, 2007; QI; WANG; FORGAC, 2007).

The enzymatic mechanism for proton pumping induces conformational changes due to a rotatory mechanism when ATP is supplied. A number of mechanisms are employed to regulate VATPase activity, including reversible dissociation of the V_1 and V_0 domains and control of the tightness of coupling of proton transport and ATP hydrolysis (CIPRIANO *et al.*, 2008; TOEI; SAUM; FORGAC, 2010). A precise regulation of V-ATPase is important for plant development and adaptation to stress. Presumably, this ATPase provides the proton gradient required for a Na^+/H^+ antiporter to Na^+ compartmentalization into vacuole, which facilitates detoxification of the cytoplasm and osmotic adjustment (BLUMWALD; AHARON; APSE, 2000; CRAIG PLETT; MØLLER, 2010).

V-PPase

The vacuolar pyrophosphatase (V-PPase) is an electrogenic proton pump, which uses inorganic pyrophosphate as a substrate to generate the proton electrochemical gradient across the vacuolar membrane, acidifying vacuoles in plant cells (MAESHIMA, 2000). In contrast to the VATPase, the V-PPase consists of a single polypeptide and exists as a dimmer of 80 kDa subunits with 16 transmembrane helices (KAJANDER; KELLOSALO; GOLDMAN, 2013). Generally, VPPase activity is high in young tissues, where PPi is synthesized in many metabolic reactions, such as DNA and RNA synthesis (MARTINOIA; MAESHIMA; NEUHAUS, 2007).

V-PPases occur in species where energy limitation is frequent and are important under stress conditions (drought, salt stress) providing ion gradients when ATP is scarce (GUO *et al.*, 2006). The regulatory mechanism of V-PPase gene expression and the post-translational regulation change according to the physiological conditions and in response to environmental stresses (PARK *et al.*, 2005). Indeed, V-PPase plays an

important role in the maintenance of the proton gradient across the vacuolar membrane and the compartmentalization of Na^+ within vacuoles.

NHX Antiporter

In plants, vacuolar Na^+/H^+ antiporter (NHX – sodium hydrogen exchanger) is a secondary transport system that move H^+ down its electrochemical potential, generated by vacuolar proton pumps, into the cytoplasm and Na^+ against its electrochemical potential into the vacuole (BASSIL; COKU; BLUMWALD, 2012; YAMAGUCHI *et al.*, 2005). Structural analysis performed with Arabidopsis NHX protein indicates 12 hydrophobic regions that potentially constitute the transmembrane helices in the conserved hydrophobic N-terminal domain, with a divergent hydrophilic C-terminal domain that would be involved in regulatory interactions (RODRÍGUEZROSALES *et al.*, 2009).

The ability to compartmentalize salt into the vacuoles is an important step towards the maintenance of ion homeostasis inside the cell (BASSIL; COKU; BLUMWALD, 2012). While salt-sensitive plants depend mainly on exclusion of Na^+ ions at the plasma membrane, salt-tolerant species accumulate large amounts of Na^+ in the vacuoles (BLUMWALD, 2000). Several studies have shown that the exposure to salt increases Na^+/H^+ antiport activity (QUEIRÓS *et al.*, 2009; SILVA *et al.*, 2009), up-regulates *NHX* genes (QIU, N. *et al.*, 2007; YU *et al.*, 2007) or increases protein abundance (QIU, N. *et al.*, 2007), suggesting a role of the exchanger in salt tolerance. Furthermore, it has been shown that *NHX* genes family also play a crucial role in pH regulation and K^+ homeostasis, regulating processes from vesicle trafficking and cell expansion of plant development (RODRÍGUEZ-ROSALES *et al.*, 2009).

P-ATPase

In plants, the plasma membrane ATPase (P-ATPase) is the primary pump responsible for the establishment of cellular membrane potential. P-ATPase uses energy derived from ATP hydrolysis to pump protons from the cytosol to the apoplast (GAXIOLA; PALMGREN; SCHUMACHER, 2007). This activity creates a proton electrochemical gradient across the plasma membrane that is utilized by membrane proteins for secondary transport, facilitating solute and ion exchange across the membrane (BLUMWALD; AHARON; APSE, 2000).

The P-ATPase is a single subunit protein with approximately 950 amino acid residues. The protein contains ten trans-membrane helices and a large cytoplasmic domain. The cytoplasmic domain consists of four domains: the nucleotide binding domain (N-domain), the phosphorylation domain (P-domain), the actuator domain (A-domain) and the regulatory domain (R-domain) (FUGLSANG; PAEZ-VALENCIA; GAXIOLA, 2011). P-ATPase activity is positively and negatively influenced by phosphorylation at multiple sites and regulation is likely fine-tuned by distinct kinases and phosphatases. In addition to regulation via phosphorylation, protein abundance

and/or localization within the plasma membrane may also play an important role in regulating the enzyme activity (ELMORE; COAKER, 2011). Besides regulation of physiological processes, PATPase also plays a role in adaptation of plants to changing conditions, especially stress conditions (JANICKA-RUSSAK, 2011).

SOS1 Transporter

The SOS1 is a plasma membrane Na^+/H^+ antiporter that belongs to Salt Overly Sensitive (SOS) pathway and is essential in regulating Na^+ efflux at cellular level as well as in facilitating long distance transport of Na^+ from root to shoot (GUPTA; HUANG, 2014). The Na^+/H^+-exchange activity is driven by the electrochemical proton gradient generated by the plasma membrane H^+ATPase (BLUMWALD; AHARON; APSE, 2000). The SOS1 activity is regulated by SOS2, a protein kinase, and SOS3, a calcium-binding protein (CRAIG PLETT; MØLLER, 2010). The Na^+/H^+ antiporter SOS1 is essential for the salt tolerance of various model plants protecting individual cells from Na^+ toxicity (QUINTERO *et al.*, 2011). At the cellular level, the SOS signaling pathway has been proposed to mediate cellular signaling under salt stress and to maintain ion homeostasis (CHINNUSAMY; SCHUMAKER; ZHU, 2004; JI *et al.*, 2013).

The latest findings accumulated over the years, has shown a high complexity of the regulatory networks in plants response to salinity. The SOS signal transduction resembles a web of signaling components allowing input from many stress sensors. Additional components must be linked somehow to SOS1, whose function is a prerequisite for salt tolerance.

4 THE SIGNIFICANCE OF VACUOLAR PROTON PUMPS AND NA^+/H^+ ANTIPORTER ON PLANT PHYSIOLOGICAL RESPONSES TO ABIOTIC STRESSES

Salinity

Cowpea, *Vigna unguiculata* (L.) Walp is one of the most widely used legumes in the tropical world. It is considered one important source of protein for human consumption. The genus *Vigna* presents several species and cultivars endowed with different degrees of salt/drought tolerance. Vita 3 and Vita 5 cultivars has been recognized as more and less tolerant to salt stress respectively (FERNANDES DE MELO *et al.*, 1994). In order to understanding the mechanisms of plant salt tolerance, our group firstly investigated the role of both vacuolar proton pumps in Vita 3 and Vita 5 cultivars in the presence of 100mM NaCl that corresponded to growth inhibition around 50%. Previous work have already characterized that Vita 5 plants are more sensible to NaCl than Vita 3, 7 days after sowing (FERNANDES DE MELO *et al.*, 1994). Otoch and collaborators (2001) showed that the tonoplast H^+-pumping V-ATPase and V-PPase in hypocotyls of Vita 5 cultivar have a differential profile concerning different

plant stages of development as well as the role of those proton pumps revealing an independently salt modulation. In the early stages of development (3 days) V-PPase showed hydrolytic and proton transport activities higher than V-ATPase activities. However, in salt conditions these activities were strongly inhibited. After 7 days of salt treatment, V-ATPase activities (hydrolysis and transport) were up regulated while PPase activities decreased when compared to control conditions. The protein level analyses of V-ATPase A and B subunits under salt conditions revealed an increase on ATPase content in parallel to their activities while PPase protein level did not exhibited the same profile suggesting a partial inactivation.

Additional data concerning V-ATPase function were obtained with Vita 3 (considered more tolerant) and Pérola (less tolerant) cultivars of *V. unguiculata* submitted to salt stress (100mM) for two weeks (OLIVEIRA, 2007). It was observed a differential regulation on V-ATPase hydrolytic activity, protein levels of V-ATPase subunit A (VHA) and transcript amounts in leaves in response to salt stress. In this study, Vita 3 cultivar showed higher V-ATPase activity and protein level than cultivar Pérola. Our results concerning the transcript levels of A, B, C, D, E, F, G, H, a, c, e, d, f subunits of V-ATPase indicate an independent transcriptional regulation for the different subunits. The response to salinity stress showed to be an intricate network of up and down regulation of the V-ATPase subunits, probably due a stoichiometric regulation or a regulation role of some of the subunits. In sum, the fine regulation of those subunits transcription and translation is important for *V. unguiculata* plant to manage salt stress without spending too much energy even if a reorganization of the V-ATPase is mandatory for a better acclimation to the constraints.

More recently, our group explored the vacuolar proton pumps regulation in Vita 3 hypocotyls at different stages of development (3, 5 and 7 days-old plants) in response to salt stress. The data highlighted that these pumps were up regulated at gene levels in all days whereas protein levels in the latest days. Nevertheless, only V-PPase activities (hydrolytic and transport) were in parallel with increases in gene expression and protein amount (SOBREIRA *et al.*, 2014).

As it is known, besides the vacuolar proton pumps there is a plasma membrane ATPase and secondary transporters responsible for Na^+ efflux through plasma membrane (SOS1) and Na^+ vacuolar influx (NHX) involved in the Na^+ network transport processes to maintain low cytoplasmic Na^+ concentrations in plant cells. Therefore, our group analyzed SOS1, P-ATPase, NHX, PPase and V-ATPase subunit A genes expression in two other *V. unguiculata* cultivars, Pitiúba and Setentão, more and less tolerant to salt stress respectively. Our latest findings revealed that these genes were differentially induced by salinity according to cultivar and tissues. An overview of their transcripts expression revealed that all evaluated genes were enhanced in Pitiúba roots while in Setentão roots their expression was variable, being some genes similarly stimulated and others less or not stimulated. On the other hand, the transcripts expression of SOS1 and NHX in the leaves of Pitiúba was slightly stimulated whereas the other genes were not.

However, in Setentão leaves SOS1 and P-ATPase transcripts expression was augmented and V-ATPase and NHX had a lower increase. Pitiuba roots proton pumps and Na^+ transporters probably were greatly efficient proteins to put out the Na^+, hindering the ion flux to their leaves while Setentão roots appeared less efficient and once the ion Na^+ arrived in the leaves, SOS1 and P-ATPase transcripts were augmented while V-ATPase and NHX transcripts slightly increased as a survival mechanism. Furthermore, it was also observed that Pitiúba, in control conditions, still presented a major proline level than Setentão revealing that the first one seemed to be more prepared to alleviate the osmotic stress component of the salt stress. So, it is clear that both cultivars envisage distinct cellular ways in response to salt stress (TORQUATO, 2014).

Another evaluation was followed with Vita 5 cultivar submitted to salt stress concerning the multigenic family NHX. These results revealed that the expression profile for both *VuNHX2* and *VuNHX6* were different in roots and leaves. The transcript levels for *VuNHX2* in seedlings submitted to 100 mM NaCl during 6, 12 and 24h revealed a higher increase in roots than in leaves while transcript expression of *VuNHX6* was higher in leaves than in roots (SOBREIRA, 2009).

Taking all into consideration, we could suggest that both vacuolar proton pumps are effective to promote available energy to secondary transports and that the cellular choice vis-à-vis one of them would depend not only on the plant species, the tissue or the development stage but even on the harvest.

Drought

Drought stress induces cellular dehydration that reduces the cytosolic and vacuolar volumes and stimulates the production of ROS which affects negatively cellular structures and plant metabolism (BARTELS; SUNKAR, 2005).

Plants acquire resistance to stress environment by reprogramming metabolism and gene expression, gaining a new equilibrium between growth, development and survival (MITTLER, 2006). In our group, the effects of drought by 200.67 $g.L^{-1}$ PEG on the gene expression of vacuolar proton pumps (*VuVHA-A*, *VuVHA-E*, *VuVHP*) and NHX antiporter (*VuNHX2* and *VuNHX6)* in leaves and roots of cowpea plants were studied (SOBREIRA, 2009). The genes for V-ATPase (*VuVHA-A* and *VuVHA-E*) were responsive for plant tolerance to drought stress. However, the *VuVHA-E* expression was organ-dependent: an up regulation was found only in roots, while in leaves a down regulation could be observed. This suggests that the *V-ATPase* genes can have a differential regulation although ATP availability is higher in leaves due to photosynthesis. Also, an important role of the V-ATPase in the tolerance of cowpea plants to osmotic stress could be evidenced. An up regulation could also be observed in *NHX* genes in both roots and leaves under 200.67 $g.L^{-1}$ PEG. A link between osmotic stress and vacuole sequestration of Na^+ has also been demonstrated in Arabidopsis where osmotic stress activates the synthesis of ABA, which in turn up regulates the expression of *AtNHX1* (SHI; ZHU, 2002).

Since drought stress enhances ABA accumulation in plants and exogenous application of ABA can have similar effects as osmotic stress, such as in gene induction, it is reasonable to hypothesize that ABA mediates osmotic stress responses, regulating plant water balance and cellular dehydration tolerance (CONDE; CHAVES; GERÓS, 2011; ZHU, 2002). Take into account these findings, our group also evaluated the effects of ABA on V-ATPase and V-PPase activities in leaves and roots of cowpea plants (REBOUÇAS, 2011). Interestingly, an organ-dependent effect was found revealing a V-ATPase activity increased in leaves, while in roots V-PPase activity was enhanced. We supposed that this organ-dependent regulation could be attributed to substrate availability (ATP or PPi) since leaves could generate ATP as a photosynthetic product, differently from roots. The prevalence of V-PPase in developing tissues supports the idea that the physiological significance of this enzyme would be to maintain the proton gradient under conditions of limited ATP supply and that PPi may serve as the key energy source during developmental stages in root cells (MAESHIMA, 2000).

Chilling

Low temperature is an important environmental factor that influences the growth, development, survival and distribution of plants (LEE, D.-G. *et al.*, 2009; RENAUT *et al.*, 2004). Chilling induces a number of alterations in cellular components, including the modification of the unsaturated fatty acids content, changes in protein and carbohydrate composition, the activation of ion channels and activation of numerous cold-inducible genes (KASAMO; YAMAGUCHI; NAKAMURA, 2000; LEE, S. H.; CHUNG; STEUDLE, 2005).

Our group studied the alterations in lipids species on vacuolar membrane and the activities of vacuolar proton pumps (V-ATPase e V-PPase) induced by chilling in cowpea plants. Three-dayold-seedlings exposed to 10 °C and 4 °C for 4 days showed that the amount of unsaturated fatty linoleic (18:2) and linolenic acid (18:3), under these conditions, was higher than in the control condition (25 °C) (OLIVEIRA *et al.*, 2010). These changes could reflect an attempt to maintain the vacuolar membrane fluidity by a higher unsaturated/saturated fatty acid rate. Furthermore, it is well known the importance of lipids in the membrane structure as well as in modulation of membranebound enzymes, such as V-ATPase and V-PPase (OLIVEIRA *et al.*, 2011; ZHANG, J. *et al.*, 2006).

Many reports showed divergent opinions about the activities of vacuolar proton pumps in response to chilling in plants including V-ATPase inactivation, no effect and enhancement of VPPase and ATPase (OLIVEIRA *et al.*, 2011).

Another approach with cowpea 7d-old seedlings grown under moderate chilling treatment (10 ^{o}C or 4 ^{o}C for 4 d) or longer chilling stress (10 ^{o}C for 6 d), revealed differential regulation for the vacuolar proton pumps. The moderate treatment increased the activities (hydrolytic and H^{+} transport) in both enzymes more than two

fold and seedlings submitted to longer chilling stress showed that V-PPase was more stable than V-ATPase. Indeed, the higher stability of V-PPase may be due to its simple structure. Nevertheless, it seems that V-PPase in cowpea plants becomes a key pump in response to chilling stress maintaining the proton motive force, essential for plant growth development (OLIVEIRA *et al.*, 2011).

5 MOLECULAR APPROACHES IN SALINITY TOLERANCE

A comprehensive understanding of the mechanisms that plants engage to respond and survive salt stress requires an integrated approach of the complex physiological traits, metabolic pathways, as well as molecular networks. Recent research has identified various acclimation responses to salinity; however, the mechanisms underlying salinity tolerance are far from being completely understood (GUPTA; HUANG, 2014). Many studies have attempted to elucidate the molecular mechanism of salinity tolerance in plants. In order to attaint this aim, it is required new genetic clues and more efficient techniques for identifying and manipulate genes implicated in salt tolerance. Indeed, every day new molecular tools for manipulating genetic resources are becoming available.

Numerous genes could be considered candidates for genetic engineering to develop salt tolerant plants. It must be highlighted that the control of Na^+ in the plant cell is crucial for the plant survival. A great number of salt responsive transcription factors and genes have been identified and characterized using transcriptomic and genomic approaches (GUPTA; HUANG, 2014).

Transformation experiments in Arabidopsis showed that an antiporter involved in tonoplast Na^+ transport (*AtNHX1*) when overexpressed improved salt tolerance in high NaCl concentration

(APSE *et al.*, 1999). Similar results were presented for tomato and brassica (FLOWERS, 2004; ZHANG, H. X.; BLUMWALD, 2001; ZHANG, H. X. *et al.*, 2001). Indeed, when the cotton orthologue, *GhNHX1*, was overexpressed in tobacco, a dramatic increase in salt tolerance was observed (WU, C.-A., 2004). There are more than 26 reports on acquired salt tolerance mediated by the overexpression of NHX genes (AGARWAL *et al.*, 2013). Specific Arabidopsis mutation, in this case, the overexpression of vacuolar H^+-PPase, AVP1, revealed important increased in salt tolerance, when the plants were grown under 250 mM salt stress, differently to wild types (GAXIOLA *et al.*, 2001).

Relative to plasma membrane, SOS1 gene from Arabidopsis was ectopically expressed for the first time in Arabidopsis plant showing reduced Na^+ accumulation in the presence of salt (SHI *et al.*, 2003). Among the genes that encode K^+ transporters and channels, HKT has been identified and cloned in various plant species. Despite the HKT transporters be important in regulation of K^+ and Na^+ transport from root to

shoots, transgenic studies have produced somewhat inconsistent results with *TaHKT1* (LAURIE *et al.*, 2002) and *AtHKT1* (RUS *et al.*, 2004). However, a knockout mutant of *AtHKT1* clearly increased salt sensitivity (RUS *et al.*, 2004), which shows that the function of HKT1 in the control of K^+ or Na^+ transport is important. The *HAL1* gene from yeast controls K^+/Na^+ selectivity and salt tolerance of yeast cells. Expression in tomato increased fruit yield and enhanced K^+/Na^+ selectivity in leaves (RUS *et al.*, 2001).

In brief, it is important to highlight the critical leaps towards understanding the molecular mechanism of salinity tolerance in plants in the last 15 years. However, many challenges still lie ahead as the regulation of gene expression and signaling cascades that regulate Na^+ transporters.

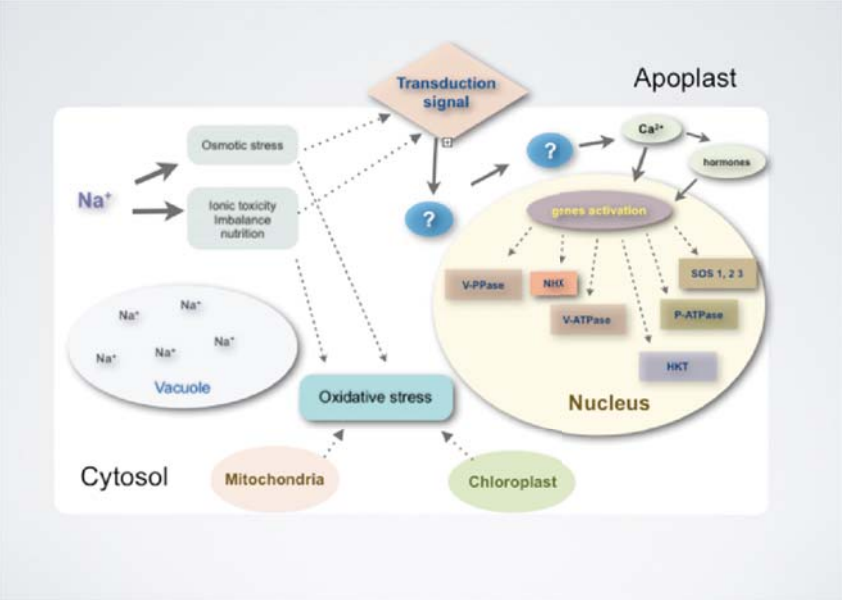

Figure 3. Acclimation mechanisms of plants under salt stress. A comprehensive understanding of the mechanisms that plants employ to respond and survive salt stress requires an integrated approach of the complex physiological traits, metabolic pathways and molecular or gene networks. Salinity induces both osmotic and ionic toxicity stress that activate a signal transduction system. How these signals are effectively is still unclear. However, it has been showed that $Ca2^+$ and hormones participate in this system and activate genes involved in the proton pumps cell energization and Na^+ transport. In *Vigna unguiculata*, it was observed regulation of the plasma membrane proton pump genes (P-ATPase), vacuolar proton pumps (V-ATPase and V-PPase) and antiporter Na^+/H^+ NHX2, 6 and SOS 1

6 CONCLUSION AND FUTURE PERSPECTIVES

Elevated temperatures caused by climate change create water-deficit (drought) conditions that contribute to increased soil salinity, and negatively impact the growth, development, and yield of crops. In recent years, the biochemical responses of plants to salt stress have been intensively studied. Information on the tolerance mechanism is useful for developing new cultivars that are tolerant to salinity environments. Due to the intricate cascade of signalization and responses, describe salt tolerance has shown to be extremely difficult since the complex nature of salt stress and the large diversity of plant responses. In addition, new investigations considering molecular approaches are needed to reveal the fundamental protection mechanisms against salt stress. In this chapter, we tried to summarize the roles of the proton pumps and the secondary transporters in a physiological, biochemical and molecular context of plant responses to abiotic stress. Some of this knowledge has led to the successfully improve plant salt tolerance comprehension and highlighted the key role of the proton pumps and the secondary transports regulation during plant stress responses. Science has made great advances in identifying genes, protein markers, and metabolites, critical to plant stress responses and the current challenge is to transfer the basic knowledge to create/breed new cultivar that cannot only withstand the severe climatic condition, but also enhance crop yield and quality. In this context, biotechnological approaches involving gene modifications and enzyme remodeling are notably important to improve plant defense mechanisms against harsh environments. Finally, as should be apparent from the studies summarized here, there is optimism that in a near future the development of new plant cultivars capable of adapting to severe environmental stresses, including those caused by global climate change will come true. However, laboratory and greenhouse research results could not rigorously be extrapolated to real field conditions, where unpredictable environmental changes or multiple stresses combination are current. This highlights the necessity to prioritize research in real-field conditions and test different crop productions system, to ultimately select crop models that are tolerant to abiotic stress conditions. So, we believe that agricultural biotechnology applications will help achieve a second green revolution in a not to distant future.

7 ACKNOWLEDGEMENTS

This research was supported by grants from INCTsal, CNPq, CAPES and FUNCAP. The origin and development of our studies of the proton pumps and transporters would not have been possible without the support, criticism and encouragement of our colleagues Maria da Guia Silva Lima, Lev Okorokov, Masoyshi Maeshima, and all those that collaborated for this work.

REFERENCES

AGARWAL, P. K. *et al.* Bioengineering for salinity tolerance in plants: state of the art. *Molecular biotechnology*, v. 54, n. 1, p. 102–23, maio 2013.

AMTMANN, A.; SANDERS, D. Mechanisms of Na+ Uptake by Plant Cells. *Advances in Botanical Research*, v. 29, p. 75–112, 1998.

APSE, M. P. *et al.* Salt tolerance conferred by overexpression of a vacuolar Na+/H+ antiport in Arabidopsis. *Science*, v. 285, n. 5431, p. 1256–8, 20 ago. 1999.

BARTELS, D.; SUNKAR, R. Drought and Salt Tolerance in Plants. *Critical Reviews in Plant Sciences*, v. 24, n. 1, p. 23–58, 23 fev. 2005.

BASSIL, E.; COKU, A.; BLUMWALD, E. Cellular ion homeostasis: emerging roles of intracellular NHX Na+/H+ antiporters in plant growth and development. *Journal of experimental botany*, v. 63, n. 16, p. 5727–40, 1 out. 2012.

BLUMWALD, E. Sodium transport and salt tolerance in plants. *Current opinion in cell biology*, v. 12, n. 4, p. 431–4, ago. 2000.

BLUMWALD, E.; AHARON, G. S.; APSE, M. P. Sodium transport in plant cells. *Biochimica et biophysica acta*, v. 1465, n. 1-2, p. 140–51, 1 maio 2000.

CHINNUSAMY, V.; SCHUMAKER, K.; ZHU, J.-K. Molecular genetic perspectives on cross-talk and specificity in abiotic stress signalling in plants. *Journal of experimental botany*, v. 55, n. 395, p. 225–36, 2 jan. 2004.

CIPRIANO, D. J. *et al.* Structure and regulation of the vacuolar ATPases. *Biochimica et biophysica acta*, From Duplicate 2 (Structure and regulation of the vacuolar ATPases. - Cipriano, Daniel J; Wang, Yanru; Bond, Sarah; Hinton, Ayana; Jefferies, Kevin C; Qi, Jie; Forgac, Michael) , v. 1777, n. 7-8, p. 599–604, 2008.

COMINELLI, E. *et al.* Challenges and perspectives to improve crop drought and salinity tolerance. *New biotechnology*, v. 30, n. 4, p. 355–61, 25 maio 2013.

CONDE, A.; CHAVES, M. M.; GERÓS, H. Membrane transport, sensing and signaling in plant adaptation to environmental stress. *Plant & cell physiology*, v. 52, n. 9, p. 1583–602, set. 2011.

CRAIG PLETT, D.; MØLLER, I. S. Na(+) transport in glycophytic plants: what we know and would like to know. *Plant, cell & environment*, v. 33, n. 4, p. 612–26, abr. 2010.

DEINLEIN, U. *et al.* Plant salt-tolerance mechanisms. *Trends in plant science*, v. 19, n. 6, p. 371–9, 6 jun. 2014.

DEMIDCHIK, V.; MAATHUIS, F. J. M. Physiological roles of nonselective cation channels in plants: from salt stress to signalling and development. *The New phytologist*, v. 175, n. 3, p. 387–404, jan. 2007.

ELMORE, J. M.; COAKER, G. The role of the plasma membrane H+-ATPase in plant-microbe interactions. *Molecular plant*, v. 4, n. 3, p. 416–27, 7 maio 2011.

FERNANDES DE MELO, D. *et al.* Effect of salt stress on mitochondrial energy metabolism of Vigna unguiculata cultivars differing in NaCl tolerance. *Plant Physiology et Biochemistry*, v. 32, n. 3, p. 405–412, 1994.

FLOWERS, T. J. Improving crop salt tolerance. *Journal of experimental botany*, v. 55, n. 396, p. 307–19, 1 fev. 2004.

FLOWERS, T. J.; COLMER, T. D. Salinity tolerance in halophytes. *The New phytologist*, v. 179, n. 4, p. 945–63, jan. 2008.

FLOWERS, T. J.; GALAL, H. K.; BROMHAM, L. Evolution of halophytes: multiple origins of salt tolerance in land plants. *Functional Plant Biology*, v. 37, n. 7, p. 604, 2 jul. 2010.

FORGAC, M. Structure and Properties of the Vacuolar (H+)-ATPases. *Journal of Biological Chemistry*, v. 274, n. 19, p. 12951–12954, 7 maio 1999.

FUGLSANG, A. T.; PAEZ-VALENCIA, J.; GAXIOLA, R. A. *Plant Proton Pumps: Regulatory Circuits Involving H+-ATPase and H+-PPase In: Transporters and Pumps in Plant Signaling*. Berlin, Heidelberg: Springer Berlin Heidelberg, 2011. v. 7. p. 39–64(Signaling and Communication in Plants).

GAXIOLA, R. A. *et al.* Drought- and salt-tolerant plants result from overexpression of the AVP1 H+-pump. *Proceedings of the National Academy of Sciences of the United States of America*, v. 98, n. 20, p. 11444–9, 25 set. 2001.

GAXIOLA, R. A.; PALMGREN, M. G.; SCHUMACHER, K. Plant proton pumps. *FEBS letters*, v. 581, n. 12, p. 2204–14, 25 maio 2007.

GUO, S. *et al.* Molecular cloning and characterization of a vacuolar H+ -pyrophosphatase gene, SsVP, from the halophyte Suaeda salsa and its overexpression increases salt and drought tolerance of Arabidopsis. *Plant molecular biology*, v. 60, n. 1, p. 41–50, jan. 2006.

GUPTA, B.; HUANG, B. Mechanism of salinity tolerance in plants: physiological, biochemical, and molecular characterization. *International journal of genomics*, v. 2014, p. 701596, jan. 2014.

HASEGAWA, P. M. Sodium (Na+) homeostasis and salt tolerance of plants. *Environmental and Experimental Botany*, v. 92, p. 19–31, ago. 2013.

JANICKA-RUSSAK, M. *Abiotic Stress Response in Plants - Physiological, Biochemical and Genetic Perspectives*. [S.l.]: InTech, 2011.

JI, H. *et al.* The Salt Overly Sensitive (SOS) pathway: established and emerging roles. *Molecular plant*, v. 6, n. 2, p. 275–86, 1 mar. 2013.

KAJANDER, T.; KELLOSALO, J.; GOLDMAN, A. Inorganic pyrophosphatases: one substrate, three mechanisms. *FEBS letters*, v. 587, n. 13, p. 1863–9, 27 jun. 2013.

KASAMO, K.; YAMAGUCHI, M.; NAKAMURA, Y. Mechanism of the chilling-induced decrease in proton pumping across the tonoplast of rice cells. *Plant & cell physiology*, v. 41, n. 7, p. 840–849, 1 jul. 2000.

KNIGHT, H.; TREWAVAS, A. J.; KNIGHT, M. R. Calcium signalling in Arabidopsis thaliana responding to drought and salinity. *The Plant Journal*, v. 12, n. 5, p. 1067–1078, nov. 1997.

KUDLA, J.; BATISTIC, O.; HASHIMOTO, K. Calcium signals: the lead currency of plant information processing. *The Plant cell*, v. 22, n. 3, p. 541–63, 1 mar. 2010.

LAURIE, S. *et al.* A role for HKT1 in sodium uptake by wheat roots. *The Plant journal : for cell and molecular biology*, v. 32, n. 2, p. 139–49, out. 2002.

LEE, D.-G. *et al.* Chilling stress-induced proteomic changes in rice roots. *Journal of plant physiology*, v. 166, n. 1, p. 1–11, 1 jan. 2009.

LEE, S. H.; CHUNG, G. C.; STEUDLE, E. Gating of aquaporins by low temperature in roots of chilling-sensitive cucumber and chilling-tolerant figleaf gourd. *Journal of experimental botany*, v. 56, n. 413, p. 985–95, 1 mar. 2005.

LIU, J. *et al.* The Arabidopsis thaliana SOS2 gene encodes a protein kinase that is required for salt tolerance. *Proceedings of the National Academy of Sciences of the United States of America*, v. 97, n. 7, p. 3730–4, 28 mar. 2000.

LIU, J.; ZHU, J. K. A Calcium Sensor Homolog Required for Plant Salt Tolerance. *Science*, v. 280, n. 5371, p. 1943– 1945, 19 jun. 1998.

MAESHIMA, M. Vacuolar H+-pyrophosphatase. *Biochimica et Biophysica Acta (BBA) - Biomembranes*, v. 1465, n. 12, p. 37–51, maio 2000.

MAHAJAN, S.; PANDEY, G. K.; TUTEJA, N. Calcium- and salt-stress signaling in plants: shedding light on SOS pathway. *Archives of biochemistry and biophysics*, v. 471, n. 2, p. 146–58, 15 mar. 2008.

MAHAJAN, S.; TUTEJA, N. Cold, salinity and drought stresses: an overview. *Archives of biochemistry and biophysics*, v. 444, n. 2, p. 139–58, 15 dez. 2005.

MARTINOIA, E.; MAESHIMA, M.; NEUHAUS, H. E. Vacuolar transporters and their essential role in plant metabolism. *Journal of experimental botany*, v. 58, n. 1, p. 83–102, 1 jan. 2007.

MITTLER, R. Abiotic stress, the field environment and stress combination. *Trends in plant science*, v. 11, n. 1, p. 15–9, jan. 2006.

MITTLER, R. *et al.* ROS signaling: the new wave? *Trends in plant science*, v. 16, n. 6, p. 300–9, jun. 2011.

MUNNS, R.; TESTER, M. Mechanisms of salinity tolerance. *Annual review of plant biology*, v. 59, p. 651–81, 29 jan. 2008.

NIU, X. *et al.* Ion Homeostasis in NaCl Stress Environments. *Plant physiology*, v. 109, n. 3, p. 735–742, nov. 1995.

OLIVEIRA, L. M. N. DE *et al.* Chill-induced changes in fatty acid composition of tonoplast vesicles from hypocotyls of Vigna unguiculata (L .) Walp . *Brazilian Journal of Plant Physiology*, v. 22, n. 1, p. 69–72, 2010.

OLIVEIRA, L. M. N. DE *et al.* Chilling-induced changes of vacuolar proton pumps in hypocotyls of Vigna unguiculata. *Plant Growth Regulation*, v. 64, n. 3, p. 211–219, 15 jan. 2011.

OLIVEIRA, L. M. N. DE. *Papel da V-ATPase e de enzimas antioxidantes nos mecanismos de ajustamento ao estresse salino em feijão-de-corda (Vigna unguiculata).* 2007. Universidade Federal do Ceará, 2007.

OTOCH, M. DE L. O. *et al.* Salt modulation of vacuolar H + -ATPase and H + -Pyrophosphatase activities in Vigna unguiculata. *Journal of Plant Physiology*, v. 158, p. 545–551, 2001.

PARK, S. *et al.* Up-regulation of a H+-pyrophosphatase (H+-PPase) as a strategy to engineer drought-resistant crop plants. *Proceedings of the National Academy of Sciences of the United States of America*, v. 102, n. 52, p. 18830–5, 27 dez. 2005.

PLATTEN, J. D. *et al.* Nomenclature for HKT transporters, key determinants of plant salinity tolerance. *Trends in plant science*, v. 11, n. 8, p. 372–4, 8 ago. 2006.

QI, J.; WANG, Y.; FORGAC, M. The vacuolar (H+)-ATPase: subunit arrangement and in vivo regulation. *Journal of Bioenergetics and Biomembranes*, v. 39, n. 5-6, p. 423–426, 27 nov. 2007.

QIU, N. *et al.* Coordinate up-regulation of V-H+-ATPase and vacuolar Na+/H+ antiporter as a response to NaCl treatment in a C3 halophyte Suaeda salsa. *Plant Science*, v. 172, n. 6, p. 1218–1225, jun. 2007.

QIU, Q.-S. *et al.* Na /H Exchange Activity in the Plasma Membrane of Arabidopsis 1. *Plant physiology*, v. 132, n. June, p. 1041–1052, jun. 2003.

QIU, Q.-S. *et al.* Regulation of SOS1, a plasma membrane Na+/H+ exchanger in Arabidopsis thaliana, by SOS2 and SOS3. *Proceedings of the National Academy of Sciences of the United States of America*, v. 99, n. 12, p. 8436– 41, 11 jun. 2002.

QIU, Q.-S. *et al.* Regulation of vacuolar Na+/H+ exchange in Arabidopsis thaliana by the salt-overly-sensitive (SOS) pathway. *The Journal of biological chemistry*, v. 279, n. 1, p. 207–15, 2 jan. 2004.

QUEIRÓS, F. *et al.* Activity of tonoplast proton pumps and Na+/H+ exchange in potato cell cultures is modulated by salt. *Journal of experimental botany*, v. 60, n. 4, p. 1363–74, 12 jan. 2009.

QUINTERO, F. J. *et al.* Activation of the plasma membrane Na/H antiporter Salt-Overly-Sensitive 1 (SOS1) by phosphorylation of an auto-inhibitory C-terminal domain. *Proceedings of the National Academy of Sciences of the United States of America*, v. 108, n. 6, p. 2611–6, 8 fev. 2011.

QUINTERO, F. J. *et al.* Reconstitution in yeast of the Arabidopsis SOS signaling pathway for Na+ homeostasis. *Proceedings of the National Academy of Sciences of the United States of America*, v. 99, n. 13, p. 9061–6, 25 jun. 2002.

RATAJCZAK, R. Structure, function and regulation of the plant vacuolar H(+)-translocating ATPase. *Biochimica et biophysica acta*, v. 1465, n. 1-2, p. 17–36, 1 maio 2000.

REBOUÇAS, D. M. *Efeito ácido abcísico nas bombas de prótons vacuolares e enzimas antioxidantes em Vigna unguiculata (L.) Walp*. Universidade Federal do Ceará. Fortaleza: [s.n.], 2011.

RENAUT, J. *et al.* Responses of poplar to chilling temperatures: proteomic and physiological aspects. *Plant biology (Stuttgart, Germany)*, v. 6, n. 1, p. 81–90, 2004.

RODRÍGUEZ-ROSALES, M. P. *et al.* Plant NHX cation/proton antiporters. *Plant signaling & behavior*, v. 4, n. 4, p. 265–76, abr. 2009.

ROY, S. J.; NEGRÃO, S.; TESTER, M. Salt resistant crop plants. *Current opinion in biotechnology*, v. 26, p. 115–24, abr. 2014.

RUS, A. *et al.* AtHKT1 facilitates Na+ homeostasis and K+ nutrition in planta. *Plant physiology*, v. 136, n. 1, p. 2500– 11, set. 2004.

RUS, A. *et al.* AtHKT1 is a salt tolerance determinant that controls Na(+) entry into plant roots. *Proceedings of the National Academy of Sciences of the United States of America*, v. 98, n. 24, p. 14150–5, 20 nov. 2001.

SCHROEDER, J. I. *et al.* Using membrane transporters to improve crops for sustainable food production. *Nature*, v. 497, n. 7447, p. 60–6, 2 maio 2013.

SCHUMACHER, K. Endomembrane proton pumps: connecting membrane and vesicle transport. *Current opinion in plant biology*, v. 9, n. 6, p. 595–600, dez. 2006.

SHI, H. *et al.* Overexpression of a plasma membrane Na+/H+ antiporter gene improves salt tolerance in Arabidopsis thaliana. *Nature biotechnology*, v. 21, n. 1, p. 81–5, jan. 2003.

SHI, H.; ZHU, J.-K. Regulation of expression of the vacuolar Na+/H+ antiporter gene AtNHX1 by salt stress and abscisic acid. *Plant molecular biology*, v. 50, n. 3, p. 543–50, out. 2002.

SILVA, P. *et al.* Role of Tonoplast Proton Pumps and Na+/H+ Antiport System in Salt Tolerance of Populus euphratica Oliv. *Journal of Plant Growth Regulation*, v. 29, n. 1, p. 23–34, 23 jul. 2009.

SOBREIRA, A. C. DE M. *et al.* Contrasting proton pumps activities reveal an important role for V-PPase in Vigna unguiculata under salt stress. *Theoretical and Experimental Plant Physiology*, v. In Press, 2014.

SOBREIRA, A. C. DE M. *Estudo da expressão dos genes das bombas de prótons (V-ATPase e V-PPase) e dos contratrasportadores vacuolares (NHX) de Vigna unguiculata (L.) Walp submetidos a estresses abióticos*. 2009. Universidade Federal do Ceará, 2009.

TOEI, M.; SAUM, R.; FORGAC, M. Regulation and isoform function of the V-ATPases. *Biochemistry*, v. 49, n. 23, p. 4715–23, 15 jun. 2010.

TORQUATO, J. P. P. *Estudo de mecanismo de regulação do sódio citoplasmático em cultivares de Vigna unguiculata (L.) Walp. submetidas a salinidade.* 2014. Universidade Federal do Ceará, 2014.

WEINL, S.; KUDLA, J. The CBL-CIPK Ca 2+ -decoding signaling network: function and perspectives. *New Phytologist*, v. 184, n. 3, p. 517–528, nov. 2009.

WU, C.-A. The Cotton GhNHX1 Gene Encoding a Novel Putative Tonoplast Na+/H+ Antiporter Plays an Important Role in Salt Stress. *Plant and Cell Physiology*, v. 45, n. 5, p. 600–607, 15 maio 2004.

WU, S. J.; DING, L.; ZHU, J. K. SOS1, a Genetic Locus Essential for Salt Tolerance and Potassium Acquisition. *The Plant cell*, v. 8, n. 4, p. 617–627, abr. 1996.

XUE, S. *et al.* AtHKT1;1 mediates nernstian sodium channel transport properties in Arabidopsis root stelar cells. *PloS one*, v. 6, n. 9, p. e24725, jan. 2011.

YAMAGUCHI, T. *et al.* Vacuolar Na+/H+ antiporter cation selectivity is regulated by calmodulin from within the vacuole in a Ca2+- and pH-dependent manner. *Proceedings of the National Academy of Sciences of the United States of America*, v. 102, n. 44, p. 16107–12, 1 nov. 2005.

YAMAGUCHI, T.; HAMAMOTO, S.; UOZUMI, N. Sodium transport system in plant cells. *Frontiers in plant science*, v. 4, p. 410, jan. 2013.

YANG, Q. *et al.* Overexpression of SOS (Salt Overly Sensitive) genes increases salt tolerance in transgenic Arabidopsis. *Molecular plant*, v. 2, n. 1, p. 22–31, 1 jan. 2009.

YU, J. N. *et al.* An Na+/H+ antiporter gene from wheat plays an important role in stress tolerance. *Journal of biosciences*, v. 32, n. 6, p. 1153–61, set. 2007.

ZHANG, H. X. *et al.* Engineering salt-tolerant Brassica plants: characterization of yield and seed oil quality in transgenic plants with increased vacuolar sodium accumulation. *Proceedings of the National Academy of Sciences of the United States of America*, v. 98, n. 22, p. 12832–6, 23 out. 2001.

ZHANG, H. X.; BLUMWALD, E. Transgenic salt-tolerant tomato plants accumulate salt in foliage but not in fruit. *Nature biotechnology*, v. 19, n. 8, p. 765–8, ago. 2001.

ZHANG, J. *et al.* Role of ABA in integrating plant responses to drought and salt stresses. *Field Crops Research*, v. 97, n. 1, p. 111–119, maio 2006.

ZHU, J.-K. Salt and Drought Stress Signal Transduction in Plants. *Annual review of plant biology*, v. 53, p. 247–73, 28 nov. 2002.

8

Recurso Água e Sensoriamento Remoto

Eunice Maia de Andrade[1], Fernando Bezerra Lopes[1] & Luiz Carlos Guerreiro Chaves[1]

[1] Universidade Federal do Ceará, Fortaleza, CE, Brasil

INOVAGRI Book 2014 - Irrigation and Salinity:
Researches and Technological Innovations
ISBN 978-85-67668-09-3

INOVAGRI
INSTITUTO DE PESQUISA E INOVAÇÃO NA AGRICULTURA IRRIGADA

Fortaleza - CE
2015

8 Recurso Água e Sensoriamento Remoto

1 INTRODUÇÃO

O conceito de qualidade da água refere-se às suas características, que podem afetar sua adaptabilidade para um determinado uso, ou seja, trata-se da relação entre a qualidade da água e as necessidades de cada usuário, podendo a mesma ser definida por uma ou mais características físicas, químicas ou biológicas (AYERS; WESTCOT, 1999).

Na região Nordeste do Brasil, de modo particular na região semiárida, a qualidade da água é merecedora de peculiar atenção em função das condições edafo-climáticas que caracterizam essa região. As altas taxas de evaporação presente nesta região conduzem a um déficit hídrico de 9 a 10 meses por ano. A evaporação pode variar de 1.000 mm ano^{-1} no litoral da Bahia e Pernambuco e atingir 2.000 mm ano^{-1} no interior, sendo que na área de Petrolina – PE, pode chegar a 3.000 mm ano^{-1} (MOURA *et al*., 2014). Adicionado a esta condição climática, a região apresenta predominância da base cristalina o que resulta em baixa infiltração e elevado escoamento superficial.

O arranjo dessas características conduziu para a construção de reservatório como a forma viável de armazenamento de água para os diversos usos deste recurso. O fato é que a elevada densidade de reservatórios no semiárido brasileiro determina ser este o semiárido mais populoso do mundo; em contrapartida se passa a ter uma maior pressão sobre este recurso. A demanda hídrica, seja para consumo humano, dessedentação, indústria ou agricultura irrigada é cada dia mais competitiva, existindo uma constante redução da água percapita.

Naturalmente, as altas taxas de evaporação do clima semiárido causam modificações nas águas dos açudes, uma vez que, ao promoverem o rebaixamento dos níveis dos reservatórios, podem levar a um aumento na concentração dos elementos que degradam a qualidade das águas (ANDRADE; MEIRELES, PALÁCIO 2010). Em adição as altas taxas de evaporação e a crescente demanda hídrica, adiciona-se a redução da disponibilidade decorrente da perda de qualidade das águas pelo uso improprio das áreas a montante dos reservatórios e no entorno da bacia hidráulica dos

mesmos. Reservatórios de grande porte como o Orós já estão eutrofizados (SANTOS *et al.*, 2014; LOPES *et al.,* 2014a) com qualidade impropria para consumo humano sem tratamento prévio.

O conhecimento e controle da qualidade das águas dos reservatórios são efetivados pelo monitoramento dos mesmos, tal ação demanda tempo, equipe campo capacidade e de custo elevados (STECH et al., 2011). Nos dias atuais novas propostas de monitoramento em escala regional vêm sendo elaboradas e propostas pelo emprego do sensoriamento remoto.

O uso de dados de sensoriamento remoto apresenta grande potencialidade para a identificação da qualidade da água, permitindo o monitoramento em diferentes escalas espacial e temporal (LOPES, 2013; LOPES *et al*., 2014b).

Com o sensoriamento remoto é possível avaliar as respostas decorrentes de perturbações introduzidas pela atividade humana, de modo a prever o impacto dessas ações sobre suas condições de sustentabilidade em médio e longo prazo (NOVO, 2005). Essas técnicas podem ser usadas de modo eficiente para prevenir, constatar e monitorar mudanças ocorridas no sistema aquático (DEKKER et al., 1992; NOVO, 2005).

Este capitulo abordar as fontes indutoras da disponibilidade hídrica, sazonalidade da salinidade das águas superficiais do estado do Ceará, bem como o emprego da técnica de sensoriamento remoto como ferramenta para monitoramento de grandes corpos hídricos.

2 PRECIPITAÇÃO

A disponibilidade hídrica de uma região é função das fontes indutoras das precipitações e das condições naturais do solo que promovem a infiltração da água e a capacidade de armazenamento da mesma. As regiões de maiores precipitações são aquelas que se encontram nas faixas de baixas pressões como a zona equatorial. Apesar do Semiárido Nordestino se encontrar inserido nesta região, está sujeito, principalmente, à influência de altas pressões subtropicais vinculadas ao anticiclone semipermanente do Atlântico sul, cuja atuação é condicionada pelas circulações de Hadley (meridional) e de Walker (zonal) em qualquer estado nordestino com exceção do Maranhão. As chuvas se devem, principalmente, ao avanço da ZCIT, entre janeiro e maio, com um máximo em março-abril sobre o Nordeste brasileiro. O movimento ascendente do ar, associado a ZCIT origina precipitações habitualmente intensas, de origem convectiva sem apresentar uma periodicidade de ocorrência bem definida; resultando em um padrão de chuva classificado como climaticamente anômalo do ponto de vista da precipitação, com uma distribuição espacial e temporal muito variável. A região se caracteriza por uma alternância dentre anos secos e anos chuvosos e poucos na normalidade.

Essa variabilidade se faz presente em toda a extensão do semiárido brasileiro. Exemplo variabilidade da precipitação em escala anual se confirma ao longo da série

de 103 anos (Figura 1) para a estação de Iguatu, localizada no Sertão Central do Estado do Ceará. Registram-se precipitações totais anuais de apenas 133 mm em 1915 e dois anos depois (1917) um total anual de 1348 mm. Variabilidade de magnitude similar ocorreu entre os anos de1983 e 1985, onde a precipitação total variou de 433 mm para 2075 mm, respectivamente.

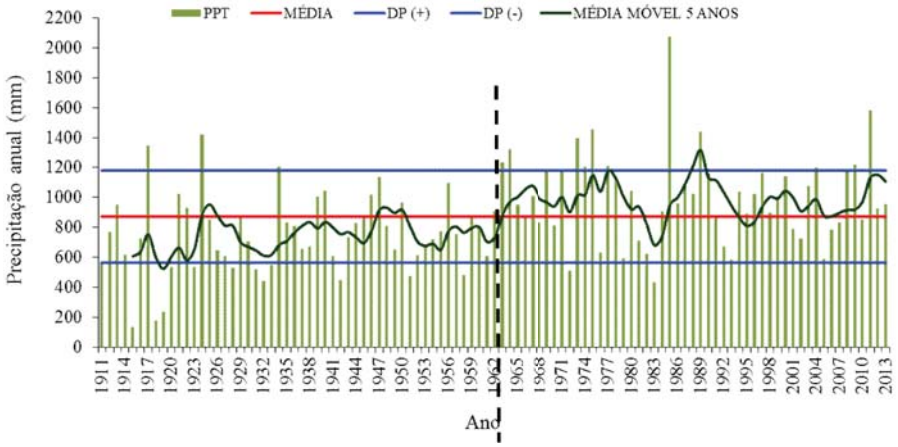

Figura 1. Série histórica (1911- 2013) da precipitação total anual para a estação de Iguatu, Ceará

Identifica-se que antes do ano de 1964, onze anos apresentaram total anual inferior a 564 mm ($\mu - \sigma$). Já para o período após 1964 somente em dois anos a precipitação total anual foi inferior a 564 mm. Em contra partida, analisando-se o limite superior do intervalo ($\mu \pm \sigma$ = 1178 mm), identifica-se que antes do ano de 1964, somente três eventos foram superiores a este limite, enquanto que nos últimos 56 anos, 9 anos registraram valores do total precipitado anual superior a 1178 mm. Esta variabilidade se confirma com a média móvel de 5 anos onde identifica-se uma tendência de aumento do total precipitado anual ao longo dos 103 anos. Tais resultados expressam a incerteza com que os eventos, mesmo em escala anual se registram no semiárido cearense (Andrade et al., 2010), e não a confirmação de mudanças climáticas. Embora 103 anos possa representar um longo período em uma escala de tempo para os humanos é um tempo ínfimo quando abordamos escalas de eras geológicas.

Um melhor conhecimento do regime pluviométrico de uma determinada região é obtido pela classificação pluviométrica quanto ao total precipitado anual empregando-se o Índice de Umidade (I_u) proposto por Navarro Hevia (2002) composto de cinco classes (Tabela 1). No cálculo do referido índice, os dados da precipitação pluviométrica total anual devem ser previamente ordenados para então determinar o Índice de Umidade (I_U) para cada ano, empregando-se a seguinte equação:

$$I_U = \frac{P}{\overline{P}}$$

onde P – Precipitação anual (mm) e P - Precipitação média anual da série histórica (mm ano $^{-1}$).

Tabela 1. Classes do Índice de Umidade (I_U) proposto por Navarro Hevia (2002)

Classificação dos anos	I_U
Muito úmido	$I_U > 1,3$
Úmido	$_U \leq 1,3$
Normal	$0,9 < I_U < 1,1$
Seco	$0,7 \leq I_U < 0,9$
Muito seco	$I_U < 0,7$

A aplicação do índice identificou que apesar da alta variabilidade interanual, existe uma distribuição muito similar do número de anos com precipitação superior ou inferior ao normal. O maior número de eventos extremos foi registrado pelos classe Muito seco. Tal fato expressa que secas não deveriam ser consideradas como eventos de anormalidade para a região de estudo, uma vez que 36% da série foi classificada como anos Secos e Muito secos (30) enquanto que os normais representam 24% da série (Tabela 2).

Tabela 2 Limites das classes do Índice de Umidade (Iu) e distribuição dos anos/classe

Classes	Limite superior (mm/ano)	Limite inferior (mm/ano)	Número de anos
Muito úmido	> 1195,74		14
Úmido	1195,74	939,51	26
Normal	939,51	768,69	25
Seco	768,69	683,28	7
Muito seco	< 683,28		31
Total de anos			103

3 ARMAZENAMENTO HÍDRICO

Em semiáridos tropicais onde a média do total anual é superior a isoieta de 750 mm ou 800 mm, a limitação da disponibilidade hídrica é decorrente das incertezas espaciais, temporais (ANDRADE *et al.*, 2010) e das elevadas taxas de evaporação, normalmente superior a 2000 mm ano^{-1}. Um bom exemplo deste tipo de ocorrência é o semiárido cearense, onde 80% dos eventos pluviométricos podem ocorrer em dois meses do ano. Tais características conduzem a anos secos alternados por anos de cheias como discutido por Ponte, 1997.

Quando esta característica climática esta associada as condições de solo rasos com o cristalino aflorando, teremos como resultados grandes rios intermitentes tão comuns em estados do Nordeste brasileiro; a exemplo cita-se o rio Jaguaribe com

uma extensão de 659 km. Em regiões com estas características é comum o uso de grandes reservatórios estratégicos para suprimento da demanda hídrica. O estado do Ceará em seus reservatórios estratégicos (um total de 149) tem um potencial de armazenamento de 18,6 bilhões de m^3, estando no momento (07/2014) com apenas 30,7% desta capacidade. Além dessa preocupação com a disponibilidade quantitativa, o estado começa a vivenciar um outro sério problema que é a eutrofização destes corpos hídricos (SILVA, 2013; SANTOS *et al.*, 2013; BATISTA *et al.*, 2014). Tal cenário determina a necessidade urgente de um monitoramento em escala regional não só da qualidade das águas, mas também das causas que promovem a eutrofização dos mesmos. As águas superficiais do estado do Ceará de forma geral apresentam boa qualidade quanto a salinidade, existindo pontos concentrados de alta salinidade como o açude Pompeu Sobrinho (CE > 5 dS m^{-1}) localizado na bacia hidrográfica Metropolitana.

4 ÁGUAS SUPERFICIAIS

As águas superficiais são aquelas tidas como águas doces que se deslocam na superfície do terreno, em função da gravidade, ocupando depressões do terreno, ficando armazenadas em barragens, açudes, lagos, represas em geral e indo lançar-se nos oceanos através dos fluxos dos rios (HOLANDA *et al*., 2010); no geral, apresentam várias substâncias dissolvidas ou suspensas (ROLIM,; LEITE JÚNIOR; GOMES FILHO, 2013) e, correspondem a apenas 0,007% volume total da água existente no planeta (TUNDISI, 2005). Mesmo o Brasil possuindo o maior volume água doce do mundo (8% do total), a situação da distribuição desse recurso no país é desigual, fazendo as Regiões do Nordeste, Sudeste e Centro-Oeste sentir problemas de escassez (HOLANADA; AMORIM, 1997).

Em se tratando da qualidade das águas superficiais merecem atenção os fatores como a eutrofização com aporte de nutrientes advindos das atividades agrícolas (nitrogênio e fósforo) e dos dejetos domésticos, que nas condições dos reservatórios superficiais elevam a população de algas; a irrigação que pode causar a elevação dos níveis de nitrato (ou até mesmo sua lixiviação para as águas subterrâneas), alterar a relação Carbono/Nitrogênio (C/N) e a Capacidade de Troca Catiônica (CTC) e, a salinização e a contaminação dos mananciais advindas do manejo inadequado das práticas agrícolas (uso de agrotóxicos e lançamento de metais pesados) (EMBRAPA, 2014).

É de nosso conhecimento que desde a construção do Açude público do Cedro em 1890, no município de Quixadá, o Estado do Ceará, continuou praticamente sem interrupção com a política de açudagem, chegando, com exceção das faixas serranas, a cobrir praticamente toda a extensão territorial do Estado. Segundo mapeamento realizado pela FUNCEME, em 2008, foram identificados 5.598 reservatórios superficiais com área de espelho d'água a partir de cinco hectares no estado do Ceará,

dos quais 12,08% são naturais (lagos e lagoas) e 87,02% são superficiais (açudes e barragens). Esse número chega a ser tão elevado que ao se visualizar uma figura da distribuição espacial desses reservatórios pode-se considerar que ela representa, quase em sua fiel condição, a forma do Estado (Figura 2).

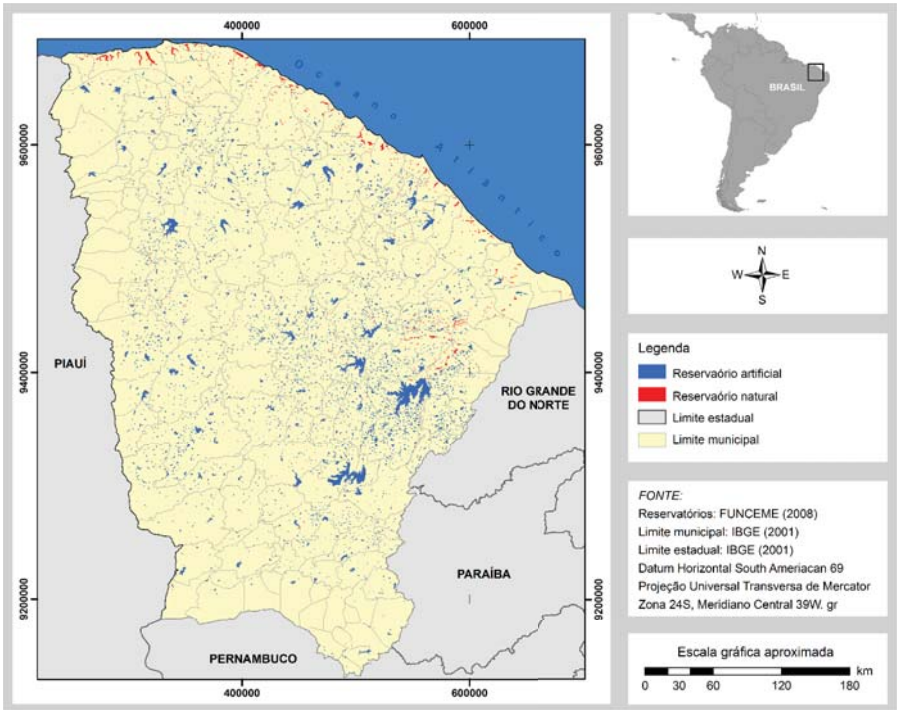

Figura 2. Distribuição espacial dos reservatórios naturais e superficiais, com área a partir de cinco hectares, no Estado do Ceará (Adaptado de Funceme, 2008)

A qualidade dessas águas, com relação à salinidade, geralmente apresenta baixas concentrações de sais totais, exceto para os Açudes Choró-Limão (Pompeu Sobrinho), localizado no município de Choró, na bacia Metropolitana e Santo Antônio de Russas, no município de Russa, bacia do Baixo Jaguaribe (ANDRADE *et al.*, 2010). De fato, as águas do Açude Pompeu Sobrinho, entre os anos de 1999 e 2000 já apresentavam valor médio de CEa de 5,5 dS m^{-1} (FUNCEME, 2002), o que o destacava como o reservatório da bacia Metropolitana em que as águas apresentavam maior salinidade. O acúmulo de sais nesse reservatório está relacionado, principalmente à litologia predominante da região, bem como ao superdimensionamento do açude, fazendo com que o mesmo passe por muitos amos sem sangrar e, consequentemente sem a renovação das suas águas que, aliada à alta evaporação, acaba por ocasionar o acúmulo dos sais. Para se ter uma noção

da importância dos fatores acima mencionados, a última sangria do Açude Pompeu Sobrinho ocorreu em 1974.

Palácio *et al*., (2011), realizando um estudo da qualidade das águas de 48 reservatórios distribuídos nas 11 bacias do Estado, entre 1998 e 2009 e levando em consideração os principais parâmetros relacionados à salinidade como: teor de Cálcio, Cloreto, Sódio e Magnésio, bem como a Condutividade Elétrica da água (CEa) e a Razão de Adsorção de Sódio (RAS), observaram que as águas superficiais se distribuem territorialmente em quatro grupos, atribuindo essa diferenciação à composição química das rochas de origem onde estão assentados os reservatórios, às condições de evaporação potencial e presença de aerossóis marinhos e, às atividades antrópicas exercidas nos entornos desses reservatórios. De fato, a antropização das áreas às margens dos açudes, ou ao longo de suas bacias de contribuição é uma situação já corriqueira tanto nos pequenos reservatórios, quanto naqueles ditos como estratégicos. No entorno do Açude Orós, por exemplo, Arraes (2010) utilizando-se de imagens de satélite investigou o uso e ocupação da terra para a bacia hidráulica desse reservatório entre os anos de 1992 e 2008, constatou que 26,94% da mesma está antropizada. Entretanto, é importante ressaltar que o termo antropizada citado neste estudo, engloba todo o solo que está sem cobertura vegetal, podendo está relacionado a áreas desmatadas, estradas, aglomerados urbanos e área de expansão urbana, áreas de culturas abandonadas ou desestruturadas, bem como aquelas para uso da pecuária.

Desde a chamada "revolução verde" o Nordeste brasileiro tem se destacado como área com considerável potencial para a irrigação. Devido ao Ceará deter 16,63% de sua área sob condições de irrigação (HEINZE, 2002) deve-se ter sempre em mente que a avaliação da qualidade da água para fins de irrigação tem se tornado fator preponderante na gestão dos Recursos Hídricos no Estado. Como, quando se trata de avaliação de qualidade da água, os parâmetros dependem da finalidade à qual se destina, no caso específico da irrigação, a qualidade das águas deve ser avaliada sob a ótica dos parâmetros físico-químicos, ou mesmo biológicos, no caso dos alimentos que são consumidos *in natura* e o sistema de classificação mais usado é o proposto pelo USDA – Salinity Laboratory, que leva em consideração a Condutividade Elétrica da água (CEa), e a Razão de Adsorção de Sódio (RAS) (RICHARDS, 1954)

Pode-se considerar que as águas superficiais do Ceará destinadas à irrigação são, em sua maioria, de boa qualidade, tanto no período seco quanto chuvoso. Foi o que observaram Chaves *et al*. (2010) em estudo realizado para o período de 1998-2006, em 48 açudes localizados ao longo do Estado (Figura 3).

É interessante observar que para o período chuvoso as águas se apresentaram com salinidade um pouco inferior, com o surgimento das classes C_3S_2 e C_4S_2. Tal fato está associado ao carreamento de sais e outros elementos superficiais pelas águas das chuvas, principalmente das regiões várzeas onde é comum o uso dessas áreas como agricultura de subsistência por pequenos agricultores, bem como, ao fato de

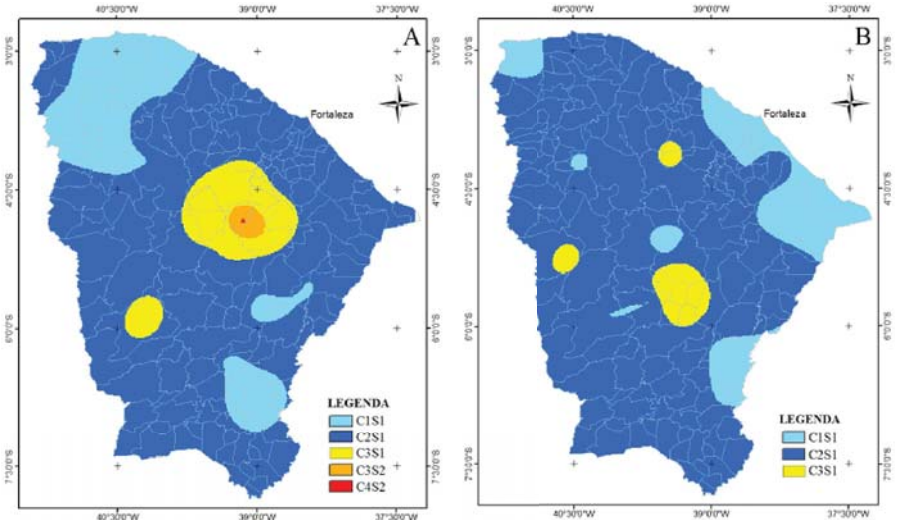

Figura 3. Distribuição espacial da qualidade das águas superficiais para fins de irrigação no Estado do Ceará, para os períodos chuvoso (A) e seco (B), de acordo com Richards (1954) (Adaptado de Chaves *et al*., 2010)

que nesta área que abrange parte das bacias Metropolitana e Banabuiú é onde está localizado o Açude Público Pompeu Sobrinho, que também segundo estudo realizada por Santos *et al*., (2010) para o mesmo período, foi onde apareceram as águas com severa restrição para uso na irrigação, quando considerado o potencial de toxicidade dos íons de Cloreto e Sódio (Figura 4).

Com enfoque na agricultura irrigada, a qualidade das águas dos açudes do Estado do Ceará monitorados pela COGERH, foram analisados por Andrade *et al.* (2010). Tomando como base as bacias hidrográficas, as bacias Metropolitana e Baixo Jaguaribe aparecem como detentoras das maiores limitações do uso da água para irrigação, com maiores valores de CEa, RAS e também de Sólidos Dissolvidos Totais (SDT). Já os maiores potenciais de água de boa qualidade para uso na irrigação estão nas bacias do Rio Salgado e Litoral (Tabela 3). É importante destacar que os SDTs além de estarem relacionados com a irrigação, causando entupimentos e corrosões nos equipamentos, também são fontes de poluição dos corpos d'água, com a diminuição da incidência de luz e, no consumo humano conferem sabor desagradáveis às águas. O CONAMA em sua Resoluções nº 357 de 2005 estabeleceu como padrão de qualidade, valores máximos permitidos para sólidos dissolvidos totais (SDT) para águas doces, classes 1, 2 e 3, de 500 mg L^{-1} e, a Portaria nº 518 de 2004 do Ministério da Saúde, estabelece valor máximo permitido de 1.000 mg L^{-1} de sólidos dissolvidos totais para águas para consumo humano. Neste parâmetro, apenas a Metropolitana apresenta valores acima do limite máximo estabelecido pelo CONAMA.

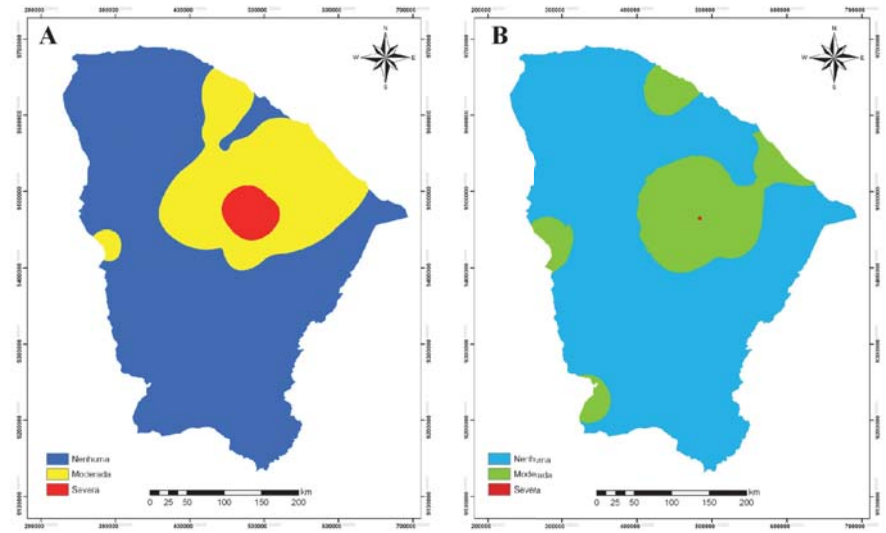

Figura 4. Mapa da classificação dos riscos de uso que podem ser gerados pelo Sódio (A) e Cloreto (B) da água de irrigação no Estado do Ceará (Adaptado de Santos *et al*., 2010)

Tabela 3. Valores médios de CEa, RAS e SDT das águas superficiais por bacia

Bacia	Nº de açudes	CE (dS m^{-1})	RAS	SDT (mg L^{-1})
Alto Jaguaribe	18	0,62	1,42	396,8
Salgado	13	0,20	1,07	128,0
Médio Jaguaribe	13	0,48	1,99	307,2
Banabuiú	18	0,74	2,68	473,6
Baixo Jaguaribe	1	1,11	1,86	710,4
Coreaú	9	0,75	2,31	480,0
Acaraú	12	0,38	1,90	243,2
Curu	12	0,71	2,14	454,4
Litoral	7	0,26	2,32	166,4
Metropolitana	17	1,48	3,13	947,2
Parnaíba	9	0,41	2,29	262,4

Fonte: Adaptada de Andrade *et al*. (2010).

5 MONITORAMENTO

O monitoramento da qualidade das águas superficiais é o conjunto de atividades que visam o acompanhamento das alterações nas características físicas, químicas e biológicas da água, resultante de processos antropogênicos e/ou naturais.

Segundo Magalhães Júnior (2000), o monitoramento deve ser visto como um processo essencial à implementação de instrumentos de gestão das águas, já que

permitem obter informações estratégicas, acompanhar as medidas efetivadas, atualizar bancos de dados e direcionar decisões. Inserido nesse contexto, o monitoramento limnológico trata especificamente da qualidade da água dos ecossistemas aquáticos continentais, incluindo rios e lagos (WETZEL, 2001) e abrange a coleta periódica associada à análise de dados e informações de qualidade da água para propósitos de efetivo gerenciamento dos ecossistemas aquáticos (BISNAS, 1990; MAROTTA et al., 2008).

O termo "qualidade de água" não se refere, necessariamente, a um estado de pureza, mas às características químicas, físicas e biológicas determinantes na estipulação de seus diferentes usos. As alterações na qualidade da água dos ecossistemas podem ser causadas por processos predominantemente naturais ou antropogênicos e seu acompanhamento rigoroso é fundamental, pois a classificação da água pode determinar o seu uso adequado.

Como uma importante ferramenta na gestão de recursos hídricos, a avaliação da qualidade da água deve abranger o acompanhamento das tendências de evolução no tempo possibilitando, dessa forma, a identificação da necessidade de medidas preventivas bem como da eficiência de algumas medidas adotadas. Segundo Freire (2000), a avaliação da qualidade da água, assim como sua evolução no tempo-espaço, só será possível com programas sistemáticos de monitoramento, que resultem em séries históricas que possam ser analisadas a fim de se estabelecerem padrões de distribuição sazonais e espaciais.

Neste sentido, o sensoriamento remoto tem grande potencial na superação da limitação espaço-temporal dos métodos tradicionais *in situ*, pois permite a aquisição das informações necessárias em diferentes escalas espacial e temporal, propiciando a análise estrutural dos ecossistemas aquáticos, assim como, sua análise funcional de modo sinóptico (VALÉRIO, 2009). Com a aplicação das técnicas de sensoriamento remoto é possível avaliar as respostas decorrentes de perturbações introduzidas pela atividade humana e processos naturais, de modo a prever o impacto dessas ações sobre suas condições de sustentabilidade em médio e longo prazo (NOVO, 2005). Essas técnicas podem ser usadas de modo eficiente para prevenir, constatar e monitorar mudanças ocorridas no sistema aquático (DEKKER et al, 1992; NOVO, 2005).

O monitoramento da qualidade da água nos dias atuais é essencial, e os dados de sensoriamento remoto podem torna-lo mais bem sucedido.

6 SENSORIAMENTO REMOTO

O conceito em si, de sensoriamento remoto, é muito amplo e existem várias definições para cada área da ciência. A definição clássica do Sensoriamento Remoto – SR refere-se a um conjunto de técnicas destinado à obtenção de informação sobre alvos (vegetação, solos, rochas, corpos d'água, etc.) sem que haja contato físico com os mesmos.

Novo (2010), após algumas considerações, definiu Sensoriamento Remoto como sendo a utilização conjunta de sensores, equipamentos para processamento de dados, equipamento de transmissão de dados colocados a bordo de aeronaves, espaçonaves, ou outras plataformas, com o objetivo de estudar eventos, fenômenos e processos que ocorrem na superfície do planeta Terra a partir do registro e da análise das interações entre a radiação eletromagnética e as substâncias que o compõem em suas diversas manifestações.

A água possui assinatura espectral distinto de acordo com as formas como se apresenta: líquida, sólida ou gasosa (Figura 5). No estado líquido a água apresenta reflectância (menor que 10%) em comprimentos de onda na faixa do visível (entre 0,38 - 0,70μm), sendo que nas demais regiões do espectro óptico há absorção da radiação incidente. A água em estado sólido apresenta reflectância em comprimentos de onda diversos, alcançando alta reflectância (80%) entre 0,7 e 1,2μm e decrescendo para valores variáveis e inferiores a 20% de reflectância em comprimentos de onda acima de 1,4μm. Para a água no estado gasoso a reflectância se mantém alta (aproximadamente em 70%) em todo o espectro óptico, porém apresentando algumas bandas de absorção em 1,0, 1,3 e 2,0 μm (NOVO, 2010).

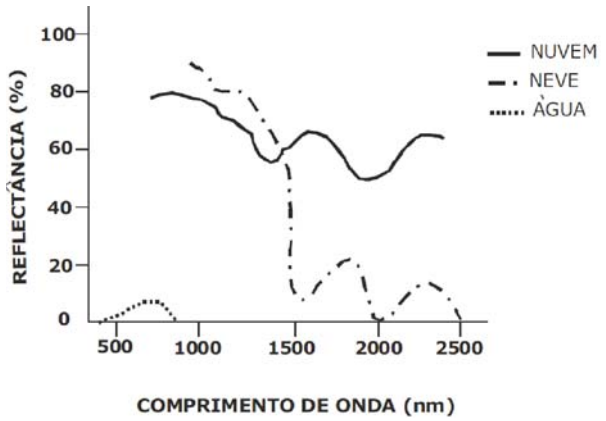

Figura 5 Curvas de reflectância da água nos estados líquidos, gasoso (nuvem) e sólido (neve) adaptada de Bowker et al. (1985)

7 PROPRIEDADES ÓPTICAS DA ÁGUA

As propriedades ópticas da água podem ser classificadas em inerentes e aparentes: As propriedades inerentes da água dependem apenas de seu conteúdo (dissolvido e/ou em suspensão). Essas propriedades não se modificam em função da mudança do campo de luz (KIRK, 2011). São propriedades ópticas inerentes: os coeficientes de absorção, espalhamento e função volumétrica de espalhamento. Essas propriedades dependem apenas do meio aquático. Os valores atribuídos aos coeficientes de absorção

e espalhamento dependem, exclusivamente, da composição do corpo d'água, ou seja, da concentração e tipo de substâncias opticamente ativas presentes na água.

A assinatura espectral da água pura é determinada, basicamente, pela absorção e espalhamento molecular nos comprimentos de onda mais curtos da radiação eletromagnética (REM). A absorção é mínima na região compreendida entre 400 e 500 nm, aumenta a partir de valor (500 nm), passando a ser significativa a partir de 580 nm e cresce rapidamente no infravermelho com máximo de absorção em 750 nm (Figura 6).

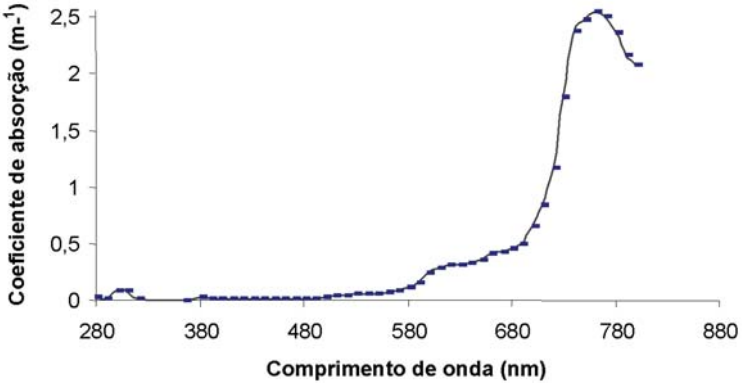

Figura 6. Coeficiente de absorção da água pura (Adaptado de Kirk, 2011)

O espalhamento da água pura, ao contrário da absorção, é máximo na região do azul e decresce exponencialmente em direção ao infravermelho (Figura 7). Além disso, a água pura apresenta alta transmitância na região do visível contribuindo para o alto coeficiente de atenuação, e para o baixo sinal de reflectância de massas de água (WOODRUFF et al., 1999). Esse comportamento do meio aquático limita os estudos de sensoriamento remoto na região entre 400 e 900 nm (BARBOSA, 2005; KIRK, 2011).

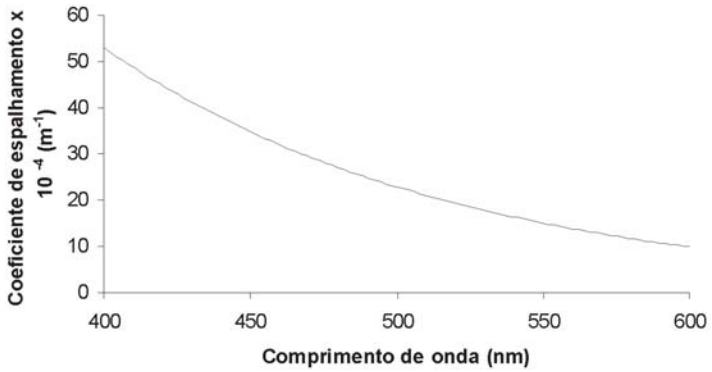

Figura 7. Coeficiente de espalhamento pela água pura (Aadaptado de Mobley, 2004)

As propriedades ópticas aparentes são afetadas pela composição da água como também pelas condições de iluminação do corpo d'água no momento da aquisição (KIRK, 2011). A reflectância da água com determinado componente pode fornecer informações a respeito das características químicas, físicas, biológicas (NOVO, 2001). Porém, tais comportamentos podem sofrer interferência das propriedades aparentes da água, que são fatores externos, como a condição de iluminação, capazes de mudar a resposta espectral do alvo. Ou seja, a água é a mesma, porém, sua resposta é modificada em função de fatores externos.

O fluxo retroespalhado, por exemplo, é uma propriedade óptica aparente visto que sua magnitude dependerá do fluxo incidente. Portanto, a irradiância descendente e a irradiância ascendente são propriedades ópticas aparentes do corpo d'água (NOVO, 2001).

Em águas naturais, a reflectância passa a ser, também, função dos Constituintes Opticamente Ativos (COAs) presentes na água (MOBLEY, 2004). As substâncias opticamente ativas são aquelas que podem afetar o espectro de absorção e espalhamento da água pura (NOVO, 2001). As principais substâncias opticamente ativas são os pigmentos fotossintetizantes, representados pela clorofila-a (Chl-a) presentes em organismos fitoplanctônicos; sólidos inorgânicos em suspensão (SIS); e matéria orgânica dissolvida (MOD) representado por ácidos húmicos ou substâncias amarelas (KIRK, 2011).

8 INTERAÇÃO DA RADIAÇÃO ELETROMAGNÉTICA COM ÁGUA

Na interação da radiação eletromagnética incidente sobre o corpo d'água pode haver absorção e espalhamento seletivo dependendo da proporção dos COAs presentes (DURAND et al., 2000), Figura 8. O sinal captado pelo sensor é o balanço entre a radiação espalhada e absorvida seletivamente pelos COAs.

Os fatores/processos que influenciam a radiação que emerge um corpo de água são ilustrados na Figura 8.

9 PROPRIEDADES ÓPTICAS DOS COMPONENTES OPTICAMENTE ATIVOS NA ÁGUA DO RESERVATÓRIO ORÓS, CEARÁ

A curva espectral da água pura apresenta o coeficiente de espalhamento máximo na região do azul decrescendo em direção ao infravermelho próximo. Em águas naturais, a presença de determinadas substâncias interfere na absorção e espalhamento da energia modificando o comportamento espectral da curva de reflectância o que resulta em feições específicas relacionadas ao tipo de componente presente na água (NOVO, 2001). A resposta espectral de um corpo de água é moldada pela composição e concentração dos componentes opticamente ativos presentes. A dinâmica espaço-temporal da composição e concentração das massas de água no reservatório Orós, foi

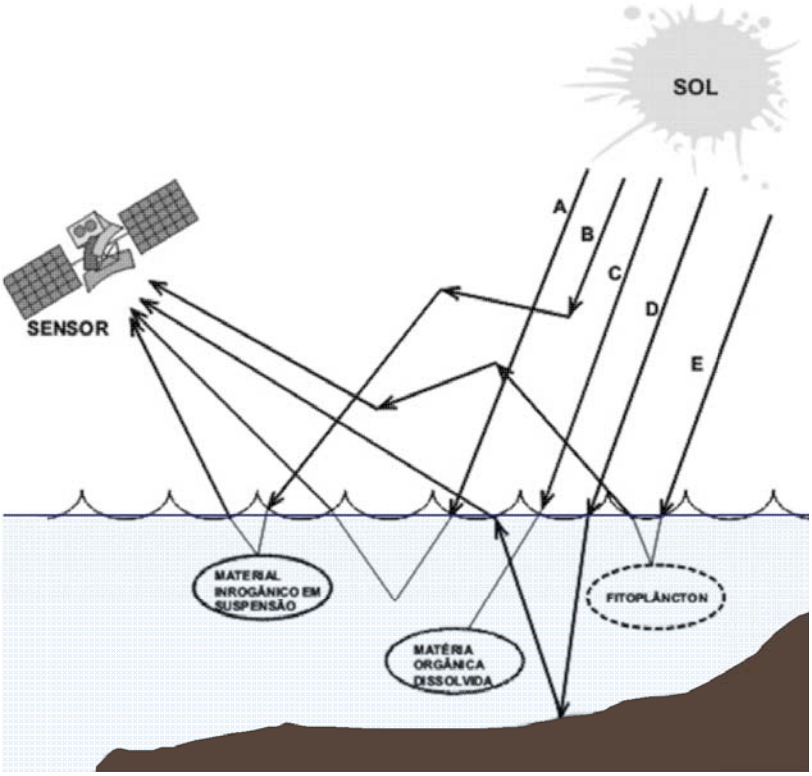

A – Retroespalhamento pelas moléculas de água; B – Retroespalhamento pelo material inorgânico em suspensão; C – Absorção pela matéria orgânica dissolvida; D – Reflexão do fundo; E – Retroespalhamento pelo fitoplâncton.

Figura 8. Fatores que determinam a intensidade e a forma dos fluxos de radiação detectados pelo sensor (Adaptado de IOCCG, 2000)

refletida de maneira significativa na forma e amplitude dos espectros conforme pode ser observado na Figura 9 na qual se apresentam os conjuntos de espectros obtidos durante as campanhas de campo realizadas nos meses de março de 2011 e agosto de 2012 (Figura 9).

Em termos de amplitude, os espectros dos pontos amostrais localizados na parte alta do reservatório Orós, P01, P02, P03, P05, P09, P10, P11 e P12 (Figura 9A), referentes ao período da estação chuvosa, foram os que apresentaram maior reflectância. Considerando-se que a magnitude da reflectância é função do coeficiente de retroespalhamento e que este, por sua vez, é altamente correlacionado com a concentração de sólidos em suspensão. O maior valor de sedimentos inorgânicos em suspensão (Apêndice 1), para os pontos localizados na parte alta do reservatório, explica os maiores valores de reflectância espectral.

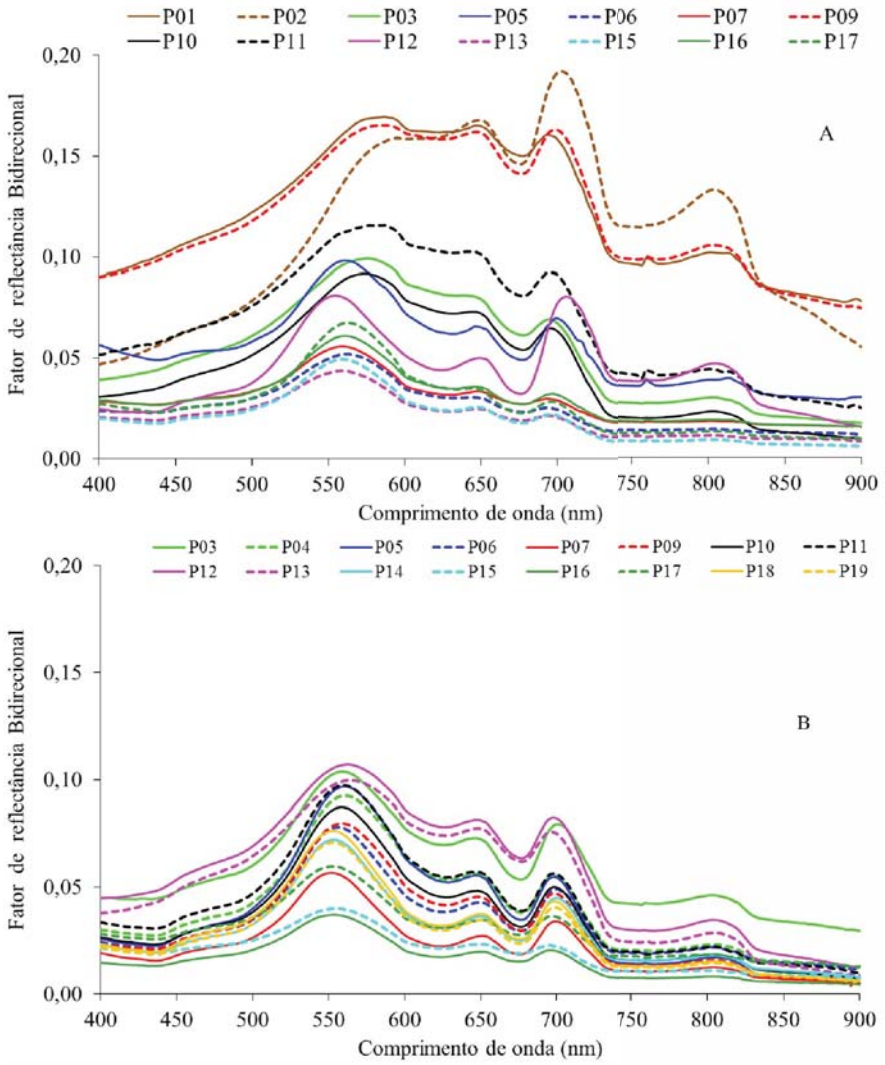

Figura 9. Comportamento espectral do sistema aquático do reservatório Orós, para as campanhas de campo realizadas em março de 2011 (A) e agosto de 2012 (Adaptado de LOPES, 2013)

Verifica-se que o fator de reflectância para os pontos P06, P07, P13, P15, P16 e P17, de março de 2011 (Figura 9A) e para todos pontos de agosto de 2012 (Figura 9B) feições características do comportamento espectral de águas ricas em fitoplâncton (RUNDQUIST, et al. 1996; GITELSON, 1992). Observa-se, uma baixa reflectância entre 400 e 500 nm, devido a absorção da luz azul com um mínimo em

438 nm, considerado o primeiro pico de máxima absorção por clorofila-a; um pico de reflectância máxima no verde, entre 550 e 560 nm (GITELSON, 1992); um pequeno ponto de inflexão em torno de 640 nm, devido ao retroespalhamento causado por pigmentos acessórios (GITELSON, 1992); um ponto clássico de absorção no vermelho em ≈ 675 nm, associado ao segundo ponto de absorção máxima por clorofila-a (Apêndices 1 e 2); um pico bem definido de reflectância no infravermelho próximo em torno de 700 nm atribuído a ambos, fluorescência dos pigmentos fotossintetizantes e absorção mínima por todos os componentes opticamente ativos, incluindo a água pura (GITELSON, 1992; RUNDQUIST et al., 1995); e finalmente, um pico menor em ≈ 810 nm, possivelmente causado pelo retroespalhamento de matéria orgânica (células algais) (MANTOVANI, 1993, NOVO, 2001; RUNDQUIST et al., 1996).

Os principais componentes opticamente ativos na modelagem da forma dos espectros são os sedimentos em suspensão, a própria água, clorofila-a e a matéria orgânica dissolvida. Constata-se que as regiões de absorção em torno de 438 e 670 nm e os picos de reflectância em torno de 550 nm e 700 nm estão presentes nas curvas dos espectros (Figura 9), devido a presença de clorofila-a (Apêndices 1 e 2). Resultados semelhantes foram encontrados por Rundquist et al. (1995) e Rundquist et al. (1996).

10 MODELOS DE ESTIMATIVAS DE VARIÁVEIS LIMNOLÓGICAS USANDO DADOS DE SENSORIAMENTO REMOTO

As bandas espectrais, cujos valores do fator de reflectância apresentaram os melhores resultados de correlação, foram testadas para estimar as variáveis: Sólidos Inorgânicos Suspensos – SIS, turbidez, transparência e condutividade elétrica – CE para as estações amostradas em março de 2011 no reservatório Orós.

O comprimento de onda de 720 nm apresentou correlação positiva com a variável Sólidos Inorgânicos Suspensos – SIS, sendo que o modelo potencial ($SIS = 860{,}1679 * FR_{\lambda 720}^{1/0{,}6427}$) (Figura 10A) teve melhor desempenho que o modelo linear. Resultados semelhantes foram encontrados por Lodhi et al. (1997) que, pesquisando o potencial do sensoriamento remoto para estimativas das concentraçõe de sedimentos em suspensão em água superficiais, determinaram o modelo potencial com R^2 de 0,96 em 855 nm. Diferentemente das regressões lineares obtidas por Chen et al. (1992); Han; Rundquist (1997) e Lopes et al. (2013) o ajuste da regressão entre os dados de sensoriamento remoto hiperespectrais de campo e as concentrações de sedimentos inorgânicos em suspensão foi não linear. Portanto, águas continentais da região semiárida (resevartório Orós), apresentam uma maior complexidade óptica. Resultados semelhantes foram encontrados por Rudorff et al. (2007) caracterizando a composição de águas opticamente complexas na Amazônia.

Para a variável turbidez, o modelo de regressão ajustado ($Turb = (FT_{\lambda 720} - 0{,}0217)/0{,}0017$) apresentou coeficiente de determinação (R^2) de 0,90 e $p < 2{,}9 \times 10^{-8}$. À medida que aumenta a turbidez, o fator de reflectância em 720 nm também aumenta

(Figura 10B). Resultados semelhantes foram encontrados por Barros et al. (2003) estimando a turbidez da água a partir de dados sensoriamento remoto.

O modelo de regressão ajustado para a transparência das águas do reservatório Orós foi, Transp = $(-FR_{\lambda 653} + 0,171)/0,1375$ com um coeficiente de determinação (R^2) de 0,92 (Figura 10C), caracterizado como bom, de acordo com Milton (1992). Pereira et al. (2011) estudando a transparência da água no reservatório de Itupararanga, São Paulo, a partir de imagens multiespectrais IKONOS e espectrorradiometria de campo encontraram R^2 ajustado explicando 47,8% da variabilidade dos dados.

O modelo de regressão ajustada para a condutividade elétrica das águas do reservatório Orós foi CE = $(-FR_{\lambda 632} + 0,5352)/1,6278$, que apresentou coeficiente de determinação (R^2) igual a 0,93 (Figura 10D). Resultados semelhantes foram encontrados por Choubey (1994) e Lopes et al. (2013), estimando a condutividade elétrica da água a partir de dados de sensoriamento remoto. Apesar da condutividade elétrica da água não ser um componente opticamente ativo e não ter uma assinatura espectral, mas no caso de Orós, ela co-varia com sedimentos em suspensão que é um componente opticamente ativo. A condutividade elétrica da água apresentou correção com a turbidez de 0,95 e 0,77 para os sólidos inorgânicos suspensos. Lopes et al. (2013), observaram alta correlação entre as concentrações de sedimentos inorgânicos em suspensão e condutividade elétrica da água com coeficientes de $R^2 = 0,95$ e $r = 0,97$. Todas as correlações para os modelos foram significativas (Figura 10).

De acordo com o resultado obtido para as bandas selecionadas, os modelos (Figura 10) foram validados (Figura 11) com base em amostras coletadas *in situ* para a campanha de campo realizada em agosto de 2012 no reservatório Orós, Ceará.

Os parâmetros usados para analisar o desempenho do modelo para a variável SIS apresentam R^2 de 0,83, r de 0,91, d de 0,79 e NSE 0,44, classificados, como forte para o R^2 e r, satisfatório para o d e aceitável para o NSE, Figura 11A. O modelo apresenta baixo erro de estimativa com EMA de 1,84 e RQEM de 2,08 (mg L^{-1}).

O desempenho do modelo para a variável turbidez apresentou R^2 de 0,91, r de 0,95, d de 0,89 e NSE 0,81, classificados respectivamente, como forte para o R^2 e r, satisfatório e adequado, Figura 11B. O modelo apresenta erro de estimativa com EMA de 4,28 e RQEM de 5,03 (UNT). O modelo tende a superestimar os baixos valores e subestimar os valores altos de turbidez. Essa variável é influenciada pela presença de sólidos em suspensão como o silte, argila, sílica, coloides e matéria orgânica.

O modelo para a variável condutividade elétrica apresentou R^2 de 0,72, r de 0,85, ambos classificados como moderado, índice de Willmontt (d) de 0,53, abaixo do valor considerado satisfatório (0,75) e NSE de 0,76, considerado satisfatório (Figura 11D). O modelo apresenta baixo erro de estimativa com EMA de 0,0217 e RQEM de 0,0224 (dS m^{-1}). Apesar de o modelo subestimar as concentrações de condutividade elétrica, apresenta a mesma tendência, ou seja, de subestimar os valores menores e maiores de condutividade elétrica da água.

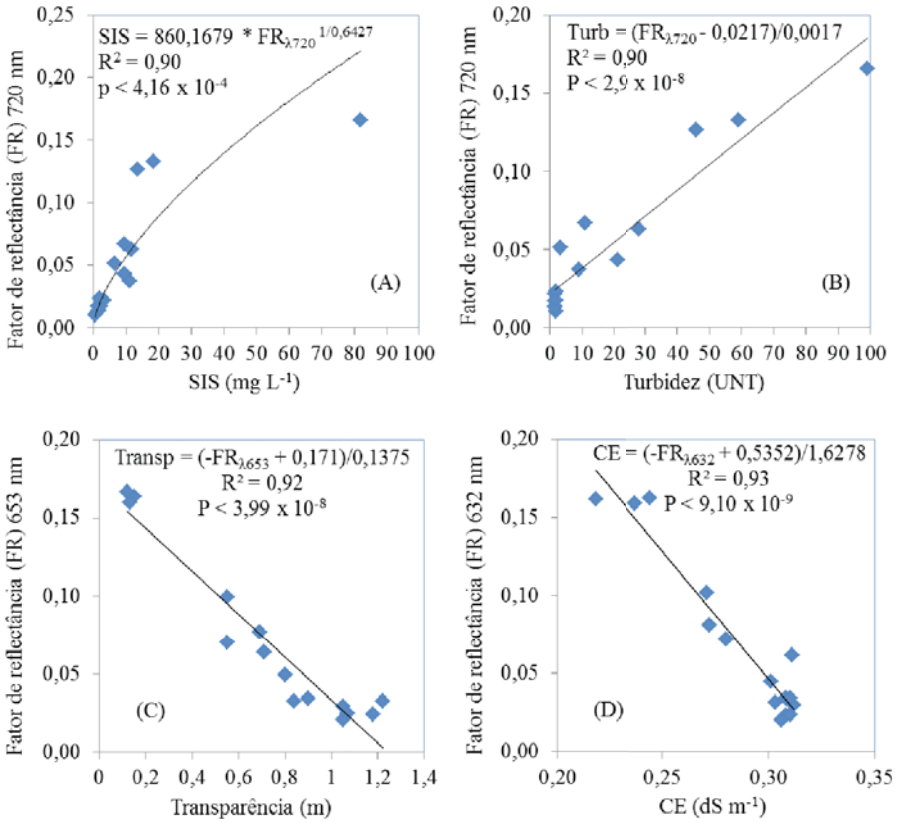

Figura 10. Modelos para estimativas das variáveis limnológicas (A) Sólidos Inorgânicos Suspensos – SIS (B) turbidez, (C) transparência e (D) condutividade elétrica – CE (Adaptado de LOPES et al., 2014b)

Verifica-se pelos índices aplicados, que os modelos ajustados apresentam desempenhos aceitáveis. Os mesmos apresentam relação significativa estatisticamente a 1%, entre os dados medidos e estimados (Figura 11). Observa-se que os modelos desenvolvidos para as variáveis limnológicas, Figura 10, mostraram-se confiáveis, indicando que estas variáveis podem ser quantificadas remotamente a partir dos dados de sensoriamento remoto de campo.

11 CONSIDERAÇÕES FINAIS

A limitação da disponibilidade hídrica é função não só do quantitativo, mas do qualitativo. Atualmente, facilmente encontramos corpos hídricos onde a água já não se tem acessibilidade na sua forma natural, é requerido tratamentos prévios para

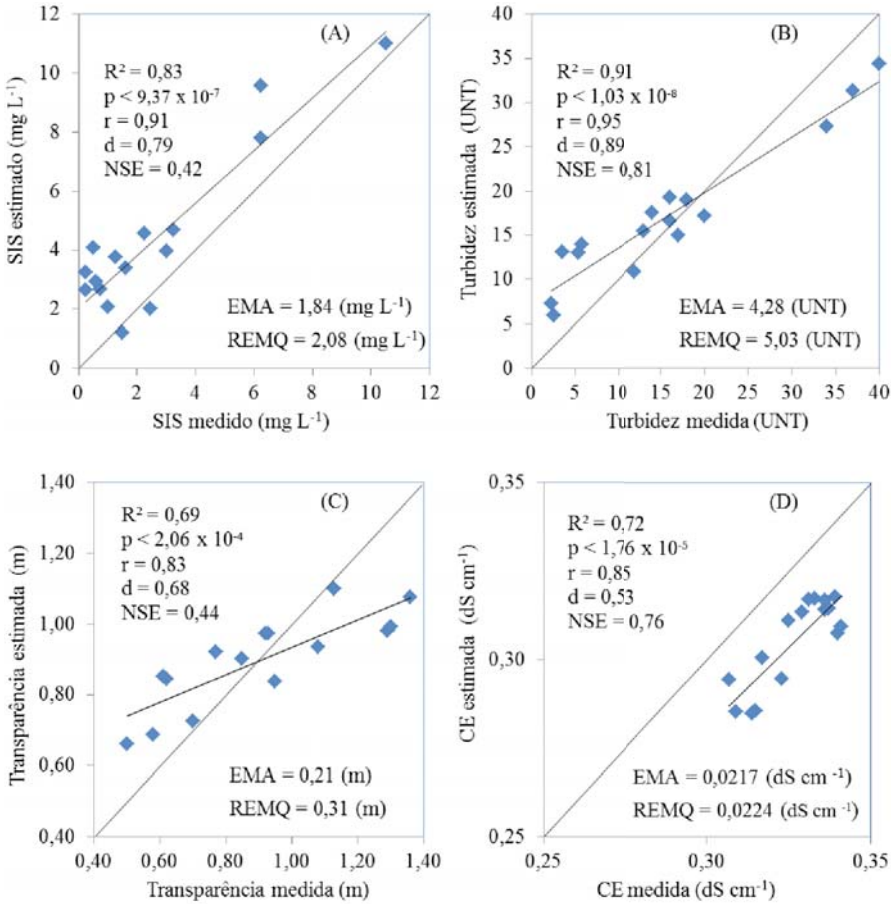

Figura 11. Validação dos modelos para quantificação das concentrações das variáveis limnológicas (A), Sólidos Inorgânicos Suspensos – SIS (B), turbidez, (C) transparência e (D) condutividade elétrica – CE (Adaptado de LOPES et al., 2014b)

leva-la a condição de potabilidade. Tais fatos apontam a necessidade de mudanças de paradigmas do uso dos recursos naturais em escala global, uma vez que o problema já não é pontual.

Uma técnica que vem se mostrando adequada em grandes escalas é o sensoriamento remoto, onde pode-se efetuar monitoramentos em tempos reais em escala de grandes bacias hidrográficas a partir de dados de sensoriamento remoto, através de dados espectrais "in situ".

Portanto, com o uso do sensoriamento remoto é possível melhorar o gerenciamento dos recursos hídricos, uma vez que auxilia na formação de banco de dados e apresenta a vantagem na superação da limitação espacial dos monitoramentos tradicionais *in situ*,

gerando informações úteis à tomada de decisões pelos gestores, e interação contínua e permanente entre gerentes e pesquisadores da área básica, vital para a implantação de políticas públicas em nível municipal, regional, estadual e federal.

REFERÊNCIAS

ANDRADE, E. M.; MEIRELES, A. C. M.; PALÁCIO, H. A. Q. O semiárido cearense e suas águas. In: ANDRADE, E. M.; PEREIRA, O. J.; DANTAS, F. E. R. (Org.). **Semiárido e o manejo dos recursos naturais: uma proposta de uso adequado do capital natural**. Fortaleza: Imprensa Universitária, 2010, cap.3, p.56-80.

ARRAES, F. D. D. **Dinâmica do balanço de energia na bacia hidráulica do Açude Orós e suas adjacências**. 2010. 89f. Dissertação (Mestrado em Engenharia Agrícola) – Universidade Federal do Ceará, Fortaleza, 2010.

AYERS, R. S.; WESTCOT, D. W. **A qualidade da água na agricultura**. Estudos FAO, Irrigação e Drenagem, 29, revisado 1, 2ª ed. Campina Grande, UFPB, 1999, 153 p.

BARBOSA, C. C. F. Sensoriamento remoto da dinâmica da circulação da água no sistema planície de Curuai/Rio Amazonas. 281f, Tese (Doutorado em Sensoriamento Remoto) – Instituto Nacional de Pesquisas Espaciais, São Jose dos Campos. 2005.

BARROS, R. S.; CRUZ, C. B. M.; MEDEIROS, A. F. F.; SEABRA, V. S. Estimativa de turbidez e temperatura da água a partir de dados dos sensores TM e ETM+ para a Baía de Guanabara. In: XII Simpósio Brasileiro de Sensoriamento Remoto, **Anais...** Belo Horizonte, Brasil, INPE, 2003. p. 2435 - 2442.

BATISTA, A. A *et al.* Sazonalidade e variação espacial do índice de estado trófico do açude Orós, Ceará, Brasil. **Revista Agroambiente On-line,** v.8, n.1, p.39-48, 2014.

BISNAS, A. K. **Monitoramento eficiente de lagos**. Shiga: ONU, 1990. 541 p.

BOWKER, D. E.; DAVIS, R. E.; MYRIC, D. L.; STACY, K.; JONES, W. T. **Spectral reflectance of natural targets for use in remote sensing studies**. Hampton, 1985. (NASA Reference Publication, 1139).

BRASIL. Ministério da Saúde. Portaria nº 518, de 25 de março de 2004. **Dispõe sobre os**

BRASIL. Ministério do Meio Ambiente. CONAMA. Resolução nº 357, de 17 de março de 2005. **Dispõe sobre a classificação dos corpos de água**. Diário Oficial [da] República Federativa do Brasil, Poder Executivo, Brasília DF 18 de março. 2005.

CHAVES, L. C. G. *et al*. Distribuição espacial da qualidade da água superficial para irrigação no Estado do Ceará. *In*: SIMPÓSIO BRASILEIRO DE SALINIDADE, 1., Fortaleza**. Anais...** Fortaleza: INCTSal, 2010.

CHEN, Z.; CURRAN, P. J.; HANSON, J. D. Derivative refrectance spectroscopy to estimate suspended sediment concentration. **Remote Sensing of Enviromment**, n.40, p. 67-77, 1992.

CHOUBEY, V. K. Monitoring surface water conductivity with Indian remote sensing satellite data: a case study from central India. Hydrological, Chemical and Biological Processes of Transformation and Transport of Contaminants in Aquatic Environments (Proceedings of the Rostov-on-Don Symposium). IAHSPubl. no. 219, p.317-326. 1994.

DEKKER, A.G.; MALTHUS, T.J.; WIJNEN, M.M. Spectral band location for remote sensing of turbid and/or eutrophic waters. **Emerging Technologies and Systems**, p. 955-970, 1992.

DURAND, D., J. BIJAOUI, e F. CAUNEAU. Optical remote sensing of shalowwater environmental parameters: A feasibility study. **Remote Sensing of Environment**, v.73, p.152-161, 2000.

EMBRAPA MEIO AMBIENTE. Empresa Brasileira de Pesquisa Agropecuária. **Recursos hídricos no Semi-árido**. Disponível em: <http://www.cnpma.embrapa.br/projetos/ecoagua/princip/rechidro.html>. Acesso em: 03 jun. 2014.

FREIRE, R. H. F. Aspectos Limnológicos de três reservatórios que abastecem a Região Metropolita- Fortaleza – Açudes Pacajus, Pacoti e Gavião. Fortaleza, Ceara. 2000. 308 f. Dissertação (Mestrado em Engenharia Civil área de concentração Saneamento Ambiental), Universidade Federal do Ceará.

FUNCEME. Fundação Cearense de Meteorologia e Recursos Hídricos. **Mapeamento dos espelhos d'água do Brasil - Relatório técnico**. Fortaleza: FUNCEME/MIN, 2008, 108 p.

GITELSON, A. A. The peak near 700 nm on radiance spectra of algae and water: relationships of its magnitude and position with chlorophyll concentration. **International Journal of Remote Sensing**, v.13, n.17, p.3367-3373, 1992.

HAN, L.; RUNDQUIST, D.C. Comparison of NIR/RED ratio and first derivative of reflectance in estimating algal-chlorophyll concentration: a case study in a Turbid Reservoir. **Remote Sensing of Environment**, v.62, p.255-261, 1997.

HEINZE, B. C. L. B. **A importância da agricultura irrigada para o desenvolvimento da Região Nordeste**. 2002. 59f. Monografia (MBA em Gestão Sustentável da Agricultura Irrigada) - ECOBUSINESS SCHOOL/Fundação Getúlio Vargas, Distrito Federal, 2002.

HOLANDA, J. S. *et al*. Qualidade da água para irrigação. *In*: GHEYI, H. R.; DIAS, N. S.; LACERDA, C. F. (Ed.). **Manejo e controle da salinidade: estudos básicos e aplicados**. Fortaleza: INCT Sal, 2010. cap. 4, p. 43-61.

HOLANDA, J. S.; AMORIM, J. R. A. Qualidade da água para irrigação. *In*: GHEYI, H. R.; QUEIROZ, J. E.; MEDEIROS, J. F (Ed.). **Manejo e controle da salinidade da agricultura irrigada**. Campina Grande: UFPB, 1997. cap. 5, p. 137-169.

IOCCG - International Ocean Colour Coordinating Group. Remote sensing of ocean colour in coastal, and other optically-complex waters. Dartmouth: 2000. 139 p.

KIRK, J. T. O. **Light and photosynthesis in aquatic ecosystems**. 3rd ed. New York: Cambridge University Press, 2011.

LODHI, M. A.; RUNDQUIST, D. C.; HAN, L.; KUZILA, M. S. The Potential for Remote Sensing of Loess Soils Suspended in Surface Waters. **Journal of the American Water Resources Association**. v. 33, n. 1, p. 111 – 117, 1997.

LOPES, F. B. *et al.* Assessment of the water quality in a large reservoir in semiarid region of Brazil. **Revista Brasileira de Engenharia Agrícola e Ambiental**, v.18, n.4, p.437-445, 2014a.

LOPES, F. B. *et al.* Modelagem da qualidade das águas a partir de sensoriamento remoto hiperespectral. **Revista Brasileira de Engenharia Agrícola e Ambiental**, v. 18, p. 13-19, 2014b.

LOPES, F. B. Uso de sensoriamento remoto como suporte ao monitoramento da qualidade das águas superficiais da região semiárida do Brasil. 202f, **Tese** (Doutorado em Engenharia Agrícola) – Universidade Federal do Ceará, Fortaleza 2013.

LOPES, F. B.; SALES, A. G. C.; CHAVES, L. C. G.; MEIRELES, A. C. M.; ANDRADE, E. M. Modelos para estimativas de sedimentos em suspensão e da condutividade elétrica da água usando dados de sensoriamento remoto. In: XLII Congresso Brasileiro de Engenharia Agrícola – CONBEA, **Anais...** Fortaleza – CE, p.1-10, 2013.

MAGALHÃES JUNIOR, A. P. A situação do monitoramento das águas no Brasil -Instituições e iniciativas. **Revista Brasileira de Recursos Hídricos**, v.5, nº3, p.113-115. 2000.

MANTOVANI, J. E. Comportamento espectral da água: faixas espectrais de maior sensibilidade ao fitoplâncton na presença de matéria orgânica dissolvida e matéria inorgânica particulada. 1993. 119 f. **Dissertação** (Mestrado em Sensoriamento Remoto) – Instituto Nacional de Pesquisas Espaciais, São José dos Campos.

MAROTTA, H.; SANTOS, R. O.; ENRICH-PRAST, A. Monitoramento limnológico: um instrumento para a conservação dos recursos hídricos no planejamento e na gestão urbano-ambientais. **Ambiente & Sociedade**. v.11, n.1, p.67-79, 2008.

Milton, J. S. Statistical methods in the biological and health sciences. 2ed. New York: McGrow-Hill, 1992. 526p.

MOBLEY, C. D. **Light and water Radiative transfer in natural waters**. Academic Press. 2004, 593p.

MOURA, M. S. B. *et al*. **Clima e água de chuva no semi-árido**. Disponível em: <http://ainfo.cnptia.embrapa.br/digital/bitstream/CPATSA/36534/1/OPB1515.pdf>. Acesso em 26 mai. 2014.

NAVARRO HEVIA, J. Control de la erosión em desmontes originados por obras de infraestructura viária: aplicación al entorno de Palencia capital. 2002. 316 p. **Tesis** (Doctorado en Ingenieria de Montes). Universidad Politécnica de Madrid.

NOVO, E. M. L. M. **Comportamento Espectral da Água**. In: Sensoriamento Remoto – Reflectância dos Alvos Naturais. Organizadores: Paulo Roberto Meneses e José da Silva Madeira Netto. Brasília, Editora UnB, 2001. 262 p. 203-222.

NOVO, E. M. L. M. Sensoriamento remoto aplicado à ecologia aquática In: ROLAND, F.; CÉSAR, D.; MARINHO, M. (Ed.). **Lições de limnologia.** São Carlos: RiMa, 2005. cap.5, p.417-432.

NOVO, E. M. L. M. **Sensoriamento remoto**: princípios e aplicações. 4ª Ed. São Paulo: Blucher, 2010. p. 387.

PALÁCIO, H. A. Q. *et al*. Similaridade e fatores determinantes na salinidade das águas superficiais do Ceará, por técnicas multivariadas. **Revista Brasileira de Engenharia Agrícola e Ambiental**, v. 15, n. 4, p. 395-402, 2011.

Pereira, A. C. F.; Galo, M. L. B. T.; Velini, E. D. Inferência da transparência da água - reservatório de Itupararanga/SP, a partir de imagens multiespectrais IKONOS e espectrorradiometria de campo. **Revista Brasileira de Cartografia**, n.63/01, p.179-190, 2011.

PONCE, V.M. Management of droughts and floods in the seiarid Brazilian Northeast – the case for conservation. **Journal of Soil and Water Conservation**, v. 50, p.422-431, 1997.

procedimentos e responsabilidades relativos ao controle e vigilância da qualidade da água para consumo humano. Diário Oficial [da] República Federativa do Brasil, Poder Executivo, Brasília DF 26 de março. 2004.

RICHARDS, L. A. (Ed.) **Diagnosis and improvement of saline and alkali soils**. USDA Agricultural Handbook 60. Washington: U.S: Departament of Agriculture, 1954. 160p.

ROLIM, H. O.; LEITE JÚNIOR, J. B.; GOMES FILHO, R. R. (Org.) Qualidade da água. *In*: **Gestão de Recursos Hídricos: conceitos e experiências em bacias hidrográficas**. Goiânia: Gráfica Editora América, e co-edição com a Editora da UEG, 2013. cap. 8, p. 217-253.

RUDORFF, C. M.; NOVO, E. M. L. M.; GALVÃO, L. S.; FILHO, W. P. Análise derivativa de dados hiperespectrais medidos em nível de campo e orbital para caracterizar a composição de águas opticamente complexas na Amazônia. **Acta Amazonica,** v. 37, n.2, p. 279-290, 2007.

RUNDQUIST, D. C., SCHALLES, J. F.; PEAKE, J. S. The response of volume reflectance to manipulated algal concentrations above bright and dark bottoms at various depths in experimental pool. **Geocarto International**, v.10, n.4, p.5-14. 1995.

RUNDQUIST, D. C.; HAN, L.; SCHALLES, J. F.; PEAKE, J. S. Remote measurement of algal chlorophyll in surface waters: the case for the first derivative of reflectance near 690 nm. **Photogrammetric Engineering & Remote Sensing**, v. 62, n.2, p.195-200, 1996.

SANTOS, J. C. N. *et al*. Espacialização da potencialidade de uso das águas superficiais do Estado do Ceará, quanto ao cloreto e sódio, com auxilio de SIG. *In*: SIMPÓSIO BRASILEIRO DE SALINIDADE, 1., Fortaleza**. Anais...** Fortaleza: INCTSal, 2010.

SANTOS, J. C. N. *et al.* Land use and trophic state dynamics in a tropical semi-arid reservoir. **Revista Ciência Agronômica**, v.45, n.1, p.35-44, 2014.

SILVA, M. D. **Diagnóstico da comunidade fitoplanctônica de um reservatório no semiárido nordestino**. 2013. 97 f. Disertação (Mestrado em Ecologia e Recursos Naturais) – Centro de Ciências. Universidade Federal do Ceará.

STECH *et al.* Uso de tecnologia espacial para coleta automática de dados limnológicos e meteorológicos: aplicações nos reservatórios hidrelétricos de Manso e Corumbá. In: ALCÂNTARA, E. H.; NOVO, E. M. L. M.; STECH, J. L. (Ed.). **Novas tecnologia para o monitoramento e estudo de reservatórios hidrelétricos e grandes lagos**. Rio de Janeiro: Parêntese, 2011. cap.4, p.163-191.

TUNDISI, J. G. **Água no século XXI: enfrentando a escassez.** São Carlos: RiMa, IIE, 2.ed, 2005, 248 p.

VALÉRIO, A. M. O uso do sensoriamento remoto orbital e de superfície para o estudo do comportamento do corpo de água do reservatório de Manso, MT, Brasil. 2009. 119 f. **Dissertação** (Mestrado em Sensoriamento Remoto), Instituto Nacional de Pesquisas Espaciais.

WETZEL, R. G. **Limnology: lake and river ecosystems**. 3. ed. California: Academic Press, 2001. 1006p.

WOODRUFF, D. L.; STUMPF, R. P.; SCOPE, J. A.; PAERL, H. W. Remote estimation of water clarity in optically complex estuarine waters. **Remote Sensing of Environment**, v.68, p. 41-52, 1999.

APÊNDICE

Apêndice 1 Constituintes opticamente ativos (COAs) da água e parâmetros limnológicos para a coleta de março de 2011

Pontos	pH	CE (dS m^{-1})	Cl-a (μg L^{-1})	SST	SIS	SSV	Turbidez (UNT)	Transparência (m)
				(mg L^{-1})				
P1	8,15	0,244	43,04	18,75	13,50	5,25	46,00	0,15
P2	8,29	0,218	21,68	99,00	82,00	17,00	99,00	0,12
P3	8,90	0,272	30,97	16,25	9,50	6,75	21,00	0,69
P5	9,10	0,311	35,78	15,00	6,50	8,50	3,30	0,71
P6	8,39	0,312	23,92	4,00	1,25	2,75	1,60	1,05
P7	8,44	0,303	57,19	7,25	3,25	4,00	1,50	1,22
P9	8,36	0,237	30,81	30,00	18,25	11,75	59,00	0,13
P10	8,70	0,280	31,24	15,25	11,00	4,25	9,10	0,55
P11	8,92	0,271	22,43	16,50	11,75	4,75	28,00	0,55
P12	9,02	0,301	25,69	18,25	9,50	8,75	11,00	0,80
P13	8,30	0,308	14,79	4,00	1,50	2,50	1,60	1,18
P15	8,65	0,310	27,61	6,00	1,25	4,75	1,60	1,07
P16	8,79	0,308	23,55	10,25	2,00	8,25	1,80	0,90
P17	8,99	0,310	22,16	7,25	2,25	5,00	1,90	0,84

Fonte: Lopes (2013).

Apêndice 2 Constituintes opticamente ativos (COAs) da água e parâmetros limnológicos para a coleta de agosto de 2012

Pontos	pH	CE (dS m^{-1})	Cl-a (μg L^{-1})	SST	SIS	SSV	Turbidez (UNT)	Transparência (m)
				(mg L^{-1})				
P1	7,09	0,238	----	9,75	4,00	5,75	33,00	0,67
P2	7,05	0,222	25,90	9,50	4,00	5,50	36,00	0,35
P3	7,14	0,220	38,39	16,25	10,50	5,75	40,00	0,70
P4	7,47	0,236	33,75	11,50	3,25	8,25	16,00	0,62
P5	7,52	0,236	41,22	15,00	3,00	12,00	20,00	0,61
P6	7,34	0,204	48,59	9,50	0,50	9,00	14,00	1,08
P7	7,18	0,203	45,18	8,25	1,00	7,25	12,00	1,78
P9	7,66	0,230	38,39	8,25	0,25	8,00	17,00	0,77
P10	7,73	0,228	≤ LQ	11,25	1,25	10,00	16,00	0,85
P11	7,77	0,225	36,05	11,75	2,25	9,50	18,00	0,95
P12	7,79	0,222	49,72	12,00	6,25	5,75	37,00	0,50
P13	7,82	0,223	32,47	12,00	6,25	5,75	34,00	0,58
P14	7,26	0,205	7,53	7,00	1,60	5,40	13,00	1,29
P15	7,24	0,203	0,96	5,50	1,50	4,00	2,30	1,36
P16	7,24	0,205	18,80	6,67	2,44	4,22	2,60	1,13
P17	7,29	0,201	22,37	5,00	0,75	4,25	3,50	1,30
P18	7,4	0,201	41,97	7,00	0,60	6,40	5,80	0,93
P19	7,52	0,204	40,80	7,25	0,25	7,00	5,40	0,92
P20	7,64	0,202	-----	6,60	0,40	6,20	6,20	0,88
P21	7,67	0,207	6,73	10,75	1,75	9,00	6,00	0,85

Fonte: Lopes (2013).

9

Remotely Sensed Estimates of Actual Evapotranspiration and Water Stress

Virginia Venturini[1], Daniela Girolimetto[1] & Leticia Rodríguez[1]

[1] Universidad Nacional del Litoral, Santa Fe, Argentina

INOVAGRI Book 2014 - Irrigation and Salinity:
Researches and Technological Innovations
ISBN 978-85-67668-09-3

INOVAGRI
INSTITUTO DE PESQUISA E INOVAÇÃO NA AGRICULTURA IRRIGADA

Fortaleza - CE
2015

9 Remotely Sensed Estimates of Actual Evapotranspiration and Water Stress

1 INTRODUCTION

Water resources will determine the Countries welfare and wealth in the coming centuries. Freshwater is essential for food and energy production, yet it is unevenly distributed over the Earth´s surface. Thus, some areas suffer from water shortage whilst others are blessed with abundant water resources. In this context, measuring, modeling and assessing freshwater resources is a non-delegable scientific undertaking. In the end, the obtained results would contribute to assess is whether there is a scarcity situation or not (Islam and Susskind, 2011).

Evapotranspiration (ET) is the most significant water withdrawal of the water balance. Therefore, iIn recent years the scientific community has given special attention to the ET impact on global circulation models, devoting efforts to estimate how much water is globally evaporating (Vinukollu et al., 2011). Even today, a precise ET calculation is a real challenge for agronomists and water resources engineers and managers since the world´ food security depends largely on water availability. Thus, it is critical to assist farmers to optimize water use in order to maximize food production for mankind.

The need to monitor extensive regions has motivated the development of new methods for calculating ET from remote sensing data. Satellite remote sensing significantly enhances ground data increasing the coverage area while complementing costly field data collection from traditional stations. Most of the satellite sensors cover remote areas that may be impossible to survey from ground stations or field campaigns. Consistent, frequent coverage enable monitoring changes on the land cover and other surface parameters, even for those that require fine spatial resolution (i.e. urban and suburban surfaces). One of the main disadvantages of optical and thermal sensors is the unfeasibility to obtain data through cloud cover, on the contrary, microwave sensors image the surface through clouds. In addition, the need to correct for atmospheric gas absorption and scattering can make it difficult to obtain certain information on particular variables.

Although thermal infrared sensors fail to deliver information throughout clouds, the advent of this technology allowed monitoring land surface temperature (T_s) relating it to vegetation index (VI) to estimate ET. The simplicity and robustness of these type of semi-empirical models made them a widely applied tool with varying results (Jiang and Islam, 2001; Nishida et al., 2003; Norman et al., 2003; Venturini et al., 2004). Water stress (WS) indexes were also derived from Et models, e.g., Jackson et al., (1977), Moran at al., (1994), Pertovt et al., (2008), Mendez-Barroso et al., (2008), Girolimetto and Venturini, (2013).

In the last decade, after Ramirez et al. (2005) publication, the complementary ET relationship (Bouchet, 1963; Granger, 1989) gotresearchers´ attention. Ramirez et al. (2005) work provided direct observational evidence of the complementary relationship in regional ET hypothesized earlier by Bouchet in 1963. Since then, Venturini et al. (2008), Szilagyi and Jozsa (2008, 2009), Crago et al. (2010) among others, developed new methods based on the complementary relationship using remotely sensed data.

Residual methods, that calculate ET as the residual of the energy budged, also employ remote sensing data, for instance SEBAL approach (Bastiaanssen, 2000) and METRIC approach (Tasumi and Allen, 2007) are widely use.

Since three decades ago, the scientific community is making research efforts witha common goal, i.e. to achieve reliable and accurate estimates of ET and its sub-products. In this work, two methods to calculate ET and water stress indexes are presented. The first is the simple Jiang and Islam (2001) method, applicable with most of the satellite data available nowadays. Girolimetto and Venturini (2013) models make use of atmospheric products, such as MODIS products. An error analysis complement the models presentation and results discussion.

2 METHODS DESCRIPTION

Jiang e Islam (2001) ET Model (ET_{J-I})

The Jiang-Islam´s interpretation of the NDVI-T_s relationship provides the basis to estimate ET by modifying Priestley and Taylor's equation (Priestley and Taylor, 1972). Jiang and Islam introduced a coefficient φ to account for unsaturated areas, which replaced the original Priestley and Taylor's coefficient (α). The resulting modified equation is

$$ET_{J-I} = \phi\left(\frac{\Delta}{\Delta+\gamma}\right)\left(R_n - G\right) \quad (1)$$

where φ is Jiang-Islam's parameter, Δ is the slope of the saturation vapor pressure curve, γ is the psychrometric constant, R_n is the net radiation at the surface level and G is the soil heat flux.

The parameter φ varies from zero, for a dry bare soil surface, to 1.26 for a saturated or well vegetated surface, i.e. it becomes equal to the parameter in Priestley and Taylor's equation. This parameter φ is calculated by a simple two-step linear interpolation between the sides of the NDVI- T_s triangle, as shown in Figure 1. Jiang and Islam interpreted the upper edge, with high temperatures and low values of φ, as the minimum value of ET for each class of NDVI, while the cold edge, associated with low T_s and maximum values of φ, represents maximum ET rate. Therefore, the value of φ vary within the limits of the triangle.

These authors proposed a two-step linear interpolation scheme to obtain φ value for each pixel image. The first step is to get upper and lower bounds of φ value for a specific interval of NDVI (NDVI >0). The global minima and maxima of φ can be easily determined ($\varphi^{min} = 0$ for the driest bare soil pixel, and φ^{max} can be found on the pixel with the maximum NDVI). Given these two bounds (NDVI = 0, φ^{min}), (NDVI = $NDVI^{max}$, φ^{max}) and the range of NDVI, the φ_i^{max} can be linearly interpolated for each NDVI interval ($NDVI_i^{max}$). The φ_i^{max} for each $NDVI_i$ can be obtained from the pixel corresponding to the lowest surface temperature within each NDVI interval.

After the lower and upper bounds of φ values for each NDVI class have been determined, the second step is to interpolate within each NDVI class between the lowest temperature pixels, i.e. the pixels with highest evaporation within this NDVI class, i.e., (T_i^{min} , φ_i^{max}), and the highest temperature pixel, where the evaporation is lowest within this NDVI class, i.e., (T_i^{max} , φ_i^{min}). Consequently, the φ values for each pixel can be ascertained using the surface parameters estimated from the aforementioned interpolation, as follows:

$$\phi_i = 1.26 \frac{T_{max} - T_i}{T_{max} - T_{min}} \quad (2)$$

where T_{max} and T_{min} are the maximum and minimum T_s for a given vegetation class, respectively, and T_i is the radiometric temperature for a given pixel. The value of T_{max} is the temperature obtained extrapolating the upper edge of the triangle to intersect the T_s axis (Figure 1) for a NDVI = 0, while T_{min} is obtained as the average T_s of those pixels identified as water, i.e. with NDVI < 0. A full description of φ calculation can be found in Jiang and Islam (2001).

The Water Stress Index Based on Jiang and Islam method

Moran et al. (1994) developed the Water Deficit Index (WDI) based on the interpretation of the trapezoidal VI – (T_s-T_a) plot, where T_a is the air temperature.

The WDI considers two important assumptions associated to the relationship between VI and the difference T_s-T_a. First, the authors assume that the difference T_s-T_a is linearly related to the percentage of vegetated area and canopy, and soil temperatures. Another important statement made by the authors is that, given a certain R_n, the

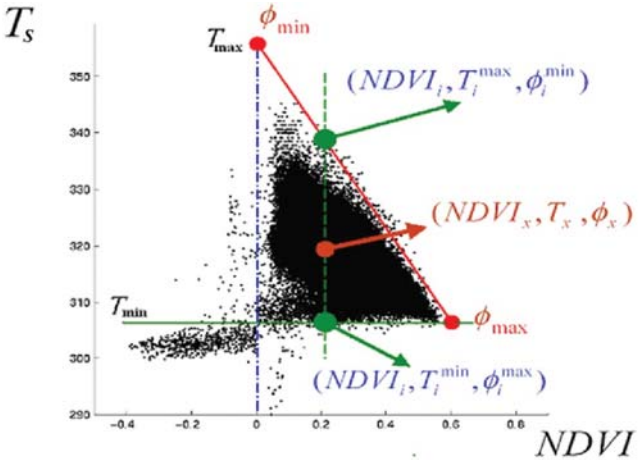

Figure 1. NDVI-Ts triangle space with upper and lower bounds and Jiang- Islam´s parameters

temperature of the foliage and soil are linearly related to transpiration and evaporation, respectively. Therefore, the variations in T_s-T_a would be associated to ET, as follows:

$$WDI = 1 - \frac{ET}{E_{pot}} \tag{3}$$

where (ET/ E_{pot}) is the relative evaporation.

In equation 3, E_{pot} assumes unlimited water supply, consistent with Penman-Monteith equation (Monteith and Unsworth, 1990) with the vegetation aerodynamic resistance (r_{cp}) close to zero, without being canceled out. Therefore, it can be assumed that in this formulation, the surface water supply is the limiting factor and the vegetation stress is mainly caused by deficit of moisture at the root zone.

In the absence of water, moisture content in the root zone will be reduced as a result of crop intake. In turn, water stress causes the closure of the plants stoma and, hence, a reduction in the transpiration rate. Then, the wet environment evapotranspiration (E_w) only considers the surface moisture and the available energy, as in Priestley and Taylor´s equation. Thus, E_w can replace E_{pot} in equation (3), so the WDI can be written as

$$WDI = 1 - \frac{ET}{E_w} \tag{4}$$

In this new form of WDI, ET can be replaced by equation 1 and E_w by the Priestley and Taylor´s equation. The new index, WSI_{Ew}, is

$$WSI_{Ew} = 1 - \frac{\phi}{\alpha} \quad (5)$$

replacing φ by equation 2, the WSI_{Ew} becomes

$$WSI_{Ew} = \frac{T_i - T_{min}}{T_{max} - T_{min}} \quad (6)$$

where T_i is the radiometric temperature for a given pixel and T_{max} and T_{min} are the Jiang and Islam´s parameters.

Venturini et al. (2008) Model ($ET_{V\text{-}V}$)

Granger (1989) derived a physically based complementary relationship between ET, E_w and E_{pot}, proposing the inequality $E_{pot} \geq E_w \geq ET$,where E_w can be either Penman or Preitley-Taylor equations. Granger (1989) demonstrated the following relationship:

$$ET + E_{pot}\frac{\gamma}{\Delta} = E_w\left(\frac{\Delta + \gamma}{\Delta}\right) \quad (7)$$

where ET is not symmetric with respect to E_{pot} and E_w.

Granger and Gray (1989) proposed their ET model for unsaturated surfaces following the combination approach and the relative evaporation concept. The relative evaporation expression proposed by these authors is based on a Dalton-type equation:

$$GG = \frac{ET}{E_{pot}} = \frac{f_u\left(e_s - e_a\right)}{f_u\left(e_s^* - e_a\right)} \quad (8)$$

where f_u is a function of the wind speed and the canopy height, e_s is the surface actual water vapor pressure, e^*_s is the surface saturation water vapor pressure, and e_a is the air actual water vapor pressure.

Venturini et al. method uses Granger's methodology, particularly the relative evaporation expression coefficient, to modify equation 7. Simplifying equation 7 would render an expression of ET as a function of only one potential evaporation concept, E_w. Furthermore, the advantage of using the ratio ET/E_{pot}, is that eliminating the wind speed function and resistance factors reduces the uncertainty and complexity of the ET calculation, as will be shown later.

A key difficulty in applying equation (8) lies in the estimation of $(e_s\text{-}e_a)$, since there is no simple way to relate e_s to any readily available surface temperature. Thus, the authors assumed that f_u affects similarly ET and E_{pot} and defined a new temperature T_u as the temperature of the surface if it is brought to saturation without

changing the actual surface vapor pressure, which is analogous to the dew point temperature.

Considering that the water vapor pressure can be calculated from the SVP curve with the corresponding temperatures, see Figure 2, F is approximated as follows,

$$F = \frac{ET}{E_{pot}} = \frac{(e_s - e_a)}{(e_s^* - e_a)} \cong \frac{(T_u - T_d)\Delta_1}{(T_s - T_d)\Delta_2} \tag{9}$$

where T_d is the dew point temperature. Δ_1 and Δ_2 are the slopes of the SVP curve at T_d and T_s, respectively.

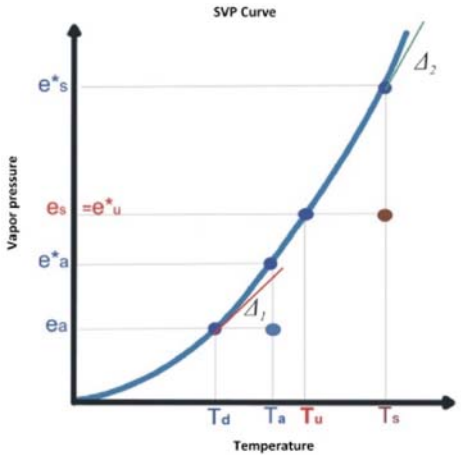

Figure 2. SVP curve, T_u, T_s, e_s, e^*_s relationship in de T_s context

Therefore, from equation (9), E_{pot}= ET/F . If combined with Granger´s complementary equation [ET+ E_{pot} (γ/Δ)=E_w(Δ+γ)/Δ], renders ET as a function of E_w,

$$ET + \frac{ET\gamma}{F\Delta} = E_w\left(\frac{\gamma + \Delta}{\Delta}\right) \tag{10}$$

In this case, the Priestley and Taylor´s equation (Priestley and Taylor, 1972) was used to compute E_w. Consequently, by combining Priestley and Taylor´s expression with equations (9) and (10), the following model was derived,

$$ET_{V-V} = \alpha\left(\frac{F\Delta}{F\Delta + \gamma}\right)(R_n - G) \tag{11}$$

where α is a Priestly-Taylor parameter, assumed equal to 1.26 for saturated surfaces.

In this formulation it is necessary to determine the new variable , T_u, in order to calculate e_s and then F (see equation 9). The authors estimated T_u from the SVP curve using T_s and T_d (see Figure 2), however they recognized that T_u calculation did not follow the physics of the problem (Venturini et al., 2011),

$$T_u = \frac{\left(e_s^* - e_a\right) - \Delta_2 T_S + \Delta_1 T_d}{\Delta_1 - \Delta_2} \tag{12}$$

Once T_u is estimated, e_s can be computed, and then F and ET.

Girolimetto and Venturini (2013) ET Model ($ET_{G\text{-}V}$)

The e_s estimation could be enhanced by using a surface variable such as surface moisture content. The new e_s calculation involves the surface water availability proposed by Barton (1979) as follows,

$$\sigma = \frac{e_s}{e_s^*} \tag{13}$$

where σ is an indicator of the near surface moisture availability (Barton, 1979).

Barton (1979) analyzed ground evaporation data in terms of σ that is directly related to soil moisture (SM) content. Hence, the author empirically related σ to bare SM data for the Deniliquin (Australia) region calculated with data from active microwave sensors. He also proposed site-specific relationships, difficult to extrapolate to other areas. Barton derived σ for bare soil surfaces, though it is not evident how it varies for mixed soil-vegetation. For instance, Deniliquin is a semi-arid region where the bare soil surface saturates for moisture contents larger than 37.5% (Barton, 1979). The soil is clayey with a patchy vegetation pattern dominated by mesophytic species forming a relatively dense sward. In this region the mean annual rainfall and evaporation are 40 cm and 161 cm, respectively and the mean temperature varies from 40 C in July and 24 C in January.

From the remote sensing point of view, the shortwave infrared (SWIR) energy is absorbed by water; therefore, these bands are sensitive to the surface moisture content variations (Chen et al., 2005). Many authors combined near-infrared (NIR) and SWIR reflectance to study changes in foliar water content (Penuelas et al., 1997; Hunt et al., 1987; Gao, 1996; Ceccato et al., 2001; Fensholt and Sandholt, 2003; Sims and Gamon, 2003; Zarco-Tejada et al., 2003; Maki et al., 2004; Chen et al., 2005; Cheng et al., 2006; Trombetti et al., 2008). Fensholt and Sandholt (2003) explained that even though the atmosphere, leaf/surface internal structure and dry matter content might affect vegetation SWIR reflectance, these effects are negligible compared with water absorption. Simulations of leaf reflectance of SWIR bands showed that over 50% of

the changes in reflectance of the SWIR region are due to the absorption caused by the water content in the vegetation (Cecatto et al., 2002a).

The strong water absorption occurring at wavelengths > 1.0 μm makes the mix surface moisture the main cause of the SWIR variation. Thus, the SWIR reflectance of the soil and vegetation are negatively related to moisture (Zerco-Tejada et al., 2003; Yilmaz et al., 2008). Consequently, considering the surface as a vegetation-soil complex, and assuming that the decrease of the reflectance in the SWIR is essentially due to the water content of the surface, we approximate σ as,

$$\sigma = \frac{\text{Rsat}}{\text{Ri}} \tag{14}$$

where Rsat is the SWIR reflectance of a saturated surface and Ri is the SWIR reflectance of any i^{th}-pixel.

Rsat is easily obtained from the relation between Ri and SM, where ground data are available. Otherwise, it can be calculated from the mean Ri of the pixels identified as water in an image. In any case, the values of Ri close to zero would be associated to saturated pixels and can be considered as Rsat.

Knowing Rsat, it is possible to estimate σ and apply equation (13) to estimate e_s ($e_s = \sigma e^*_s$). Introducing e_s in equation (9),

$$F = \frac{\sigma e^*_s - e_a}{e^*_s - e_a} \tag{15}$$

Thus, ET is estimated from equation (11) with the new F which incorporates the physically consistent T_u estimation. This modified form of Venturini et al.´s model will be referred hereinafter as $ET_{G\text{-}V}$.

The Water Stress Index Derivation from Girolimetto and Venturini ET Method

It is possible to rewrite Moran et al. (1994) formulation replacing ET/E_{pot} by F (see equation 3), as follows:

$$WSI_F = 1 - F = 1 - \frac{\left(e_s - e_a\right)}{\left(e^*_s - e_a\right)} = \frac{e^*_s - e_s}{e^*_s - e_a} \tag{16}$$

Knowing $e_s = \sigma e^*_s$, with σ determined from the SWIR reflectance, WSI_F can be re-writen as follows,

$$WSI_F = \frac{e^*_s - e_s}{e^*_s - e_a} = \frac{\left(e^*_s - \sigma e^*_s\right)}{\left(e^*_s - e_a\right)} \tag{17}$$

The new index tends to zero when σ tends to 1, i.e. for a saturated surface, e_s tends to the saturation vapor pressure (e^*_s) [see equation (17)], so the WSI_F would tend to zero indicating a non-stress condition. In the contrary, when σ tends to zero, e_s tends to e_a and WSI_F would be close to 1 reflecting a full stress condition.

3 APPLICATION

The methods described in previous sections have been derived from universal relationships. Moreover, data sources do not pose a limitation for their applicability, nonetheless remotely sensed data such as that provided by MODIS atmospheric products would empower the potential applications of the methods.

Terra, the first EOS satellite, was launched on December 18, 1999. MODIS (Moderate Resolution Imaging Spectroradiometer) is one of the five sensors onboard. This sensor has 36 spectral bands between 0.405 and 14.385 μm whose spatial resolution ranges from 250 to 500 and 1000 m. Another MODIS sensor is onboard of EOS-Aqua satellite, launched in May 2002..

Daytime MODIS- Aqua images for nine days in years 2009, 2010 and 2011 in Spring and Summer, with at least 82% of the study area free of clouds, were selected to apply the models described. The products MYD02, MYD07 and MYD11 were used to compute the models parameters and variables.

TheMOD021KM product was utilized since it provides calibrated digital numbers for 36 bands at 1.09 km spatial resolution. Besides the channel digital number of each pixel, the geolocation, i.e., latitude, longitude and viewing angle, are also available from the same product. MODIS Atmospheric Profile product consists on several parameters: total-ozone burden, atmospheric stability, temperature and moisture profiles, and atmospheric water vapor. All hese parameters are produced day and night for Level 2 at 5×5 km pixel. MYD07_L2 contains data collected from the Aqua platform. MODIS temperature and moisture profiles are produced at 20 vertical levels. A simultaneous direct physical solution to the infrared radiative-transfer equation in a cloudless sky is used. The profiles are also used to correct for atmospheric effects for some of the MODIS products (e.g., sea-surface and land-surface temperatures, ocean aerosol properties, etc) as well as to characterize the atmosphere for global greenhouse studies. MYD11, the Land Surface Temperature and Emissivity (LST/E) products, provide per-pixel temperature and emissivity values. Average temperatures are extracted in Kelvin with a day/night LST algorithm applied to a pair of MODIS daytime and nighttime observations. This method yields 1 K accuracy for materials with known emissivities, the view angle information is included in each LST/E product. The LST/E algorithms use MODIS data as input, including geolocation, radiance, cloud masking, atmospheric temperature, water vapor, snow, and land cover (Wan and Dozier, 1996; Venturini et al, 2004; Venturini et al, 2010).

In this chapter, results obtained for the Southern Great Plains (SGP) region in USA are presented. The region is a flat terrain, with heterogeneous land cover and seasonal variations of temperature and humidity. It extends over the State of Oklahoma and southern parts of Kansas, ranging in longitude from 95.5º W to 99.5º W and in latitude from 34.5º N to 38.5º N (See Figure 3).

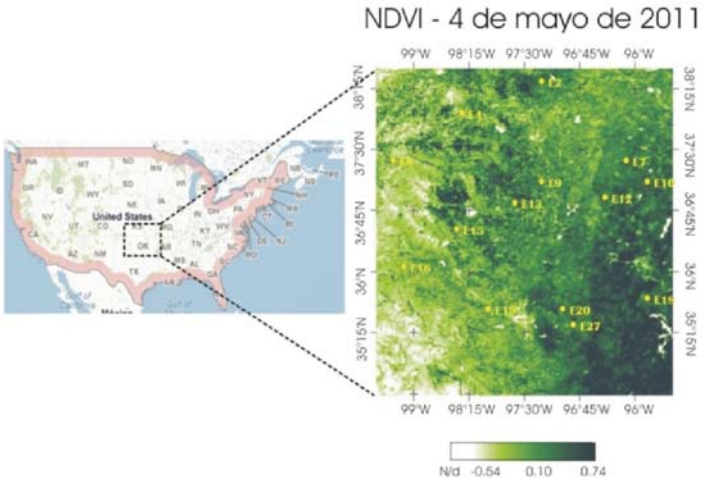

Figure 3. Southern Great Plain and NDVI map for 04-05-2011

This region was the first field measurement site established by the Atmospheric Radiation Measurement (ARM) program. At present, the ARM program has three experimental sites. Scientists all over the World have access and utilize the information generated at this site to improve the performance of atmospheric general circulation models used for climate change research. This region has a relatively extensive and well-distributed coverage of surface flux and meteorological observation stations.

Each image was geo-registered from the Lat-Lon coordinates available within each of them. T_a and T_d images were resized to obtain pixels of $1km^2$, a resolution comparable to the resolution of other images used in the models implementation. Then, the study area is extractedfrom each image in a grid of 467 columns by 444 rows, in pixels of approximately 1 km resolution.

Red (R) and near infrared (NIR) images were used to get the NDVI as (NIR-R/NIR+R), which was plotted against T_s to attain NDVI-T_s scatter plot. Jiang and Islam´s main parameters, i.e. T_{max} and T_{min}, were estimated from the NDVI-T_s graphs as shown in Figure 4. For each analyzed day, φ was computed from T_{max} and T_{min}; then ET_{J-I} and WSI_{Ew} were estimated using equations (1) and (6), respectively.

On the other hand, T_a and T_d images were used to compute Venturini et al.´s parameters, T_u and F. Then, ET_{V-V} was calculated with equation (11).

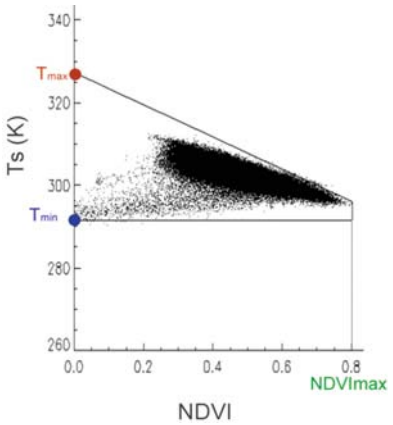

Figure 4. NDVI – Ts and trapezoid bond plot for day 04-05-2011

In order to apply Girolimetto-Venturini´s ET model, R_{sat} parameter must be estimated to obtain σ from equation (14). R_{sat} was attained from MODIS band 7 (R7) and gravimetric soil moisture SM content. These data indicate that R7 turn out to be asymptotic at 0.06 for SM values greater than 25%, suggesting the saturation condition of the surface for this region (see Figure 5).

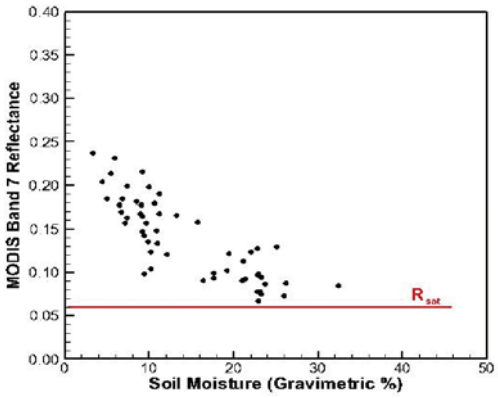

Figure 5. R7 *versus* soil moisture (gravimetric %) plot where Rsat limit is indicated

Then, σ was obtained with R_{sat} and R7 of each pixel for each selected day. $ET_{G\text{-}V}$ was calculated with equation (11) and F as a function on σ.

4 ET AND WSI ERRORS

The ET estimates ($ET_{modeled}$) from the three models, $ET_{V\text{-}V}$, $ET_{G\text{-}V}$ and $E_{J\text{-}I}$, were contrasted with observed ET (ET_{ground}).

The bias and the root mean square error (RMSE) were used to analyse the reliability of the new model in 54 ground observation points . Table 1 shows the RMSE and bias for each analyzed day for ET_{V-V}, ET_{J-I} and ET_{G-V} models. In general, the RMSEs for ET_{G-V} model are lower than 13% of the mean ET_{ground} of each day; the biases are up to 8% of the observed mean ET. Only the day 04/06/2010 presented a RMSE of 18% with a bias of the same order. The image quality of that day is poor, few stations are free of clouds, which may cause uncertainties in the imagery. The ET_{V-V} method presents RMSE maximum values of approximately 30% of the observed ET mean and the ET_{J-I} model presents RMSE and bias much higher than those for ET_{V-V} and ET_{G-V} models.

Table 1. Contrast between ET_{obs} and $ET_{calculated}$ for each study day in terms of RSEM and bias

Day	# of observations	ET_{J-I}		ET_{V-V}		ET_{G-V}	
		RMSE	Bias	RMSE	Bias	RMSE	Bias
April 6th 2011	4	39.08	-30.24	20.95	-10.84	16.97	- 7.01
May 4th 2011	8	37.78	-8.66	55.42	-24.16	36.78	18.82
May 26th 2011	6	110.24	-79.83	96.52	-28.74	44.34	-23.07
May 29th 2011	6	91.77	-79.77	98.84	-70.95	36.03	23.83
June 5th 2011	6	47.92	10.38	70.63	-3.54	39.15	23.77
April 10th 2010	5	64.89	-62.71	44.67	-42.42	29.63	8.75
June 4th 2010	4	45.69	9.06	51.69	19.97	84.05	74.97
June 5th 2009	8	37.61	5.32	65.95	24.67	31.53	19.95
August 22th 2009	7	36.53	-29.18	34.24	11.94	25.85	2.92
RMSE y bias global	54	61.58	-28.23	65.89	-13.10	39.92	14.69

ET_{G-V} model would imply a significant improvement in ET estimates with remotely sensed data. For instance, Venturini et al. (2008) published of RMSE and bias values of about 18% and 15% of the observed mean ET, respectively, for the same region. Kalma et al. (2008) conducted a thorough analysis summarizing results from about 30 published ET validation studies. These authors reported RMSE values of about $50 Wm^{-2}$ and relative errors of about 15 to 30%. Long and Singh (2012) recently found RMSE values of 45.6 Wm^{-2} and 63.1 Wm^{-2} using Landsat TM/ETM+ and ASTER images, respectively.

The preliminary results presented here suggest that ET_{G-V} model correlates more closely r with ET measurements than ET_{V-V} model results.

Figure 6 shows the comparison between models results and ground observations. ET obtained with Priestley and Taylor´s model is included in the figure since it is the base equation for all of the three models discussed in this work, ET estimated with Priestley and Taylor´s model represents E_w (red squares). ET_{J-I} and ET_{V-V} models overestimate observation values, while ET_{G-V} model results (pink diamonds) present less dispersion around the 1:1 line.

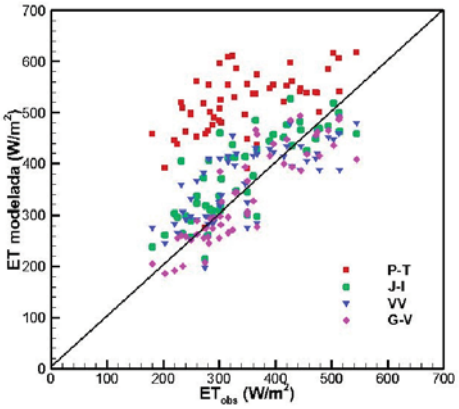

Figura 6. ET_{obs} vs $ET_{calculada}$

The state of the surface moisture introduced by σ is consistent with the definition of T_u and e_s, consequently σ improves the results of the ET_{V-V} model. The new ET_{G-V} method yields robust ET estimates being simple to apply with remotely sensed data and easily coded for routinely applications withoutuser´s supervision.

Regional statistics of WSI_{Ew} were computed. Since Jiang and Islam´s method requires free water pixels to estimate T_{min}, the minimum WSI_{Ew} is always equal to 0 The minimum temperature represents $ET=E_w$, i.e. a no-stress condition; thus, no-stress pixels are always exist in this methodology. The regional maximum ranges from 0.50 to 0.72. Mean values of WSI_{Ew} vary from 0.14 to 0.42. The relationship between WSI_{Ew} and SM (R^2=0.52) provides interesting information. In Figure 7 one can observe that a soil with 5% moisture matches a WSI_{Ew} of about 0.45. On the other

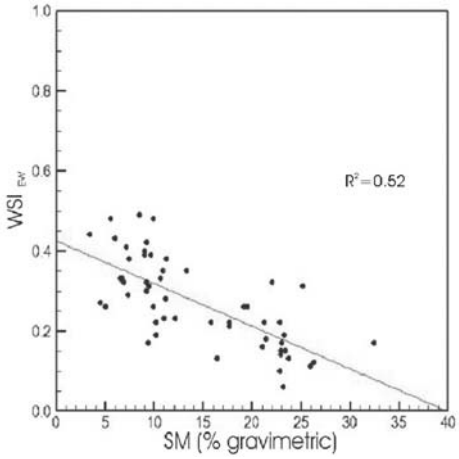

Figure 7. *WSI_{Ew} vs* observed SM (at 5 cm)

end, a SM of 30% agrees with a WSI_{Ew} of 0.1. In other words, WSI_{Ew} would not get close to 1 although the SM indicates a dry surface.

Values of WSI_F regional average are greater than 0.50 for all analyzed dates, suggesting that the region is within a moderately stressed period. The value of WSI_F standard deviations varies between 0.097 and 0.234, which is consistent with different degrees of dispersion around the mean and different regional surface moisture distributions.

The relationship between WSI_F and SM (R2=0.8) provides information about the index limits. For instance, a soil with 5% of moisture matches a WSI_F of about 0.8 and a SM of 30% agrees with a WSI_F of about 0.3. WSI_F would get close to 0 for surfaces with SM in the order of 25-30%, which is a near saturation point for many soils (see Figure 8).

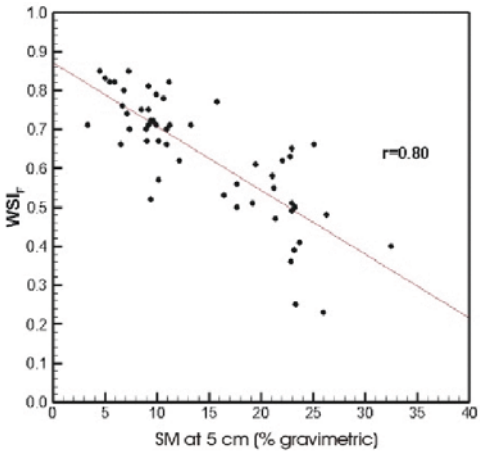

Figure 8. WSI_F *vs* observed SM (at 5 cm)

A simple contrast between both indexes is displayed in Table 2, where their background assumptions are remarked. The varying range of both indexes is different and should be taken into account when the results are contrasted. Maps of WSI_{Ew} and

Table 2. Contrast between WSI_{Ew} and WSI_F

	WSI_F	WSI_{Ew}
Surface moisture effects	Yes	Yes
Atmospheric effects	Yes	No
SM associated	**WSI**	
5%	0.8	0.4
15%	0.6	0.3
25%	0.4	0.2
	Expected Variation Range	
	1 to 0	0.5 to 0

WSI_F for day May 4th 2011 are displayed in Figure 9, (a) and (b), respectively. In these maps the spatial differences between both indexes can be identified, although the southeastern area is stressed in both maps, the magnitude of the deficit varies from one index to the other.

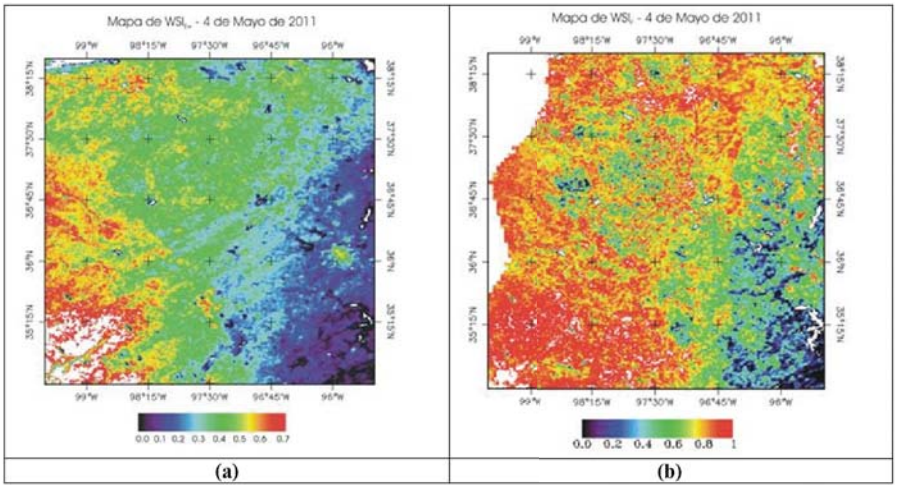

Figure 9. Water Stress indexes maps for day May4th 2011. (a) WSI_{Ew} and (b) WSI_F

REFERENCES

Bastiaanseen, W.G.M. (2000). SEBAL-based sensible and latent heat fluxes in the irrigated Gediz Basin, Turkey, *Journal of Hydrology*, 229, pp. 87-100, ISSN 0022-1694.

Barton, I.J., 1979. A parameterization of the evaporation from nonsatured surfaces. *Journal of Applied Meteorology*, 18, 43-47.

Bouchet, R.J. (1963). Evapotranspiration rèelle et potentielle, signification climatique. International Association of Scientific Hydrology. *General Assembly of Berkeley, Transactions*, *2*, Evaporation, Berkeley, California- USA.

Ceccato, P., Flasse, S., Tarantola, S., Jacquemoud, S., Gregoire, J. M., 2001. Detecting vegetation leaf water content using reflectance in the optical domain. *Remote Sensing of Environment*, 77, 22–33.

Ceccato, P., Gobron, N., Flasse, S., Pinty, B., Tarantola, S., 2002a. Designing a spectral index to estimate vegetation water content from remote sensing data: Part 1. Theoretical approach. *Remote Sensing of Environment*, 82, 188–197.

Chen, D., Huang, J., Jackson, T., 2005. Vegetation water content estimation for corn and soybeans using spectral indices derived from MODIS near- and short-wave infrared bands. *Remote Sensing of Environment*, 98, 225–236.

Cheng, Y.B., Zarco-Tejada, P.J., Riano, D., Rueda, C.A., Ustin, S. L., 2006. Estimating vegetation water content with hyperspectral data for different canopy scenarios: Relationships between AVIRIS and MODIS indexes. *Remote Sensing of Environment*, 105, 354−366.

Crago R. D., Qualls R. J., & Feller M. (2010???) A calibrated advection-aridity evaporation model requiring no humidity data . *Water Resources Research*, 46, W09519, 8 PP., 201. ISSN. 0043-1397

Fensholt, R., and Sandholt, I., 2003. Derivation of a shortwave infrared water stress index from MODIS near- and shortwave infrared data in a semiarid environment. *Remote Sensing of Environment*, 87, 111−121.

Gao, B. C., 1996. NDWI-A normalized difference water index for remote sensing of vegetation liquid water from space. *Remote Sensing of Environment*, 58, 257– 266.

Girolimetto, D. and Venturini, V. 2013. Water Stress Estimation from NDVI-Ts Plot and the Wet Environment Evapotranspiration. Advances in Remote Sensing. 2:283-291.

Granger, R.J., 1989. A complementary relationship approach for evaporation from nonsaturated surfaces. *Journal of Hydrology*, 111, 31-38.

Granger, R.J., and Gray, D.M., 1989. Evaporation from natural nonsaturated surfaces. *Journal of Hydrology*, 111, 21-29.

Hunt, E.R., Rock, B.N., Nobel, P.S., 1987. Measurement of leaf relative water content by infrared reflectance. *Remote Sensing of Environment*, 22, 429– 435.

S. Islam and L. Susskind. 2011. Water Diplomacy: Managing the science, policy, and politics of water networks through negotiation. General Assembly of the European Geosciences Union, Vienna, Austria, April 3-8.

Jiang, L., and Islam, S., 2001. Estimation of surface evaporation map over southern Great Plains using remote sensing data. Water Resources Research, 37(2), 329-340.

Jackson R.D, Reginato R.G., Idso S.B., 1977. Wheat canopy temperature: A practical tool for evaluating water requirements. *Water Resources Research*. 13: 651-656.

Kalma, J.D., McVicar T.R., McCabe, M.F., 2008. Estimating Land Surface Evaporation: A Review of Methods Using Remotely Sensed Surface Temperature Data. *Surveys in Geophysics*. Volume 29, Numbers 4-5, 421-469

Long, D., and Singh, V.P., 2012. A Two-source Trapezoid Model for Evapotranspiration (TTME) from satellite imagery. Remote *Sensing of Environment*, 121, 370–388.

Maki, M., Ishiahra, M., Tamura, M., 2004. Estimation of leaf water status to monitor the risk of forest fires by using remotely sensed data. *Remote Sensing of Environment*, 90, 441-450.

Mendez-Barroso L.A., Garatuza-Payan J., Vivoni E.R., 2008. Quantifying water stress on wheat using remote sensing in the Yaqui Valley, Sonora, Mexico. *Agricultural Water Management*. 95 (6), 725-736.

Monteith, J.L. & Unsworth, M. (1990). Principles of Environmental Physics. Butterworth-Heinemann, 2nd edition. Burlington-MA, 304 pages. ISBN: 071312931X .

Moran M.S., Clarke T.R., Inoue Y., Vidal A., 1994. Estimating crop water deficit using the relation between surface-air temperature and spectral vegetation index. *Remote Sensing of Environment*. 49 (3), 246-263.

Nishida, K., Nemani, R.R., Running, S.W., Glassy, J.M., 2003. An operational remote sensing algorithm of land evaporation. *Journal of Geophysical Research*, 108, D9, 4270.

Norman J.M., Anderson M.C., Kustas W.P., French A.N., Mecikalski J., Torn R., 2003. Remote sensing of surface energy fluxes at 101-m pixel resolutions. *Water Resources Research*. 39(8), 1221−1232.

Penuelas, J., Piñol, J., Ogaya, R., Filella, I., 1997. Estimation of plant water concentration by the reflectance water index (R900/R970). *International Journal of Remote Sensing***,** 18, 2869–2875.

Pertovt L.E., Rivas R., Schirmbeck J., Coelho W.O.G., Vives L., 2008. Análisis de condicionantes ambientales del estrés hídrico de la vegetación en el sur de Brasil mediante imágenes NOAA - AVHRR. Boletín Geológico y Minero. 119 (1): 119-124.

Priestley, C.H.B., and Taylor, R.J., 1972. On the Assessment of Surface Heat Flux and Evaporation Using Large-Scale Parameters. *Monthly Weather Review,* 100, 81–92.

Ramírez, J. A., Hobbins, M.T. & Brown T. (2005). Observational evidence of the complementary relationship in regional evaporation lends strong support for Bouchet's hypothesis. *Geophysical Research Letters*, 32, L15401, ISSN 0094-8276.

Sims, D.A., and Gamon, J.A., 2003. Estimation of vegetation water content and photosynthetic tissue area from spectral reflectance: a comparison of indices based on liquid water and chlorophyll absorption. *Remote Sensing of Environment,* 84, 526-537.

Szilagyi J., & Jozsa J. (2008). New findings about the complementary relationship based evaporation estimation methods. *Journal of Hydrology,* 354, pp. 171– 186, ISSN 0022-1694

Szilagyi J., & Jozsa J. (2009). Analytical solution of the coupled 2-D turbulent heat and vapor transport equations and the complementary relationship of evaporation . *Journal of Hydrology,* 372, pp. 61–67, ISSN 0022-1694

Tasumi, M. and Allen, RG. 2007 Satellite-based ET mapping to assess variation in ET with timing of crop development. Agricultural Water Management 88 (1), 54-62

Trombetti, M., Riano, D., Rubio, M.A., Cheng, Y.B., Ustin, S.L., 2008. Multi-temporal vegetation canopy water content retrieval and interpretation using artificial neural networks for the continental USA. *Remote Sensing of Environment*, 112, 203-215.

Venturini, V., Bisht, G., Islam, S., Jiang, L., 2004. Comparison of evaporative fractions estimated from AVHRR and MODIS sensors over South Florida. *Remote Sensing of Environment*, 93, 77-86.

Venturini, V., Islam, S., Rodríguez, L., 2008. Estimation of evaporative fraction and evapotranspiration from MODIS products using a complementary based model. *Remote Sensing of Environment*, 112, 132-141.

Venturini V., Rodríguez L., Bisht G. (2010). A comparison among different modified Priestley and Taylor's equations to calculate actual evapotranspiration with MODIS data. *International Journal of Remote Sensing,* 32(5), 1319-1338.

Vinukollu, R.K., Wood, E.F., Ferguson, C.R. and Fisher, J.B., 2011. Global estimates of evapotranspiration for climate studies using multi-sensor remote sensing data: Evaluation of three process-based approaches. *Remote Sensing of Environment*, 111, 801–823.

Wan, Z., and Dozier, J.A., 1996. A generalized split-window algorithm for retrieving land-surface temperature from space. *IEEE Transactions on Geoscience and Remote Sensing*, 34(4), 892−905.

Yilmaz, M.T., Hunt Jr. E.R., Goins, L.D., Ustin, S.L., Vanderbilt, V.C., Jackson T.J., 2008. Vegetation watercontent during SMEX04 from ground data and Landsat 5 Thematic Mapper imagery. *Remote Sensing of Environment*, 112, 350–362.

Zarco-Tejada, P.J., Rueda, C.A., Ustin, S.L., 2003. Water content estimation in vegetation with MODIS reflectance data and model inversion methods. *Remote Sensing of Environment*, 85, 109−124.

10

Sistema Solo-Água-Planta-Atmosfera e Manejo da Irrigação em Plantas Perenes

Lucas Melo Vellame[1] & Alisson Jadavi da Silva[1]

[1] Universidade Federal do Recôncavo da Bahia, Cruz das Almas, BA, Brasil

INOVAGRI Book 2014 - Irrigation and Salinity:
Researches and Technological Innovations
ISBN 978-85-67668-09-3

INOVAGRI
INSTITUTO DE PESQUISA E INOVAÇÃO NA AGRICULTURA IRRIGADA

Fortaleza - CE
2015

10 Sistema Solo-Água-Planta-Atmosfera e Manejo da Irrigação em Plantas Perenes

1 INTRODUÇÃO

Informações a respeito das relações água-solo-planta-atmosfera são fundamentais para o desenvolvimento de estratégias no manejo dos recursos naturais. Essas informações são a base para projeto, planejamento e manejo da irrigação. Medidas meteorológicas e de variação de armazenamento de água do solo são as estratégias mais utilizadas por produtores e pesquisadores que visam uma irrigação racional. Essas estratégias têm se mostrado simples e eficazes em cultivos anuais que cobrem uniformemente o solo, a aplicação de água também é uniforme e atende a evapotranspiração de forma potencial. Entretanto, essas condições nem sempre são satisfeitas e as metodologias usuais podem se tornar bastante ineficientes.

Esse capítulo traz algumas considerações e resultados de pesquisa de dois jovens pesquisadores com as relações hídricas em plantas de banana e laranja. O texto busca mais do que recomendar estratégias de manejo da irrigação explicitar alguns problemas passiveis de maiores estudos.

2 MANEJO DA IRRIGAÇÃO – CONTROLE DE PROCESSO

A irrigação tem sido definida como um "processo" artificial de reposição da água do solo. Considerando a irrigação um "processo", o manejo da irrigação pode ser analisado como um sistema de controle de processo. As variáveis de processo são condições internas ou externas que afetam o desempenho de um processo. A variável controlada de um processo é aquela que mais diretamente indica a forma ou o estado desejado do produto. Os sistemas de controle mais elementares são o controle em malha fechada e o controle em malha aberta. (Figura 1)

O controle em malha fechada, também chamado de controle retroativo (realimentação ou feedback) necessita de informações da saída do controlador através de elementos sensores ou transdutores, compara o sinal da saída com o set-

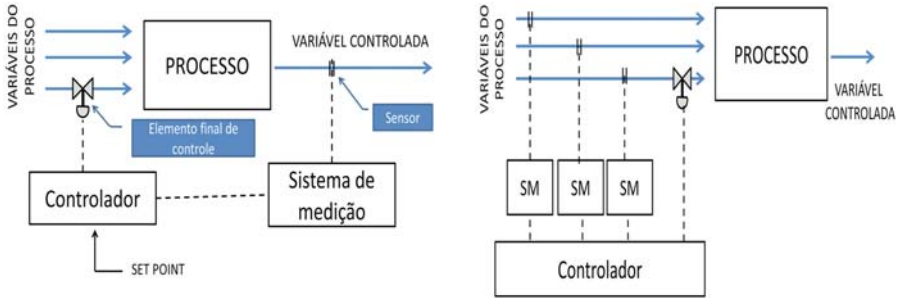

Figura 1. Controle em malha aberta e em malha fechada

point (referência) e corrige a saída caso a mesma esteja desviando-se dos parâmetros programados.

O controlador de malha aberta consiste em um sistema que não possui realimentação. Mais detalhadamente o controle em malha aberta consiste em aplicar um sinal de controle na entrada de um sistema, esperando-se que na saída a variável controlada consiga atingir um determinado valor ou apresente um determinado comportamento desejado. Nesse tipo de sistema de controle não observamos a evolução do processo para determinar o sinal de controle.

No caso da irrigação a variável controlada mais comumente utilizada é o conteúdo de água do solo e as variáveis do processo são as características da planta e as variáveis meteorológicas. Esse manejo tem como objetivo do manejo repor a água do solo para que as plantas transpirem potencialmente. No caso do manejo com a evapotranspiração de referência e KC (ALLEN et al, 1998) temos um controle em malha aberta e no caso do manejo via solo o controle em malha fechada. Ambos têm o mesmo objetivo e partem pressuposto que a transpiração potencial é a que rende maior produtividade já que a fotossíntese depende da abertura estomática.

Apesar da maior ênfase nas medidas meteorológicas e de água do solo, o monitoramento da planta começa a ter destaque para algumas culturas, a exemplo da temperatura do dossel obtido por termômetros de infravermelho. Nesse sistema de controle a variável controlada deixa de ser a umidade do solo e passa a ser a condição hídrica da planta. Esses métodos por indicarem a condição hídrica da planta são particularmente interessantes no caso da irrigação com déficit e para estresse hídrico controlado, na indução de florescimento em fruteiras e maturação da cana, por exemplo.

Medidas de resistência estomática, potencial de água na folha, temperatura do dossel e turgidez do caule (dendrômetros), entre outros, tem relatos de sucesso, na literatura cientifica, para definir indicadores da condição hídrica de diversas espécies de plantas. Entretanto, cada uma dessas técnicas apresenta limitações de uso em campo, sendo a principal limitação a pequena disponibilidade de informações quanto aos limites e índices recomendados para as culturas de interesse econômico. (MANTOVANI et al., 2007).

A automação é umas das ferramentas possíveis para tentar minimizar as perdas de água na irrigação. Muitos sistemas automáticos estão funcionando em campos de irrigação brasileiros. Todavia, o que se vê na prática é o uso de controladores importados, e geralmente dedicados, que controlam apenas os mecanismos de aplicação da água, não considerando regras de manejo para a tomada de decisão (QUEIROZ, 2007).

EVANS et. al. (2000) fazem em seu trabalhado um apanhado geral das tecnologias disponíveis para controle em irrigação de precisão. Os autores concluem que, para a irrigação de precisão ser praticada em larga escala é necessário o desenvolvimento de sensores de solo e/ou planta, de baixo custo, integrados com redes de comunicações e sistemas de controle e de apoio às decisões.

Diversos sensores para variáveis ambientais, muitos com transmissão por rádio-freqüência, estão disponíveis ou sendo desenvolvidos. Entretanto, o manejo automático da irrigação ainda é um desafio tanto em sistemas convencionais quanto por taxa variável, isso porque a ação de controle envolve uma tomada de decisão que não é simples de ser tomada pelos controladores existentes no mercado.

3 TRANSPIRAÇÃO EM LARANJEIRAS JOVENS

Os resultados apresentados nesse tópico do capitulo foram oriundos de um experimento com laranjeiras jovens no município de Piracicaba que deram origem a um trabalho de tese (Vellame, 2010) e publicado em periódico científico (Vellame et al., 2012)

Em cultivos descontínuos (florestas, pomares e vinhedos) tanto a evaporação quanto a transpiração podem assumir papeis importantes sendo necessário diferenciar de alguma forma os componentes da evapotranspiração. Muitas formas de manejar os cultivos como cobertura morta e a irrigação localizada reduzem a evaporação do solo tornando a transpiração o principal elemento do consumo hídrico.

Grande parte dos estudos sobre medidas de transpiração de plantas, principalmente em lenhosas, se baseia na estimativa do fluxo de seiva por métodos de fornecimento de calor no tronco. A estimativa da transpiração com base nesses métodos pressupõe a equivalência entre o fluxo de seiva no tronco e o fluxo transpiratório nas superfícies foliares, pressuposto válido quando se considera o fluxo em escala diária (VELLAME et al., 2009; COELHO FILHO et al., 2005; DELGADO-ROJAS et al., 2007; LU et al., 2002; VALANCOGNE e NASR, 1993).

Na Figura 2 está apresentado o curso da radiação global e do fluxo de seiva médio de 20 plantas jovens de laranja Valência em quatro dias escolhidos de forma a representar períodos com condições de baixa e alta demanda atmosférica. Verifica-se a defasagem entre o fluxo de seiva e o curso da radiação solar em todos os dias, fato este detectado por vários autores (HEILMAN e HAN, 1990; VALANCOGNE e NASR, 1993). Observa-se também que nos dias de baixa demanda (Figura 2-B)

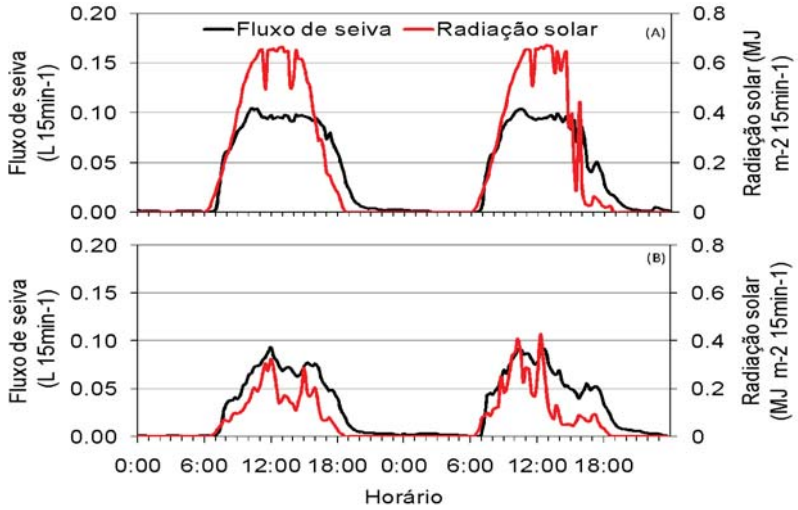

Figura 2. Curso da radiação solar global e fluxo de seiva médio de 20 plantas de laranja 'Valência' em 2 dias consecutivos de alta (A) e baixa (B) demanda evaporativa da atmosfera (Vellame et al., 2012)

o fluxo de seiva segue as variações de radiação solar. Já em dias de alta demanda (Figura 2-A) ocorrem poucas variações no fluxo de seiva em condições de radiação superiores a 0,4 MJ m^{-2} 15 min^{-1}, provavelmente, devido ao fechamento estomático. Pode ser notado que a linha que representa o curso do fluxo de seiva nos dias de alta demanda fica abaixo da linha de radiação solar, comportamento que se inverte nos dias de baixa demanda, indicando uma mudança da relação entre essas variáveis.

Na Figura 3 é relacionada a transpiração média de 20 plantas de laranja jovens com a ETo_{PM}. Observa-se que para valores de ETo_{PM} até 2,4 mm dia^{-1} existe uma tendência linear de aumento da transpiração das plantas com o aumento da demanda evaporativa da atmosfera. Para valores de ETo_{PM} entre 2,4 e 4,8 mm dia^{-1} a transpiração média das plantas foi de 4,4 L dia^{-1} com coeficiente de variação de 13,2%, indicando uma tendência de estabilização da transpiração média em maiores demandas. O valor de ETo_{PM} = 2,4 mm dia^{-1} como limite entre as faixas de alta e baixa demanda foi definido pela minimização da raiz quadrada da média dos quadrados dos desvios (RMSE) na estimativa geral da transpiração por regressão linear segmentada.

Devido aos altos desvios apresentados acreditamos que o modelo apresentado na Figura 3 não explica totalmente a transpiração das plantas. Entretanto, indica que a transpiração dessas plantas não é linear com a ETo e portanto o uso de coeficientes de cultura podem levar a erros elevados.

Plantas perenes não sofreram em sua maioria adaptação genética para transpirar potencialmente como as anuais. Os citros se caracterizam quanto à condutância foliar à difusão de vapor, por sua alta resistência e por algum tipo de resposta adaptativa,

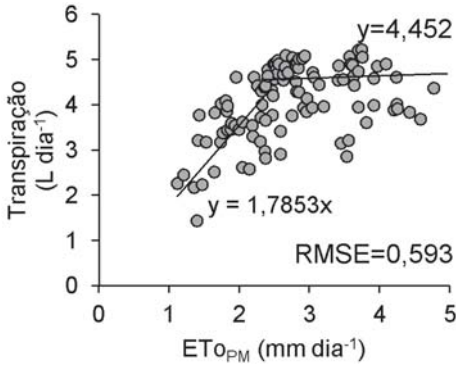

Figura 3. Transpiração média de 20 plantas de laranja 'Valência' em função da evapotranspiração de referência (Vellame et al., 2012)

quando expostos durante um tempo a demanda atmosférica elevada. Assim, tem-se verificado comportamento semelhante de demanda de água por plantas cítricas em regiões úmidas e em regiões secas (BONAN, 1996; HALL et al., 1975; SYVERTSEN e LLOYD, 1994). Quando a demanda evaporativa da atmosfera aumenta, os estômatos tendem a fechar, reduzindo as taxas de transpiração. Dessa forma, quando ocorre mudança nas condições ambientais em termos de saldo de radiação e das diferenças entre a pressão de vapor nas folhas e no ar, a planta responde aumentando a resistência estomática, diminuindo a transpiração (HALL et al.,1975; SYVERTSEN & LLOYD, 1994). Apesar desse fato ser amplamente conhecido o manejo da irrigação com o uso de coeficiente de cultura (Kc) e a ETo parte do pressuposto que a resistência estomática do dia não depende das condições meteorológicas. Algumas metodologias foram propostas a fim de corrigir os coeficientes de cultura em plantas perenes como a apresentada por ALLEN e PEREIRA (2009). A questão que levantamos é: será que criar modelos para corrigir coeficientes do modelo ETc=KcxEto, que apresentava a grande vantagem de ser simples, é o caminho a ser tomado pelo manejo da irrigação

Com o objetivo de verificar a metodologia empregada no estudo foi feita uma regressão múltipla para estimativa da transpiração média das plantas em função do dia Juliano e da ETo_{PM}. Os dados foram separados em fases fonológicas das plantas e em grupos de transpiração em dias com $ETo_{PM} < 2{,}4$ mm dia^{-1} e outro com valores acima. Só dessa forma obteve-se um bom ajuste dos dados (Figura 4). O efeito do dia Juliano foi significativo indicando que outras variáveis dependentes temporalmente devem ser consideradas para a estimativa da transpiração com precisão.

4 VARIABILIDADE DE EXTRAÇÃO DA ÁGUA DO SOLO

As variações do conteúdo de água no solo têm sido utilizadas para indicar o momento e a quantidade de água a se aplicar na irrigação. Atualmente existe um

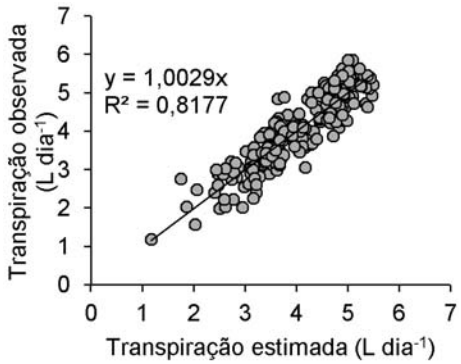

Figura 4. Relação entre a transpiração média diária observada e estimada para plantas de laranja 'Valência' (Vellame et al., 2012)

número satisfatório de métodos e instrumentos que possibilitam a determinação da quantidade de água existente em um determinado local do solo, podendo-se citar: Gravimetria, Tensiômetro, FDR (Frequency Domain Reflectometry), TDR (Time Domain Reflectometry), Sonda de Neutrons, dentre outros. A precisão e acurácia desses métodos e instrumentos, mesmo que de forma não padronizada e sem seguir as normas metrológicas, têm sido bastante reportadas na literatura. A escolha de um ou outro método decorre principalmente da praticidade, tempo em obtenção de resultados e custos.

Pouco reportado na literatura, entretanto, é a indicação do local e quantidade de sensores necessários a serem instalados na zona radicular de uma cultura. Pouco se conhece da variação espacial e temporal da extração de água no volume de solo explorado pelas raízes das plantas, sobretudo de fruteiras, levando produtores e pesquisadores a instalarem seus sensores de forma arbitrária.

Algumas recomendações de posicionamentos de sensores de leitura de umidade do solo para manejo de irrigação têm sido feita com base na distribuição de raízes no solo (Sokalska et al., 2009; Sant`Ana et al., 2012). Porém, em outros trabalhos, tem-se verificado que a extração de água pelas raízes nem sempre ocorre em direção proporcional à concentração de raízes (Clothier & Green, 1994; Silva et al., 2009; Javaux et al., 2008). Neste sentido, algumas orientações de manejo de água e nutrientes já vêm sendo realizadas levando em consideração as zonas efetivas de extração de água pelas plantas (Coelho et al., 2007; Guohua et al., 2010). Entretanto, a variabilidade da extração de água dentro dos limites tomados como efetivo, dificulta a recomendação do número e posicionamento de sensores, principalmente no caso de fruteiras que apresentam amplitude no desenvolvimento do sistema radicular.

Monitorando de forma contínua e detalhada a extração de água da bananeira, Silva (2013) verificou que devido a existência de variabilidade da extração de água na região explorada pelas raízes da cultura, instalar sensores na região de maior

intensidade de extração de água superestima os valores de evapotranspiração (ET) da cultura. As diferenças obtidas nos valores de ET devem-se justamente à variabilidade no espaço e no tempo do padrão da distribuição de extração de água do solo na região explorada pelas raízes da planta. Conforme pode-se observar na visão tri-dimensional da distribuição da extração de água da região radicular da bananeira na fase de crescimento vegetativo (Figura 5), a saída de água do perfil não é uniforme e é mais intensa próxima ao pseudocaule da planta.

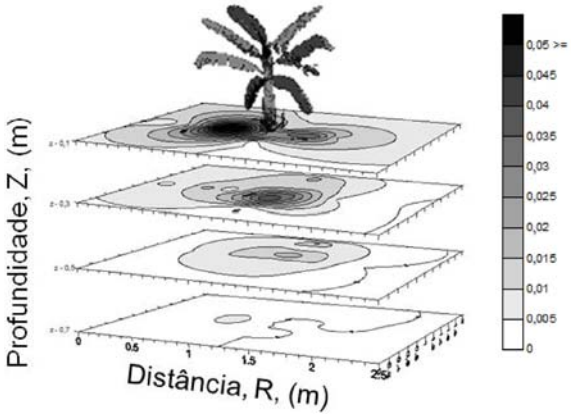

Figura 5. Distribuição tridimensional da extração de água ($cm^3\ cm^{-3}$) na zona radicular da bananeira em fase de crescimento vegetativo. Fonte: Silva (2013)

As estimativas de ET realizadas com o cálculo da variação de armazenamento de água no solo considerando dados de umidade obtidos em 1 e 2 baterias de sondas de TDR superestimaram os valores obtidos em todo perfil explorado pela zona radicular da bananeira (Figura 6). Os valores de ET estimados com uma bateria de sondas de TDR foram superestimados em 297% comparando-se aos valores estimados com dados de umidade obtidos em todo perfil. Os valores estimados com 2 baterias superestimam os valores obtidos no perfil inteiro em 288%.

O curioso a se observar é que há na literatura pesquisas que fazem uso de sensores para monitorar umidade utilizando uma ou duas baterias no solo por planta (Silva et al., 2009; Souza et al., 2013; Montenegro et al., 2008). Nosso entendimento é de que assumir que as variações de umidade na região radicular de uma cultura pode ser representada por poucos pontos de coleta de umidade é um risco, pois em regiões onde existe maior intensidade de extração tem-se maior variação de armazenamento de água. Tendo em vista que os dados de extração de água de uma cultura podem apresentar alta variabilidade e não seguir uma distribuição normal, o uso do valor médio também é visto como um risco de pouca representatividade. Portanto, é mais seguro monitorar a umidade do solo em vários pontos na região explorada pelas raízes das plantas, tornando mais

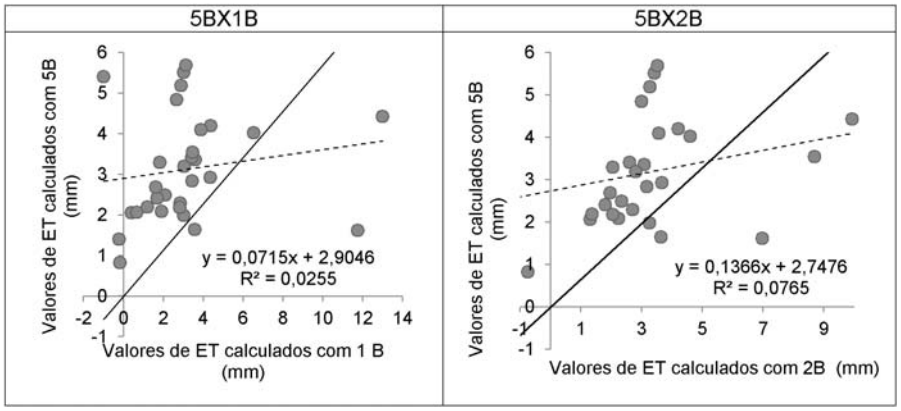

Figura 6. Relação entre valores de evapotranspiração da banana estimada pelo balanço hídrico no solo com um número variado de baterias de sondas de TDR instaladas no perfil. 1B – uma bactéria, 2B – Duas baterias, 5B – cinco baterias. Cada bateria (B) foi composta por 4 sondas instaladas às profundidades de 0,1m; 0,3m; 0,5m e 0,7m. As baterias foram distanciadas entre por 0,2m.

completo o cálculo do balanço hídrico. Para tanto, existe ainda a necessidade, para uma dada condição, estabelecer o número mínimo de sensores necessários a se instalar no perfil.

5 CONSIDERAÇÕES FINAIS

Plantas perenes não sofreram em sua maioria adaptação genética para transpirar potencialmente como as anuais. Dessa forma a relação com a demanda de água pela atmosfera nem sempre é linear e o uso do Kc pode levar a erros expressivos.

Devido à variabilidade espacial e temporal da extração de água na rizosfera, mesmo em condição de molhamento uniforme, a estimativa da variação de armazenamento se torna complicada exigindo um grande número de sensores para uma estimativa confiável.

O manejo da irrigação com déficit deve ser muito mais preciso e erros na estimativa de variáveis como a profundidade do sistema radicular, armazenamento de água do solo e a evapotranspiração podem levar a resultados indesejáveis.

Se por um lado, em algumas condições, as metodologias tradicionais de quantificação das relações hídricas podem ser ineficientes, as soluções apresentadas até o momento não são simples de serem aplicadas. Dessa forma, o debate e esforços/investimentos em pesquisa e extensão na área ainda são extremamente necessários. O anseio em fornecer recomendações práticas para uso em campo pelos irrigantes não deve suprimir os questionamentos necessários a investigação científica.

REFERÊNCIAS

ALLEN, R.G.; PEREIRA, L.S.; RAES, D.; SMITH, D. Crop evapotranspiration: Guides for computing crop water requirements Food and Agriculture Organization of the United Nations FAO;Rome, 1998. 300 p. (FAO Irrigation and Drainage Paper,56.)

ALLEN, R. G.; PEREIRA, L. S. Estimating crop coefficients from fraction of ground cover and height. Irrigation Science, v. 28, n. 1, p. 17-34, 2009

CLOTHIER B. E., GREEN S. R. Rootzone Processes and the efficient use of irrigation water. Agricultural Water Management. vol. 25, p. 1-12, 1994.

COELHO, E. F.; SANTOS, D. B. dos and AZEVEDO, C. A. V. de. Sensor placement for soil water monitoring in lemon irrigated by micro sprinkler. Rev. bras. eng. agríc. ambient. vol.11, n.1, pp. 46-52, 2007.

COELHO FILHO, M.A.; ANGELOCCI, L.R.; CAMPECHE, L.F.S.M.; FOLEGATTI, M.V.; BERNARDES, M.S.B. Field determination of young acid lime plants transpiration by the stem heat balance method. Scientia Agricola, Piracicaba, v. 62, n. 3, p. 240-247, 2005.

DELGADO-ROJAS, J.S.; ANGELOCCI, L.R.; FOLEGATTI, M.V. ; COELHO FILHO, M.A. Desempenho da sonda de dissipação térmica na medida da transpiração de plantas jovens de Lima Ácida. Engenharia Agrícola, Jaboticabal, v. 27, n. 2, p. 404-413, 2007.

EVANS, R. G., et al. Controls for precision irrigation with self-propelled systems. National irrigation symposium. Proceedings of the 4th Decennial Symposium, Phoenix, Arizona, 2000.

GUOHUA,L.; KANG, Y.; LI, L.; WAN, S.; Effect of irrigation methods on root development and profile soil water uptake in winter wheat. Irrigation Science, vol.28, p.387-398, 2010.

HALL, A.E.; CAMACHO, B.S.E.; KAUFFMAN, M.R. Regulation of water loss by citrus leaves. Physiologia Plantarum, Copenhagen, v. 33, p. 62-65,1975.

HEILMAN, J.L.; HAM, J.M. Measurement of mass flow rate of sap in Ligustrum japonicum. Hortscience, Stanford, v.25, n.4, p.465-467, 1990

JAVAUX, M.; SCHRODER, T.; VANDERBORGHT, J.; VEREECKEN, H. Use of a Three-Dimensional Detailed Modeling Approach for Predicting Root Water Uptake. Vadose Zone Journal. vol. 7, n. 3, p. 1079-1088, 2008.

LU, P.; WOO, K. C.; LIU, Z. T. Estimation of whole-plant transpiration of bananas using sap flow measurements. Journal of Experimental Botany, Oxford, v. 53, n. 375, p.1771-1779, 2002.

MANTOVANI E. C.; BERNARDO, S. e PALARETTI, L. F. Irrigação: Princípios e Métodos. Viçosa: UFV. 2007. 358p

QUEIROZ, T. M. Desenvolvimento de um sistema automático para irrigação de precisão em pivô central. Piracicaba: ESALQ-USP, 2007. 141 p. Tese – Doutorado).

SYVERTSEN. J.P.; LLOYD, J.J. Cítrus. In: SCHAFFER, B.; ANDERSEN. P.C. (Ed.) Handbook of environmental physiology of fruits crops: subtropical and tropical crops. Boca Raton: CRC Press, 1994. v. 2, p. 65-99.

SOKALSKA, D. I.; HAMAN, D.Z.; SZEWCZUK, A.; SOBOTA, J.; DEREN, D. Spatial root distribution of mature Apple trees under drip irrigation system. Agricultural Water Management. vol. 96, p. 917-924, 2009.

SANT'ANA, J. A. V.; COELHO, E. F.; FARIA, M. A.; SILVA, E. L.; DONATO, S. L. R. Distribuição de raízes de bananeira 'Prata-Anã' no segundo ciclo de produção sob três sistemas de irrigação. Revista Brasileira de Fruticultura. v. 34, p.124-133, 2012.

SILVA, A. J. P. Estimação da percolação em lisímetros de drenagem e evapotranspiração da bananeira usando TDR. Tese de Doutorado, Universidade Federal do Recôncavo da Bahia, Cruz das Almas-BA, 2013.

SILVA, A. J. P. da; COELHO, E. F.; MIRANDA, J. H. de and WORKMAN, S. R. Estimating water application efficiency for drip irrigation emitter patterns on banana. Pesquisa Agropecuária Brasileira. vol.44, n.7. 2009.

VALANCOGNE, C.; NASR, Z. Measuring sap flow in the steam of small trees. In: BORGHETTI, M.; GRACE, J.; RASCHI, A. Water transport in plants under climatic stress. Cambridge: Cambridge University Press, 1993. p.166-173.

VELLAME, L. M. Relações hídricas e frutificação de plantas cítricas jovens com redução de área molhada do solo. 2010.128 p. 2010. Tese de Doutorado. Tese (Doutorado em Irrigação e Drenagem)–Escola Superior de Agricultura "Luiz de Queiroz", Universidade de São Paulo, Piracicaba.

VELLAME, L. M.; COELHO, R. D.; TOLENTINO, J. B. Transpiração de plantas jovens de laranjeira'Valência'sob porta-enxerto limão'Cravo'e citrumelo'Swingle'em dois tipos de solo. Revista Brasileira de Fruticultura, v. 34, n. 1, p. 24-32, 2012.

VELLAME, L.M.; COELHO FILHO, M.A.; PAZ, V.P.S. Transpiração em mangueira pelo método Granier. Revista Brasileira de Engenharia Agrícola e Ambiental, Campina Grande, v. 13, n. 5, p. 516–523, 2009.

11

Strawberry Irrigation in the Environment of the National Park of Doñana (Spain). Evapotranspiration, Crop Coefficients and Irrigation Efficiency

Pedro Gavilán Zafra[1], David Lozano Pérez[1] & Natividad Ruiz Baena[1]

[1] IFAPA Centro Alameda del Obispo, Córdoba, Spain

INOVAGRI Book 2014 - Irrigation and Salinity:
Researches and Technological Innovations
ISBN 978-85-67668-09-3

INOVAGRI
INSTITUTO DE PESQUISA E INOVAÇÃO NA AGRICULTURA IRRIGADA

Fortaleza - CE
2015

11 Strawberry Irrigation in the Environment of the National Park of Doñana (Spain). Evapotranspiration, Crop Coefficients and Irrigation Efficiency

ABSTRACT

This paper reports the results of an experiment for the determination of strawberry crop evapotranspiration (ET_c), crop coefficient (K_c) and the irrigation efficiency using different amounts of water applied for *Sabrina* variety in the vicinity of P.N. Doñana, Southern Spain. The ET_c of a strawberry crop was around 88% of the estimated reference evapotranspiration under greenhouse. The K_c was highly dependent on crop cover, reaching a maximum value of 1.1 when 95% coverage was reached. An irrigation efficiency of 83% was achieved when a volume of irrigation of 5500 m^3 ha^{-1} was applied (treatment T1), but higher amounts of water applied implied efficiencies of 70% and lower (T2 and T3). In all treatments production exceeded 1,000 g $plant^{-1}$, resulting in 5% reduction of significant production in the first two treatments with respect to the third. If the application of an irrigation schedule to T1 having a coefficient of less than the actual crop resulted in a production higher than 1,000 g $plant^{-1}$, one would think that a slight increase of irrigation at the end of the season, accompanied by a decrease of it at the beginning, could have resulted in obtaining similar productions in T1 and T2 with a significantly lower amount of water. Using an irrigation schedule based on meteorological data and crop coverage, accompanied by measurements of soil moisture, can result in significant water savings without any loss in production

1 INTRODUCTION AND OBJECTIVES

According to estimates by the Council of Agriculture, Fisheries and Rural Development of the Government of Andalusia, the surface of strawberry cultivated in the province of Huelva has reached 7,500 ha in the 2013/2014 season, which is an increase of 10% in relation to the average one of the years 2004/2007, which reached values close to 6,900 hectares, a period in which the average annual production reached 300,000 tons (Consejería de Agricultura y Pesca, 2012). Strawberry is a generator of high economic value and employment. However, its location in the vicinity of the

National Park of Doñana requires the reconciliation of environmental conservation and productive activity.

Despite the widespread use of drip irrigation in this crop, there is great uncertainty about the strawberry irrigation requirements (Hanson y Bendixen, 2004). Most research on strawberry irrigation have been performed in California and Florida (USA), where the strawberry is cultivated outdoors (Clark y col., 1996; Grattan y col., 1998; Hanson y Bendixen, 2004; Trout y Gartung, 2004). However, in the province of Huelva the whole of this crop is performed under plastic, particularly in greenhouses of macrotunnel type. Up to this project, the values of crop coefficients (Kc) necessary to calculate the strawberry water requirements had been determined for growing outdoors in the climatic conditions of California or Florida (USA). For the state of California and outdoor growing, Hanson and Bendixen (2004) reported estimated maximum values of K_c equal to 0.7, when the maximum coverage was no greater than 75%. However, these authors did not get to measure crop evapotranspiration (ET_c), but measured its coverage and used the ratios obtained by Grattan et al. (1998) for estimating the crop coefficient and therefore ET_c. Jakson (1992) also reported maximum values of K_c equal to 0.7 for coverage of 75%. Finally, the FAO-56 Irrigation and Drainage Paper (Allen et al., 1998) advices maximum values of Kc equal to 0.85, independent of the maximum crop coverage. However, no studies have been performed to estimate these coefficients for strawberries under plastic in the growing conditions of the Huelva coast, where sandy soils predominate. From the 2011/2012 season, IFAPA is carrying out studies on the strawberry water requirements for advising farmers on more efficient irrigation management. These studies have included measurement of evapotranspiration and estimation of crop coefficients, the determination of irrigation efficiency and calculating water productivity. Moreover, irrigation systems commonly used in the Doñana area for strawberry production were evaluated.

The objectives of this study were: 1) determining evapotranspiration of a strawberry cultivation, variety *Sabrina*, in a macrotunnel greenhouse 2) estimating the evolution of its crop coefficient, 3) determining irrigation efficiency for different volumes of water applied, 4) calculating the irrigation water productivity in each case and 5) obtaining a production function of irrigation water in the trial conditions.

2 MATERIALS AND METHODOLOGY

The work was carried out in T. M. Almonte, near the village of "El Rocio", on a commercial strawberry farm of the *Sabrina* variety (*Fragaria x ananassa*). The soil of the study area is classified as sandy (USDA classification), with 90% sand and 10% clay. The company did all the tasks for strawberry cultivation in the trial (including fertilizer). They also took care of the irrigation management to build the bed, to maintain the structure before planting and of sprinkler irrigation applied to ensure plant establishment after transplant. The transplant was performed on 9

October 2012 with a planting density of 71,888 plants per ha. The trial ended on 6 June 2013. As we mentioned before, with the exception of fertirrigation, the trial plants received the same tasks as the commercial part of the farm. The culture was planted in 0.60 m trapezoidal bed larger base, smaller base of 0.50 and 0.50 m high, with a separation between them of 1.1 m. Two rows of plants were placed by ridge with a drip irrigation tape in the center. The used tape was able to apply 5 l m-1 h-1 at a pressure of 0.55 MPa.

A trial with three treatments with different irrigation volumes was applied and a randomized block design with four replications was conducted. The experimental unit was a complete tunnel 70 x 6.6 m2, so that the essay consisted of 12 tunnels. Using the entire tunnel as the experimental unit allowed the farmer to compare the results with the production and irrigation applied in the rest of the farm. The first treatment (T1) was designed to apply the crop water requirements, using an irrigation efficiency of 85%. T2 and T3 respectively applied 25% and 50% more water than T1.

Irrigation scheduling was programmed based on the soil water balance method (Allen et al., 1998), using a value of estimated reference evapotranspiration inside the greenhouse ($ET_{o\ gre}$) and the values of the crop coefficients (K_c) recommended by Hanson and Bendixen (2004), reaching maximum values of 0.7 at the end of the season with a maximum coverage of 75%. As shown below, the use of this maximum value of crop coefficient had influence on the production of treatment T1. The $ET_{o\ gre}$ was estimated using a model based on solar radiation measured inside the tunnels proposed by Fernández et al. (2010). Meteorological data measured inside a greenhouse with similar characteristics and proximity to trial, from one station close to the "Aldea de El Rocío" belonging to the Agroclimatic Information Network of Andalusia (SIAR) (Gavilán et al., 2008), were used. For this purpose, an automatic weather station was used for measuring temperature and relative humidity of the air (HMP 45C probe, Vaisala) and solar radiation (pyranometer CM3, Kipp and Zonen), controlled by a datologger CR10X (Campbell Scientific). The solar radiation values measured inside the greenhouse during the 2011/2012 season helped to set a value of average transmissivity of plastic (τ) that could be used in the case of not having a weather station in the greenhouse, as in most of farms. During a measurement campaign performed during 2011/2012 it was estimated that an average value of 0.7 for τ would be suitable for this type of greenhouses.

To measure crop evapotranspiration (ET_c), lysimeters drainage were installed in each treatment, made of polyester, reinforced with fiberglass and with the next dimensions 0.30 m x 1.40 m x 0.62 m. The lysimeters were buried at ground level and then rebuilt the bed where strawberries grow. In each lysimeter 11 plants were planted to an identical distance to the rest of the bed. Daily, readings of the drainage lysimeters were taken for obtaining ET_c based on water balance method.

The amount of water applied to each treatment was measured using flowmeters. Flowmeters were installed at the head of each treatment, which allowed knowing the

volume applied to the set of the four tunnels. Moreover, in the beds where the lysimeters were located, flowmeters of ½" were installed to measure the amount of water applied. With this information the amount of water supplied to each lysimeter was calculated.

The soil moisture was measured in each of the treatments using ECH2O (Decagon Devices) and EasyAG (Sentek Technologies) probes. The EasyAG probe was used to monitor the moisture content of the T1 treatment, which received the least amount of water. The EasyAG probe was connected to an Internet server, such that the values of soil moisture could be displayed remotely, facilitating irrigation decisions. The soil moisture values were used to correct the weekly storage soil moisture to estimate ET_c values and to determine the moisture content in each of the treatments. This allowed adjust the irrigations based on changes in soil moisture due to the different weather conditions along the season.

3 RESULTS AND DISCUSSION

Irrigation Applied on Each of the Treatments

At the start of the campaign, using historical data of ET_o and values of the crop coefficient described above, the target irrigation was planned. To satisfy the crop water requirements an irrigation volume of 5.500 m^3 ha^{-1} was estimated. An irrigation efficiency of 85% was assumed. This irrigation was applied to the treatment T1. However, the irrigation schedule was modified along the season depending on the weather conditions. In the end, the volumes delivered to each of the treatments were 5.610 m^3 ha^{-1} in T1, 6.876 m^3 ha^{-1} in T2 and 7.957 m^3 ha^{-1} in T3. This represented for T2 and T3 applying 23 and 42% more water and fertilizer. Though the target of 25 and 50% values could not be achieved due to the high sensitivity of the drip tape to pressure differences, these values may be considered acceptable considering the emitters were not self-compensating. In treatment T1, November was the month that less water was applied (216 m^3 ha^{-1}), while in May the maximum values of water applied was reached (1.524 m^3 ha^{-1}).The irrigation target was achieved since only 2% more water than we expected was applied in treatment T1.

Along the season, drainage lysimeters indicated that the maximum coefficient of 0.7, proposed by Hanson and Bendixen (2004), was insufficient to meet the crop water requirements from early April. It was decided to use a coefficient of 0.8 from 19 April and subsequently one of 0.9 from the 1st of May, which was used until the end of the campaign. However, this increase was insufficient to meet the crop water requirements. The maximum value of the crop coefficient measured in the essay was 1.1 at the end of the crop cycle.

Evapotranspiration and Crop Coefficients

The greenhouse reference evapotranspiration ($ET_{o\ gre}$) along the irrigation season was 523 mm. The precipitation recorded at Almonte meteorological station, belonging

to the SIAR Network in Andalusia during this period was 580 mm. The average ET_c measured with lysimeters was 463 mm, ranging from 430 mm (T3) to 498 mm (T2). These variations were mainly due to differences in plant growth within the lysimeters and the moisture measurement uncertainty, used to correct the soil water balance. However, these differences can be considered acceptable given the constraints resulting from the use of drainage lysimeters. The maximum evapotranspiration month was May, in which a cumulative average value of 145 mm was reached. In November the reached value was 15 mm. The average crop evapotranspiration along the season was 1.9 mm d^{-1}.

To calculate the actual crop coefficient, the ratio of crop evapotranspiration and greenhouse reference evapotranspiration was used. The evapotranspiration was measured by the water balance in the drainage lysimeters. The initial crop coefficient was around 0.2, when coverage reached values of about 15% in early November (Figure 1). This ratio rose progressively until mid-March, reaching values close to 0.8, with 70% coverage. From that moment, crop coefficient slowly increased to reach a peak of 1.1 in mid-May, with a maximum coverage of about 95%. Using a maximum value of 0.9 for crop coefficient could lead to a little stress in T1 treatment plants and consequently, a small loss of production.

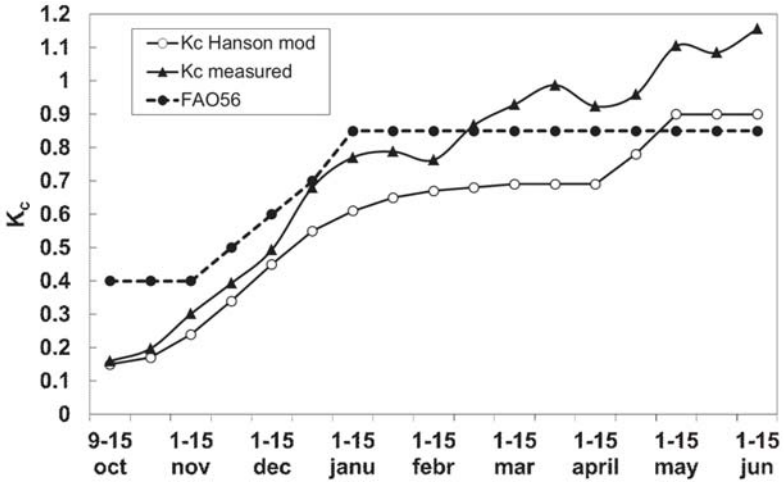

Figure 1. Evolution of crop coefficients applied in irrigation scheduling (Hanson and Bendixen modified), and estimated by lysimeter (average value)

Irrigation Efficiency

Knowing irrigation efficiency is crucial, because it is an indicator of the amount of water taken up by plants in relation to the total applied water. It is also an indicator of the efficiency of fertilizer, as water drainage carries nutrient solution supplied by fertigation, causing what is called diffuse pollution. The irrigation efficiency values

that appear in the literature are illustrative and must be verified under actual conditions. A value of irrigation efficiency of 85% is difficult to achieve without appropriate irrigation management, especially in very sandy soils, such as those we find in the vicinity of the "Village of El Rocío", near the Doñana National Park.

The use of lysimeters allows measuring irrigation efficiency, which is more reliable than its estimation. Treatment T1 reached maximum efficiency with an average annual value of 83%, close to the target value of 85%. The efficiency was variable along the campaign, starting from values lower than 20% immediately after planting, reaching values around 85% from February onwards, and maximum values near 100% from the end of April onwards, even when irrigation became deficit. T2 and T3 treatments had annual average efficiencies of 67 and 58% respectively.

In Figure 2 we can see the difference between an irrigation of 5,500 m^3 ha^{-1} (treatment T1) or 8,000 m^3 ha^{-1} (T3 treatment). This means having an irrigation efficiency equal to 85% or 55%, respectively, and implies a reduction in the volumes of water and fertilizer applied around 45%. Furthermore, in terms of environmental impact, Figure 2 shows the volumes of drainage, which explain how the increase in contamination of T3 relative to T1 is about 300%. Therefore, an irrigation of 8,000 m^3 ha^{-1} would contaminate almost three times that one of 5,500 m^3 ha^{-1}

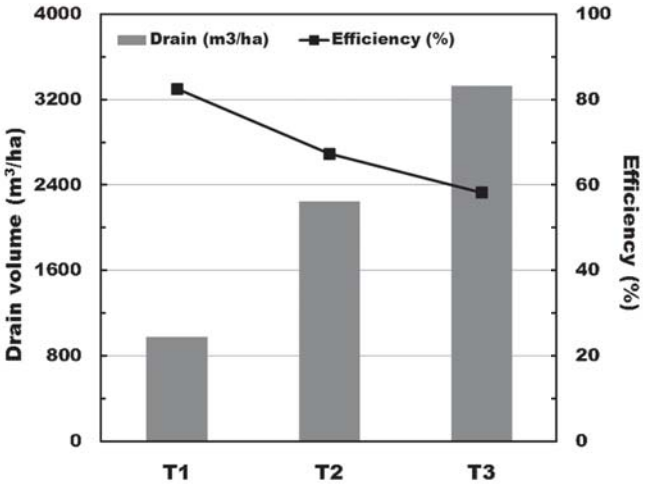

Figure 2. Drainage volumes (m^3 ha^{-1}) and irrigation efficiency (%) for the different treatments of the trial

Yields, Water Productivity and Production Function

In all the treatments the production was over 1000 g $plant^{-1}$ (Figure 3). In T1 and T2, yields of 1.039 and 1.040 g $plant^{-1}$ were respectively achieved with no significant differences between them. This indicates that T1 treatment cannot be considered deficient. If T2 was in deficit, T1 would have had significantly less production than T2.

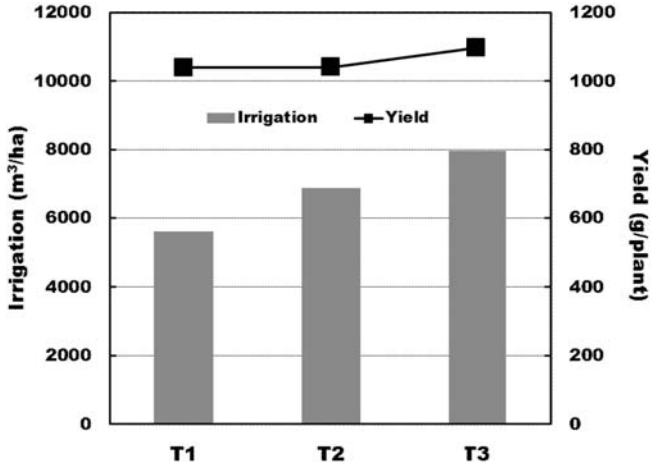

Figure 3. Irrigation Volume (m^3 ha^{-1}) and yield (g $plant^{-1}$) in each treatment

The T3 treatment reached a production of 1,097 g $plant^{-1}$ (5% more than T1 and T2) and was statistically different from T1 and T2. This happened because the calculation of irrigation requirements in the months of April and May was performed with a crop coefficient lower than the real one. Finally, water productivity in each treatment was 13.31, 10.9, 9.9 kg m^{-3}, for T1, T2 and T3, respectively.

4 CONCLUSIONS AND RECOMMENDATIONS

The ET_c of a strawberry crop was around 88% of $ET_{o\ gre}$. This data has not been reported yet in the strawberry bibliography. Furthermore, ET_c was highly dependent on crop coverage, which alerts us to be cautious in extrapolating the results to other varieties, such as *Antilla*, which has a maximum coverage of 65%. The crop coefficient was very dependent on coverage, reaching maximum values of 1.1 for 95% coverage. Therefore, it is necessary to measure the percentage of crop coverage to make decisions about which crop coefficient should be used. For treatment T1, an irrigation efficiency of 83% was reached. Higher amounts of applied water accounted efficiencies of 70% and under. Finally, if the implementation of an irrigation schedule to T1 with a lower crop coefficient resulted in a yield of 1,000 g $plant^{-1}$, one would think that a slight increase of irrigation at the end of the season, accompanied by a water reduction at the beginning, similar productions to T3 could have been obtained with significantly less water. However, it is necessary to test this hypothesis. However, we can say that the use of an irrigation scheduling based on metereological data and crop coverage, accompanied by measurements of soil moisture, could result in significant savings in water and fertilizer without declines in production, and could also significantly reduce environmental impact in terms of diffuse pollution.

5 ACKNOWLEDGMENTS

This work has been funded by TRANSFORM project "Irrigation Advisory Service" (PP.TRA.TRA2010.1), co-financed with FEDER funds. The work would not have been performed without the sponsorship of the company Surexport SL. We also thank all the staff of Surexport S.L.

REFERENCES

Allen, R.G., Pereira, L.S., Raes, D., Smith, M., (1998) Crop evapotranspiration. Guidelines for computing crop water requirements. FAO irrigation and drainage paper 56. FAO, Roma.

Clark, G.A., Albregts, E.E., Stanley, C.D., Smajstrla, A.G., Zazueta, F.S., 1996. Water requirements and crop coefficients of drip-irrigated strawberry plants. Transactions of ASAE 39(3):905-913.

Consejería de Agricultura y Pesca, 2012. Memoria Anual de la Consejería de Agricultura y Pesca 2009. Junta de Andalucía.

Fernández, M.D., Bonachela, S., Orgaz, F., Thompson, R., López, J.C., Granados, M.R., Gallardo, M., Fereres, E., 2010. Measurement and estimation of plastic greenhouse reference evapotranspiration in a Mediterranean climate. Irrigation Science 28:497-509.

Gavilán, P., Estévez, J., Berengena, J., 2008. Comparison of standardized reference evapotranspiration equations in Southern Spain. Journal of Irrigation and Drainage Engineering 134(1):1-12.

Grattan, S.R., Bowers, W., Dong, A., Snyder, R.L., Carrol, J.J., George, W., 1998. New crop coefficients estimate water use of vegetables, row crops. California Agriculture 52(1):16-21.

Hanson, B., Bendixen, W., 2004. Drip irrigation evaluated in Santa Maria Valley strawberries. California Agriculture 58(1):48-53.

Jackson, A., 1992. Central Coast Crop Coefficients for Field and Vegetable Crops. California Department of Water Resources, Water Conservation Office. University of California (UC)

Trout, T.J., Gartung, J., 2004. Irrigation water requirements of strawberries. Acta Horticulturae 664:665-671.

REALIZAÇÃO

INOVAGRI
INSTITUTO DE PESQUISA E INOVAÇÃO NA AGRICULTURA IRRIGADA

Instituto Nacional de Ciência e Tecnologia Engenharia da Irrigação

APOIO

INSTITUTO FEDERAL DE EDUCAÇÃO, CIÊNCIA E TECNOLOGIA CEARÁ Campus Sobral

CNPq
Conselho Nacional de Desenvolvimento Científico e Tecnológico

CAPES

Agência Brasileira do ISBN
ISBN 978-85-67668-09-3

INOVAGRI BOOK 2014 – Irrigation and Salinity: Researches and Technological Innovations